# LRP1 - a master regulator of the contractile activity of myofibroblasts

Inaugural Dissertation
submitted to the
Faculty of Biology and Chemistry
in partial fulfillment of the requirements
for the degree *doctor rerum naturalium* (Dr. rer. nat.)
of the Faculty Biology and Chemistry
of the Justus Liebig University Giessen

by
Schnieder, Jennifer
of
Langenberg, Germany

Giessen 2018

From the Biochemistry Institute:
Director: Prof. Dr. Lienhard Schmitz
of the Faculty of Medicine of the Justus Liebig University Giessen

First Supervisor and Committee Member: Prof. Dr. Adriaan Dorresteijn

Second Supervisor and Committee Member: Prof. Dr. Malgorzata Wygrecka-Markart

Committee Members: Prof. Dr. Saverio Bellusci
Prof. Dr. Kai Thormann

# I. TABLE OF CONTENTS

# II. LIST OF FIGURES

# III. LIST OF TABLES

# IV. LIST OF ABBREVIATIONS

| | |
|---|---|
| Akt | Protein kinase B |
| ALT | Alanine aminotransferase |
| apoER2 | Apolipoprotein E receptor 2 |
| ARDS | Acute respiratory distress syndrome |
| AST | Aspartate aminotransferase |
| ATP | Adenosine triphosphate |
| BALF | Bronchoalveolar lavage fluid |
| BSA | Bovine serum albumin |
| CTGF | Connective tissue growth factor |
| dNTP | Deoxynucleotide Triphosphate |
| DAPT | N-[N-(3,5-Difluorophenacetyl)-L-alanyl]-S-phenylglycine t-butyl ester |
| DMEM | Dulbecco's Modified Eagle Medium |
| DMSO | Dimethyl sulfoxide |
| ECM | Extracellular matrix |
| EDTA | Ethylenediaminetetraacetic acid |
| EGF | Epidermal growth factor |
| EGTA | Ethylene glycol tetraacetic acid |
| EMT | Epithelial-mesenchymal transition |
| ERK | Extracellular signal-regulated kinase |
| FA | Focal adhesion |
| FAK | Focal adhesion kinase |
| FCS | Fetal calf serum |
| FoxO3a | Forkhead box O3a |
| GFP | Green fluorescent protein |
| GM-CSF | Granulocyte-macrophage colony-stimulating factor |
| GPI | Glycosylphosphatidylinositol |
| HDM | House dust mite |
| HEPES | 4-(2-Hydroxyethyl)-piperazine-1-ethanesulfonic acid |
| ICD | Intracellular domain |
| IPF | Idiopathic pulmonary fibrosis |
| ITGB1 | Integrin β1 |

| | |
|---|---|
| JNK | c-Jun N-terminal kinase |
| LAP | Latency associated peptide |
| LDLR | Low density lipoprotein receptor |
| LPA | Lysophosphatidic acid |
| LPS | Lipopolysaccharide |
| LRP1 | Low density lipoprotein receptor-related protein 1 |
| LTBP | Latent TGF-β-binding protein |
| MAPK | Mitogen-activated protein kinase |
| MEK1/2 | MAPK/ERK kinase 1/2 |
| MEF | Mouse embryonic fibroblast |
| MLC | Myosin regulatory light chain |
| MLCK | Myosin light chain kinase |
| MMP | Matrix metalloproteinase |
| NaOH | Sodium hydroxide |
| N-cadherin | Neural cadherin |
| OB-cadherin | Osteoblast cadherin |
| Opti-MEM$^{TM}$ I | Opti-Minimal Essential Medium I |
| PAGE | Polyacrylamide-gel electrophorese |
| PAI-1 | Plasminogen activator inhibitor-1 |
| PBGD | Porphobilinogen deaminase |
| PBS | Phosphate-buffered saline |
| PDGF | Platelet-derived growth factor |
| PI3K | Phosphatidylinositol 3-kinase |
| PMSF | Phenylmethylsulfonyl fluoride |
| PVDF | Polyvinylidene fluoride |
| qPCR | Real-time PCR |
| RIPA | Radioimmunoprecipitation assay buffer |
| ROCK | Rho-associated protein kinase |
| R-SMAD | receptor-activated SMAD |
| RT | Reverse transcriptase |
| SDS | Sodium dodecyl sulfate |
| siRNA | Small interfering RNA |
| α-SMA | α-Smooth muscle actin |
| SMAD | Mothers against decapentaplegic homolog |

| | |
|---|---|
| suFA | Supermature focal adhesion |
| TBS-T | Tris-buffered saline with Tween 20 |
| TG2 | Transglutaminase 2 |
| TGF-β1 | Transforming growth factor-β1 |
| TGFBRI | TGF-β receptor type I |
| TGFBRII | TGF-β receptor type II |
| tPA | Tissue plasminogen activator |
| TRIS | Tris(hydroxymethyl)aminomethane |
| uPA | urokinase-type plasminogen activator |
| uPAR | urokinase-type plasminogen activator receptor |
| VLDLR | Very low density lipoprotein receptor |

# V. SUMMARY

During wound healing, fibroblasts migrate into the wound where they proliferate and eventually differentiate to myofibroblasts. The latter produce extracellular matrix (ECM) components and thus participate in the formation of a new ECM in the lesion. The characteristics of myofibroblasts are the expression of α-smooth muscle actin (α-SMA) and high contractile activity. The acquisition of the myofibroblast phenotype during wound healing is regulated in a combinatory way by cytokines, e.g. transforming growth factor-β1 (TGF-β1), and matrix rigidity. Low density lipoprotein receptor-related protein 1 (LRP1) was also found to control fibroblast to myofibroblast transdifferentiation in kidney and liver. Depending on the organ, this endocytic receptor promotes or suppresses α-SMA expression in fibroblasts. In kidney, LRP1 exerts its functions by modulating the TGF-β1 response. However, it remains elusive whether LRP1 regulates the induction of the myofibroblast phenotype in lung fibroblasts from patients with idiopathic pulmonary fibrosis (IPF).

In order to decipher the role of LRP1 in lung fibroblast differentiation, LRP1 was knocked-down in IPF and donor lung fibroblasts. The microarray analysis revealed that LRP1-deficiency significantly perturbs Kegg pathways which describe processes of cytoskeleton modulation in IPF lung fibroblasts but not in donor lung fibroblasts. In contrast, Kegg pathways which describe endocytic processes were significantly perturbed in donor lung fibroblasts but not in IPF lung fibroblasts following LRP1-depletion. The α-SMA expression was investigated in the IPF lung fibroblasts which were derived from different IPF patients. Levels of LRP1 mRNA and α-SMA mRNA negatively correlated in these cells. In addition, knock-down of LRP1 led to the increase of α-SMA protein expression in IPF lung fibroblasts. This effect was not mediated by the canonical TGF-β1 pathway. In detail, silencing of *SMAD3* did not block α-SMA expression after LRP1-knock-down. It was furthermore demonstrated that the expression, activation and transcriptional activity of SMAD3 is not affected by silencing of *LRP1*. Instead, it was shown that the activity of extracellular signal-regulated kinase (ERK) and c-Jun N-terminal kinase (JNK) as well as of the transcription factor c-Jun is elevated after LRP1-depletion in IPF lung fibroblasts. Pharmacological blockage of ERK or JNK in LRP1-expressing and LRP1-deficient IPF lung fibroblasts

identified JNK to mediate the suppression of α-SMA by LRP1. Combined knock-down of LRP1 and JNK1 confirmed this finding. Moreover, this experiment showed that LRP1 suppresses c-Jun, a downstream target of JNK, in IPF lung fibroblasts. c-Jun can be a component of the transcription factor AP1.
Dual-Luciferase Reporter Assay revealed that LRP1 inhibited the transcriptional activity of AP1 under basal conditions and in response to TGF-β1.
Functionally, LRP1 suppressed the contractile activity of IPF lung fibroblasts under basal conditions and after TGF-β1 treatment. Proliferation and migration were not affected by LRP1-depletion.

Collectively, the present study describes the mechanism by which LRP1 inhibits the differentiation of IPF lung fibroblasts to myofibroblasts. In detail, LRP1 limits α-SMA expression and the contractile activity of IPF lung fibroblasts by inhibiting the JNK/AP1 signaling pathway.

# VI. ZUSAMMENFASSUNG

Bei der Wundheilung migrieren Fibroblasten in die Wunde, in der sie proliferieren und sich schlussendlich zu Myofibroblasten differenzieren. Letztere produzieren Bestandteile der ECM und wirken somit bei der Erneuerung der ECM in der Läsion mit. Die Charakteristika der Myofibroblasten sind die Expression von α-SMA und die hohe kontraktile Aktivität. Das Auftreten des Myofibroblast-Phänotyps während der Wundheilung wird durch das Zusammenwirken von Zytokinen, z.B. TGF-β1, und der Matrixfestigkeit reguliert. Es wurde weiterhin demonstriert, dass LRP1 ebenfalls die Differenzierung von Fibroblasten zu Myofibroblasten in den Nieren und in der Leber kontrolliert. In Abhängigkeit vom Organ fördert oder unterdrückt dieser endozytotische Rezeptor die Expression von α-SMA in Fibroblasten. In den Nieren erfolgt dies, indem LRP1 den TGF-β1 Signalweg moduliert. Es ist jedoch nicht bekannt, ob LRP1 die Ausprägung des Myofibroblast-Phänotyps in Lungenfibroblasten von Patienten mit der idiopathischen pulmonalen Fibrose reguliert.

Um die Rolle von LRP1 in der Differenzierung von Lungenfibroblasten zu Myofibroblasten aufzuschlüsseln, wurde ein Knock-Down von LRP1 in IPF und Donor Lungenfibroblasten durchgeführt. Die Analyse mittels Microarray zeigte, dass LRP1-Defizienz diejenigen Kegg Signalwege, die Prozesse der Zytoskelettmodulierung beschreiben, in IPF Lungenfibroblasten aber nicht in Donor Lungenfibroblasten signifikant stört. Die Kegg Signalwege, die endozytische Prozesse beschreiben, waren hingegen nach LRP1-Verlust in Donor Lungenfibroblasten, jedoch nicht in IPF Lungenfibroblasten, signifikant gestört. Die α-SMA Expression wurde in den IPF Lungenfibroblasten von verschiedenen IPF Patienten untersucht. In diesen Zellen standen die Level der LRP1 mRNA und α-SMA mRNA in einer negativen Korrelation zueinander. Des Weiteren führte der Knock-down von LRP1 zu einer erhöhten α-SMA Proteinexpression in IPF Lungenfibroblasten. Dieser Effekt wurde nicht von dem kanonischen TGF-β1 Signalweg vermittelt. Das geht daraus hervor, dass Silencing von *SMAD3* nicht den Anstieg der α-SMA-Expression nach Verlust von LRP1 blockiert hat. Es wurde weiterhin gezeigt, dass *LRP1* Silencing die Expression, Aktivierung und transkriptionale Aktivität von SMAD3 nicht verändert. Stattdessen war die Aktivität der Kinasen ERK und JNK sowie des Transkriptionsfaktors c-Jun nach LRP1-

Verlust in IPF Lungenfibroblasten erhöht. Die pharmakologische Inhibition von ERK oder JNK in LRP1-exprimierenden und LRP1-defizienten IPF Lungenfibroblasten identifizierte JNK als den Vermittler der LRP1-abhängigen Suppression von α-SMA. Kombinierter Knock-Down von LRP1 und JNK1 bestätigte dieses Ergebnis. Zusätzlich zeigte dieser Versuch, dass LRP1 c-Jun in IPF Lungenfibroblasten unterdrückt. Bei diesem Protein handelt es sich um einen nachgeordneten Vermittler von JNK. c-Jun kann eine Komponente des Transkriptionsfaktors AP1 sein. Dual-Luciferase Reporter Assay zeigte, dass LRP1 die transkriptionale Aktivität von AP1 unter basalen Bedingungen und in Reaktion auf TGF-β1 inhibiert. Die Funktion der Myofibroblasten betreffend, reduziert LRP1 die kontraktile Aktivität von IPF Lungenfibroblasten unter basalen Bedingungen und nach Behandlung mit TGF-β1. Das Proliferations- und Migrationsverhalten wurden durch den Verlust von LRP1 nicht verändert.

Insgesamt wird in dieser Arbeit der Mechanismus beschrieben, mit dem LRP1 die Differenzierung von IPF Lungenfibroblasten zu Myofibroblasten inhibiert. LRP1 limitiert die α-SMA Expression und die kontraktile Aktivität von IPF Lungenfibroblasten durch Inhibierung des JNK/AP1 Signalwegs.

# 1 Introduction

## 1.1 Low density lipoprotein receptor-related protein 1

LRP1 is a member of the low density lipoprotein receptor (LDLR) superfamily which encompasses also LDLR, megalin, LRP1B, LRP3, LRP4, LRP5, LRP6, the very low density lipoprotein receptor (VLDLR) and the apolipoprotein E receptor 2 (apoER2) [1,2].

LRP1 consists of the extracellular heavy α-chain (515 kDa) and the transmembrane/cytoplasmic light β-chain (85 kDa) [3]. The α-chain contains four clusters of ligand-binding type cysteine-rich repeats of which cluster II and IV mediate ligand-binding [3,4]. Up to now, more than 100 ligands of LRP1 have been identified, amongst them are TGF-β1, platelet-derived growth factor (PDGF), matrix metalloproteinases (MMPs), urokinase-type plasminogen activator (uPA), apolipoprotein E, α2-macroglobulin, thrombospondin 1, calreticulin and lactoferrin [1,5,6]. Six epidermal growth factor (EGF) repeats non-covalently connect the α-chain to the β-chain [3]. The latter contains the single membrane-spanning segment and the cytoplasmic domain [3]. Within the cytoplasmic domain, one YXXL motif and two NPXY motifs [3] regulate the two functions of LRP1 which are endocytosis and the modulation of signaling cascades. In detail, the YXXL motif controls LRP1 endocytosis [7], whereas the NPXY motifs mediate LRP1-dependent signal transduction by serving as docking sites for cytoplasmic adaptor proteins [8–10]. Figure 1 shows the structure of LRP1.

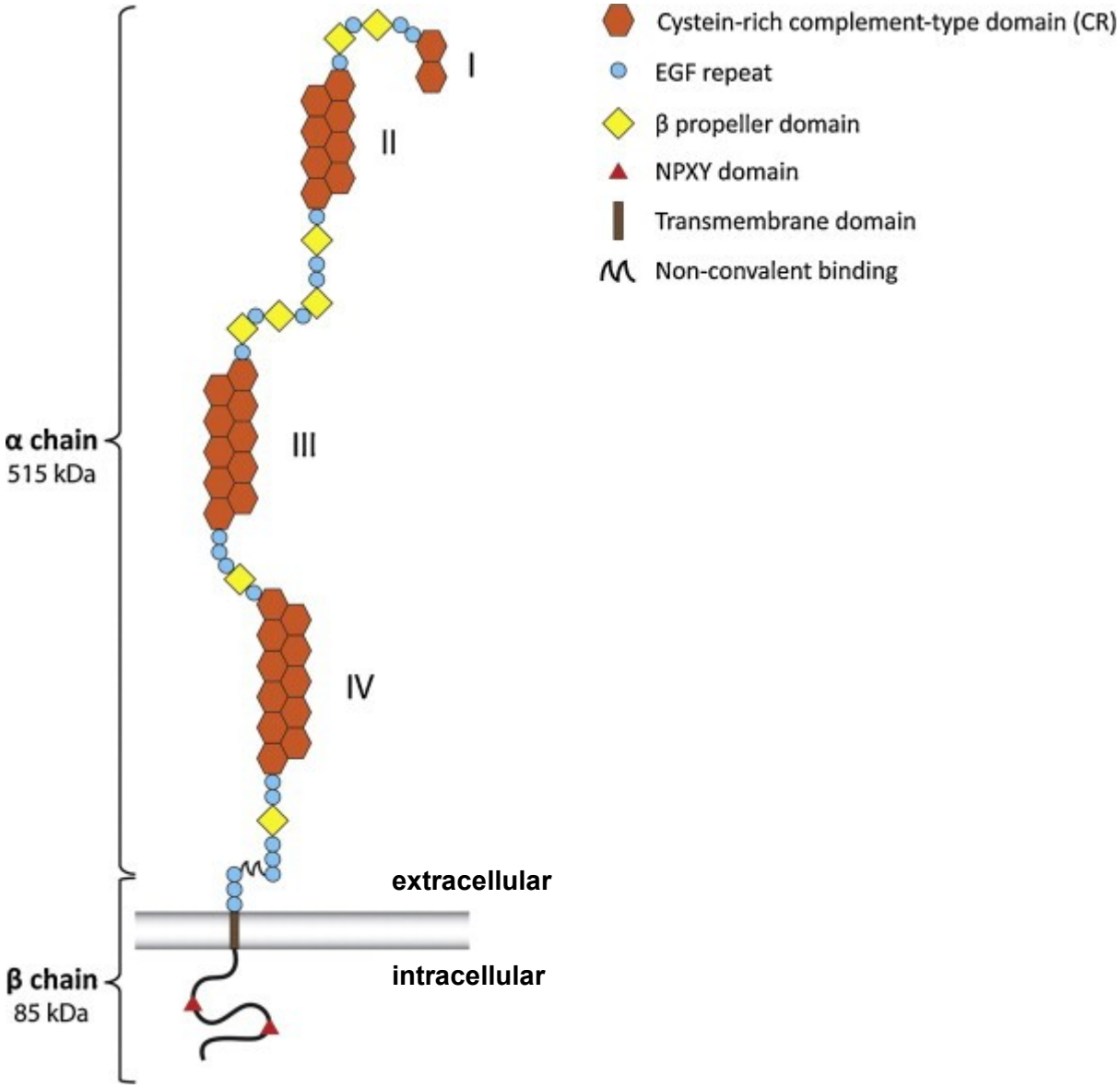


**Fig. 1: Structure of LRP1.** LRP1 consists of the extracellular α- and the transmembrane/cytoplasmic β-chain which are non-covalently connected to each other. The α-chain encompasses the four ligand-binding type cysteine-rich repeats, whereas the β-chain contains the transmembrane domain and the cytoplasmic domain with two NPXY motifs and one YXXL motif. The figure was taken from reference [11] and modified. CR: cysteine-rich repeat; EGF: epidermal growth factor.

LRP1 regulates inflammation and tissue remodeling as well as the clearance of extracellular molecules, such as amyloid-β peptide, von Willebrand factor and factor VIII [12–15]. LRP1 is involved in the pathogenesis of numerous diseases such as acute respiratory distress syndrome (ARDS), atherosclerosis, Alzheimer's disease and kidney fibrosis [16–19]. Although LRP1 is ubiquitously expressed, high levels of LRP1 are present in the lung, liver and brain [3,20]. Under physiological conditions, LRP1 controls the glucose and lipid metabolism. For instance, LRP1 regulates the levels of circulating cholesterol-rich remnant proteins [21]. In addition, LRP1 mediates

the internalization of postprandial lipids in adipocytes [22]. Mice with adipocyte-specific LRP1-deficiency are resistant to dietary fat-induced obesity and glucose intolerance [22]. In the brain, LRP1 functions as a regulator of the blood-brain barrier permeability [23].

Tissue remodeling takes place during wound healing. This process is controlled by LRP1. Tissue remodeling is characterized by dynamic changes in the ECM composition as well as by cell migration, proliferation and differentiation. Wound healing is a three-phase process [24]. In the first inflammatory phase, the coagulation cascade is activated and culminates in fibrin formation, which upon cross linking by factor XIIIa provides a stable matrix [25]. This matrix also contains fibronectin and platelets [26]. Throughout the later course of wound healing, the fibrin matrix is degraded and replaced by ECM [24]. In pleural mesothelial cells, it was demonstrated that blockage of LRP1 results in enhanced fibrin degradation [27]. The mechanisms which underlie this observation involve the uPA/uPA receptor (uPAR) system [27]. Urokinase plasminogen activator binds the cell-surface receptor uPAR and converts plasminogen to plasmin [28]. Plasmin eventually cleaves fibrin [29]. LRP1 regulates uPA levels by mediating the internalization and degradation of receptor-bound uPA [27]. Consequentially, loss of LRP1 leads to the accumulation of uPA on the cell surface and to enhanced generation of fibrin-degrading plasmin. Here it becomes evident that LRP1 may be transiently downregulated during wound healing to allow degradation of the provisional matrix.

During the first phase of wound healing, chemokines which are released by platelets attract macrophages, neutrophils as well as fibroblasts and endothelial cells to the provisional matrix [24].

The second, so called proliferative phase, starts with angiogenesis and subsequent fibroblast proliferation on the provisional matrix [24]. TGF-β1 which is expressed by inflammatory cells during wound healing is a key regulator of cell proliferation and can promote or inhibit proliferation, depending on the cell type. Interestingly, LRP1 controls the effect of TGF-β1 on fibroblast proliferation, as silencing of *LRP1* gene expression switches the function of TGF-β1 from anti-proliferative to pro-proliferative [30]. Besides its effect on fibroblast proliferation, TGF-β1 mediates the differentiation

of fibroblasts to myofibroblasts. Myofibroblasts are characterized by α-SMA expression, high contractile activity and the secretion of large amounts of ECM components, such as collagen type I and type III, which rebuild an ECM matrix in the lesion [24,31,32]. At this stage, the premature wound matrix is called a granulation tissue. The contractile activity of myofibroblasts contributes to the maturation of the granulation tissue [33]. In kidney fibroblasts, it was demonstrated that connective tissue growth factor (CTGF) mediates LRP1 phosphorylation and in consequence increases the TGF-β1-induced α-SMA expression [34]. Hence, LRP1 may promote CTGF-induced fibroblast to myofibroblast transdifferentiation. However, this conclusion is questioned by other findings. For instance, LRP1 mediates endocytosis and degradation of CTGF in hepatocytes [35]. To decipher the role of LRP1 in fibroblast to myofibroblast transdifferentiation, more investigations are needed. Besides TGF-β1, increasing stiffness of the ECM promotes the differentiation of fibroblasts to myofibroblasts. The ECM stiffness is enhanced both by the deposition and the cross linking of ECM components. LRP1 regulates these events in different manners. For instance, LRP1 is a catabolic receptor for fibronectin [36]. Hence, fibroblasts which are deficient for LRP1 accumulate fibronectin on the cell surface [36]. Furthermore, as mentioned above, downregulation of LRP1 expression leads to the accumulation of uPA on the cell surface [27]. It was shown that LRP1 loss in fibroblasts results in enhanced plasmin-mediated remodeling of the fibronectin- and collagen matrix [37]. After blockage of LRP1 uPA also promoted collagen production as shown in pleural mesothelial cells [27]. Transglutaminase 2 (TG2) is a cross linker of many ECM components, among them are collagen, fibronectin and elastin [38–40]. Furthermore, TG2 promotes the TGF-β1-mediated fibronectin production by lung fibroblasts as well as their migration and their contraction on the collagen matrix [41]. In fibroblasts, LRP1 limits TG2 activity by mediating the endocytosis and lysosomal degradation of this enzyme [42].

In the third phase, the resolution phase, the wound closes and the scar formation occurs [24]. This phase is characterized by reduced ECM deposition but enhanced remodeling of the granulation tissue, e.g. by MMPs [24]. LRP1 controls the function of MMP2 and MMP9 by mediating their endocytosis [43,44]. In ARDS, it was demonstrated that elevated levels of MMP2 and MMP9 correlate with basement membrane

destruction [16]. Shedding of LRP1 on lung fibroblasts was identified to permit the increased accumulation of MMP2 and MMP9 [16].
Wound healing ends when the myofibroblast population strongly decreases due to apoptosis of these cells [24]. Here it becomes evident, that tight control of myofibroblast acquisition is crucial for sufficient wound healing and that maladaptive tissue repair might lead to aberrant tissue remodeling such as scarring.

## 1.2 Transforming growth factor-β

The TGF-β family encompasses the three TGF-β isoforms TGF-β1, TGF-β2 and TGF-β3 as well as activins and bone morphogenic proteins in mammals [45]. TGF-β regulates cell proliferation, differentiation, ECM synthesis, apoptosis, immune responses and wound repair [46–51]. Furthermore, TGF-β is involved in embryonic development [52]. After secretion, TGF-β is stored in an inactive latent form in the ECM [53]. Latent TGF-β associates with latency associated peptide (LAP) and latent TGF-β-binding protein (LTBP) [53]. Activation of TGF-β requires removal of LAP and LTBP, a task that can be performed mechanically, e.g. by integrins [53] or enzymatically, e.g. by MMPs [54]. Active TGF-β initiates intracellular signaling through the serine/threonine kinase receptors, TGF-β receptor type I (TGFBRI) and TGF-β receptor type II (TGFBRII) [45]. Binding of TGF-β to TGFBRII results in heterodimerization of both receptors and phosphorylation of TGFBRI by the constitutive active kinase of TGFBRII [45]. Thereafter, activated TGFBRI phosphorylates the canonical signaling mediators of the TGF-β signaling pathway, the receptor-activated SMAD (R-SMAD, mothers against decapentaplegic homolog) proteins, namely SMAD2 and SMAD3, which are recruited to TGFBRI by the adaptor proteins [45]. The C-termini of SMAD2 and SMAD3 contain a conserved SS(M/V)S amino acid motif in which two serine residues are phosphorylated by TGFBRI [45]. Following activation, SMAD2 and SMAD3 form a heterocomplex with a co-SMAD, SMAD4, and are subsequently translocated to the nucleus where they serve as transcription factors [45]. The protein interactions between SMAD2, SMAD3 and SMAD4 are mediated by their C-terminal MH2-domain [45]. In the nucleus, SMAD3 and SMAD4 can directly bind *via* their N-terminal MH1-domain to DNA [55]. Furthermore, R-SMADs can interact with DNA *via* DNA-binding proteins, such as Runx, E2F4, E2F5 and ATF3 [45]. Both MH-domains of SMADs are connected by a linker region [45]. This region contains numerous phosphorylation sites [45]. Phosphorylation of the linker region was shown to mod-

ulate the transcriptional activity of SMAD2 and SMAD3 [45]. Upon binding to its receptor, TGF-β can also mediate activation of non-canonical signaling-mediators (including members of the mitogen-activated protein kinase (MAPK) pathway, Rho-like GTPases and the PI3K/Akt pathway) which are known to phosphorylate the linker region of R-SMADs [56,57]. For instance, phosphorylation of the SMAD3 linker region by p38 MAPK promotes the plasminogen activator inhibitor-1 (PAI-1) and the α2(I)-procollagen gene expression in rat myofibroblasts [58,59]. Interestingly, the p38-mediated phosphorylation of the linker region of SMAD3 is enhanced in myofibroblasts in a rat model of chronic liver injury [58]. The kinases Rho-associated protein kinase (ROCK) and JNK also promote the activity of SMAD3 by phosphorylating the linker region of this transcription factor [60–62]. Here it becomes evident that the interplay between the non-canonical and the canonical TGF-β signaling pathway allows TGF-β to exert a plethora of effects under different biological conditions. The canonical and non-canonical TGF-β signaling pathway is illustrated in figure 2.

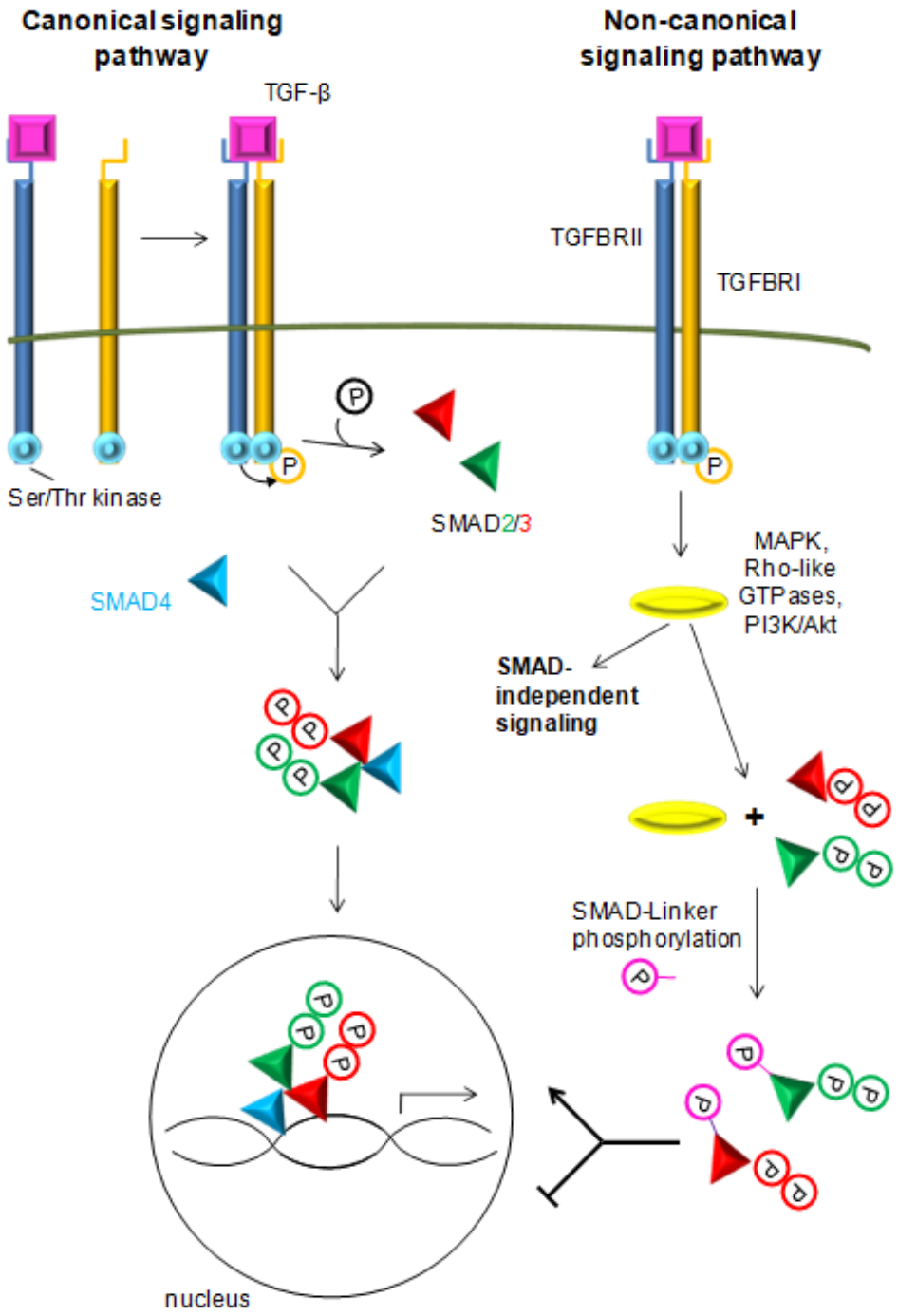


**Fig. 2: Canonical and non-canonical TGF-β signaling pathway.** In the canonical TGF-β signaling, TGF-β induces heterodimerization of TGF-β receptor II and TGF-β receptor I. Thereafter, TGFBRII phosphorylates TGFBRI which subsequently activates SMAD2 and SMAD3. In complex with SMAD4, these SMADs translocate to the nucleus where they regulate gene transcription. In the non-canonical TGF-β signaling, TGF-β induces the activation of members of the MAPK and the PI3K/Akt pathway as well as of Rho-like GTPases. These kinases mediate SMAD-independent signaling. In addition, these kinases can phosphorylate SMAD2 or SMAD3 in the linker domain. As a consequence, the transcriptional activity of SMAD2 or SMAD3 is promoted or inhibited. TGF-β: transforming growth factor-β; TGFBRII: transforming growth factor-β receptor type II; TGFBRI: transforming growth factor-β receptor type I; SMAD: mothers against decapentaplegic homolog; Ser: serine; Thr: thronine; MAPK: mitogen-

activated protein kinase; GTP: guanosine triphosphate; PI3K: phosphatidylinositol 3-kinase; Akt: protein kinase B.

## 1.3 Source of myofibroblasts in the lung

In the lung, different cell types are considered to serve as progenitors for myofibroblasts. Amongst them are resident fibroblasts, such as the perivascular and peribronchiolar adventitial fibroblasts [63]. Furthermore, pulmonary epithelial cells contribute to the myofibroblast population by undergoing epithelial-mesenchymal transition (EMT). For instance, murine primary alveolar epithelial cells undergo EMT when cultivated on fibronectin or fibrin matrices, which mimic the provisional matrix which is formed after injury [64]. In this study, it was also observed that activation of latent TGF-β1 by integrins promotes EMT [64]. The EMT-inducing function of TGF-β1 was furthermore demonstrated *in vivo*. To this end, β-galactosidase expressing alveolar epithelial cells were tested for the presence of the mesenchymal marker in TGF-β1-overexpressing mice [64]. The majority of mesenchymal cells, as assessed by vimentin expression, was positive for β-galactosidase, suggesting their epithelial origin [64]. Also in the rat, exogenous TGF-β1 promotes the expression of mesenchymal cell markers in primary alveolar epithelial cells and in the epithelial cell line RLE-6TN [65]. Nevertheless, investigations of EMT in bleomycin-induced experimental animal models of pulmonary fibrosis obtained controversial findings. Although bleomycin triggered EMT in pleural mesothelial cells *via* the canonical TGF-β pathway in mice [66], other authors did not observe EMT in mouse and rat models of bleomycin-induced lung fibrosis [67]. However, in the human system, cells expressing both epithelial markers and the myofibroblast marker α-SMA were found in lung tissue of patients with IPF, a disease characterized by the TGF-β1 overactivation [65].

Circulating fibrocytes were demonstrated to be attracted to injured lung tissue and to provide a source of fibroblasts and myofibroblasts in these depleted areas [68,69]. For instance, human fibrocytes, which were injected into the tail-vein of bleomycin-treated mice were found to migrate into the fibrotic lung [69]. These fibrocytes expressed CD45, collagen I and the chemokine CXCL12 receptor CXCR4 [69]. *In vitro* experiments showed that migration of the fibrocytes is induced by CXCL12 [69]. Moreover, it was demonstrated that allergen exposure induces the accumulation of CD34-positive fibrocytes in the bronchial mucosa of patients with allergic asthma

[70]. The fibrocytes were mainly enriched in subepithelial areas characterized by collagen I deposition [70]. Interestingly, most of these CD34-positive fibrocytes expressed procollagen I mRNA [70]. Besides this cell population, the bronchial mucosa of allergic asthma patients also contained cells that were positive for CD34, α-SMA and expressed procollagen I mRNA after allergen exposure [70]. In a mouse model of allergic asthma, repeated antigen exposure resulted in the expansion of CD34 and procollagen I positive cells in the bronchial wall [70]. In the later time course of repeated allergen exposure, CD34 and procollagen I positive cells were localized in collagen-rich subepithelial regions [70]. Furthermore, the population of CD34, procollagen I and α-SMA positive cells expanded [70]. On the contrary, only a small number of blood fibrocytes was positive for α-SMA [70]. Stimulation of human circulating fibrocytes with TGF-β1 enhanced the expression of fibronectin, collagen III and α-SMA *in vitro* [70]. Nevertheless, another study showed that green fluorescent protein (GFP) expressing bone marrow cells that were transplanted into the bone marrow of bleomycin-receiving mice migrate to the fibrotic lung and expressed collagen I but do not differentiate into α-SMA-expressing myofibroblasts [71]. Here, the heterogeneity of fibroblast-like cells which are involved in lung injury and remodeling becomes evident. Additional research effort in this field is required.

## 1.4 Mechanisms of fibroblast to myofibroblast transdifferentiation

The increase in ECM stiffness and cytokine concentration during wound healing works in concert to induce the differentiation of fibroblasts to myofibroblasts. The underlying mechanisms are described in the following.

## 1.5 Promotion of fibroblast to myofibroblast transdifferentiation by TGF-β1

The role of TGF-β1 in fibroblast to myofibroblast transdifferentiation is summarized in figure 3.

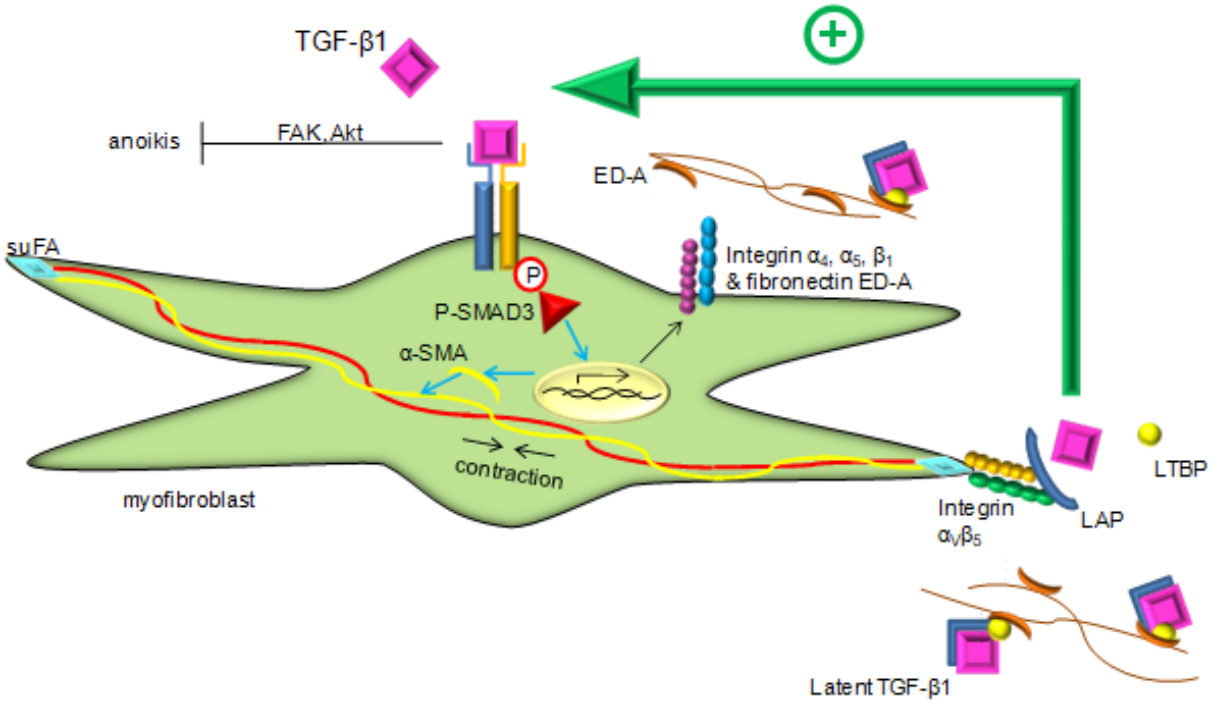


**Fig. 3: Mechanism of TGF-β1-induced fibroblast to myofibroblast transdifferentiation.** TGF-β1 mediates α-SMA expression *via* SMAD3 in fibroblasts. The incorporation of α-SMA into stress fibers enhances the contractile activity of fibroblasts and thus allows the development of suFa. The latter are required for the transmission of the high contractile forces of myofibroblasts to the environment. Integrins ($\alpha_V\beta_5$) within the suFA bind to LAP and transmit the contractile force to latent TGF-β1 complexes which are deposited in ECM. As a consequence, these complexes which consists of TGF-β1, LAP and LTBP disassemble and active TGF-β1 is liberated. Subsequently, TGF-β1 promotes fibroblast to myofibroblast transdifferentiation in a feed forward loop. TGF-β1 furthermore induces the expression of the fibronectin ligands integrin $\alpha_4$, $\alpha_5$ and $\beta_1$ as well as of ED-A fibronectin. Moreover, TGF-β1 protects myofibroblasts from anoikis by activating FAK and Akt. TGF-β1: transforming growth factor-β1; FAK: focal adhesion kinase; Akt: protein kinase B; SMAD: mothers against decapentaplegic homolog; α-SMA: α-smooth muscle actin; suFA: supermature focal adhesion; LTBP: latent TGF-β-binding protein; LAP: latency associated peptide.

### 1.5.1 Induction of α-SMA expression by TGF-β1

TGF-β1 is the key inducer of α-SMA expression during fibroblast to myofibroblast transdifferentiation [72]. *In vitro* experiments demonstrated that TGF-β1-induced α-SMA expression is mediated by the canonical signaling mediator SMAD3 [73]. Interestingly, TGF-β1 also induced the formation of actin stress fibers which are essential for the development of supermature focal adhesions during fibroblast to myofibroblast transdifferentiation [73,74]. The promoting effect of TGF-β1 on focal adhesion maturation is crucial for the TGF-β1-mediated α-SMA expression [73,75]. TGF-β1 induced the expression of fibronectin and the fibronectin receptors integrin $\alpha_4$, $\alpha_5$, and $\beta_1$

which stabilized integrin-mediated cell-matrix connections and provided a feed forward loop of TGF-β1-induced differentiation of fibroblasts to myofibroblasts [76].

### 1.5.2 The antiapoptotic effect of TGF-β1 on myofibroblasts

Besides mediating fibroblast to myofibroblast transdifferentiation TGF-β1 enhances survival of myofibroblasts by reducing their susceptibility to cell death. In detail, TGF-β1 mediates the combinatorial activation of the focal adhesion kinase (FAK) and protein kinase B (Akt) pathways which protect myofibroblasts from anchorage-dependent apoptosis [77]. This form of apoptosis is referred to as anoikis [78]. Furthermore, TGF-β1 suppresses IL-1β-induced apoptosis of myofibroblasts [79].

### 1.5.3 The impact of TGF-β1 on the contractile activity of myofibroblasts

As an inducer of α-SMA expression in fibroblasts, TGF-β1 contributes to the α-SMA-mediated increase of the contractile activity of myofibroblasts [31]. Treatment of myofibroblasts isolated from fibrotic rat lungs with a blocking anti-TGF-β antibody reduced myofibroblast-induced contraction of the collagen gels [80]. The generation of contractile forces by stress fibers in myofibroblasts as well as transmission of mechanical forces to ECM depend on the number of focal adhesions [81]. Thus, the aforementioned upregulation of fibronectin and integrin receptors by TGF-β1 contributes to both processes.

### 1.5.4 Induction of ED-A fibronectin expression by TGF-β1

Fibroblasts present in granulation tissue express ED-A fibronectin [82]. This splice variant of fibronectin includes the type III segment ED-A [83]. Moreover, it was demonstrated that TGF-β1 induces the expression of the ED-A isoform of fibronectin in skin fibroblasts *in vitro* [84,85]. An accumulating evidence suggests that ED-A fibronectin is essential for the generation of myofibroblasts in the lungs of bleomycin-treated mice as α-SMA-positive myofibroblasts were not detectable in lungs of ED-$A^{-/-}$ animals [86]. Furthermore, these mice did not exhibit elevated collagen deposition and did not develop fibrosis [86]. The importance of ED-A fibronectin for myofibroblast generation is further supported by *in vitro* data which demonstrated that cultivation of fibroblasts from ED-$A^{-/-}$ mice on ED-A fibronectin restores TGF-β1-mediated expression of α-SMA and collagen in these cells [86]. In granulation tissue, observed

in a mouse model of skin injury, fibronectin is accumulated before collagen appears [87]. Hence, expression of ED-A fibronectin might be a prerequisite for the development of collagen-producing myofibroblasts. The ED-A isoform of fibronectin is also involved in pulmonary fibrosis in humans. For instance, fibroblasts isolated from the lungs of IPF patients expressed elevated levels of ED-A fibronectin and α-SMA as compared to those isolated from control patients [86]. Furthermore, ED-A fibronectin and α-SMA were detected in fibrotic foci in IPF lungs [88]. Interestingly, ED-A fibronectin colocalized with latent TGF-β1 in the ECM produced by primary rat lung myofibroblasts *in vitro* [89]. It remains to be investigated whether ED-A fibronectin facilitates the storage of latent TGF-β1 in ECM.

### 1.5.5 Regulation of TGF-β1 expression in wound healing

There is a large body of evidence that highlights granulocyte-macrophage colony-stimulating factor (GM-CSF) as a key inducer of TGF-β1 expression in wound healing. As such, GM-CSF is an indirect activator of myofibroblasts. Adenoviral overexpression of GM-CSF in the alveolus resulted in elevated TGF-β1 levels in bronchoalveolar lavage fluid (BALF) in rats [90]. In addition, the expansion of the macrophage population in the lung was observed [90]. Macrophages which were isolated from BALF of GM-CSF overexpressing mice showed higher TGF-β1 secretion than macrophages isolated from control animals [90]. Moreover, the GM-CSF levels positively correlated with the TGF-β1 expression in alveolar macrophages [91]. Furthermore, the increase of TGF-β1 in GM-CSP positive lungs was followed by the appearance of α-SMA expressing myofibroblasts [90].

### 1.5.6 TGF-β1-activation by myofibroblasts

The permanently increasing matrix stiffness and elevated levels of active TGF-β1 in fibrotic tissue support persistent myofibroblast generation and activity. In addition, myofibroblasts promote their own maturation in two manners. First, they secrete ECM components [32] and thus enhance matrix stiffness and second they activate latent TGF-β1 which is deposited in ECM [89]. TGF-β1 which was activated by myofibroblasts induces fibroblast to myofibroblast transdifferentiation in a feed forward loop [89]. Mechanistically, the activation of latent TGF-β1 by myofibroblasts requires the interaction of integrins which are expressed on myofibroblast surface with LAP, a

component of the latent TGF-β1 complex [89]. The integrins transmit the high contractile force which is generated by α-SMA-containing stress fibers within the myofibroblast to the latent TGF-β1 complex [89]. Consequently, conformational changes are induced in the latent TGF-β1 and the active TGF-β1 is released in a protease-independent manner [89]. There is evidence that $\alpha_V\beta_5$ integrin mediates activation of latent TGF-β1 by myofibroblasts. For instance, $\alpha_V\beta_5$ integrin is mainly responsible for the generation of active TGF-β1 in primary rat lung myofibroblast [89]. In the human system it was demonstrated that $\alpha_V\beta_5$ integrin is present in fibroblastic foci in the lungs of IPF patients [92]. Functionally, myofibroblasts localized in fibroblastic foci of IPF lungs show enhanced contractile activity [93,94].

## 1.6 Induction of fibroblast to myofibroblast transdifferentiation by ECM

### 1.6.1 Development of supermature focal adhesions

In intact connective tissue, fibroblasts are protected from mechanical stress by ECM [95]. Fibroblasts exhibit a low number of matrix-cell connections and do not form stress fibers [95]. The destruction of ECM followed by the infiltration of thrombocytes and immune cells which express a number of cytokines, including TGF-β1, supports the formation of immature focal adhesions (FA) in fibroblasts [95]. These immature FA not only ensure matrix-cell contact but they also facilitate the migration of fibroblasts into the wound [95]. The increase in the matrix rigidity during wound healing promotes the assembly of mature FA and stress fibers in fibroblasts [95]. The stress fibers are built from cytoplasmic actins and myosin II, however they do not contain α-SMA [95,96]. Mature FA and actin stress fibers define proto-myofibroblasts, which represent an intermediate form in the process of fibroblast to myofibroblast transdifferentiation [97]. Stress fibers are anchored to mature FA. The latter are integrin-containing cell membrane complexes that connect cytosolic stress fibers with ECM [95]. In this function, mature FA transmit intracellular contractile forces to the ECM and sense ECM properties such as rigidity [95].

A further increase in matrix stiffness and TGF-β1 expression promotes fibroblast to myofibroblast transdifferentiation by inducing the formation of supermature FA (suFA) from mature FA [95]. As suFA are longer (8 to 30 µm) than mature FA (2 to 6 µm), they can transmit a fourfold higher external tension, such as stretch, to fibroblasts [75]. The transmission of high tension is essential for the incorporation of α-SMA into

suFa-anchored cytoplasmic actin stress fibers [75]. The high contractile activity which is generated by α-SMA-containing stress fibers, on the other hand, is crucial for the maintenance of suFA [74].

### 1.6.2 Formation of osteoblast (OB)-cadherin-type adhesive junctions in myofibroblasts

The increasing stiffness of ECM during wound healing also promotes the formation of cadherin-type adhesion junctions. These adhesion junctions are connected to stress fibers. At the beginning of fibroblast to myofibroblast transdifferentiation neural (N)-cadherin expression increases but at a later stage it decreases and gets replaced by OB-cadherin [98]. Hence, OB-cadherin adhesion junctions are characteristics for the myofibroblast phenotype [98]. The OB-cadherin adhesion junction is resistant to around twofold higher forces than N-cadherin adhesion junctions [99]. Consequently, OB-cadherin-type adhesion junctions permit enhanced intercellular adhesion which adapts myofibroblasts to the high mechanical stress which occurs during wound healing [99].

### 1.6.3 α-SMA-mediated stress fiber contraction

The incorporation of α-SMA into stress fibers allows an increase in myofibroblast contractile activity. For instance, *in vitro* experiments demonstrated that α-SMA-positive lung fibroblasts show remarkable higher contractile activity as compared to α-SMA negative cells [31]. In addition, selective removal of α-SMA from actin stress fibers by delivery of a fusion peptide containing the N-terminal sequence AcEEED of α-SMA resulted in decreased contraction of myofibroblasts [100].

Stress fibers isolated from human fibroblasts were used to investigate the mechanisms of non-muscle cell contraction *in vitro* [101]. In the presence of $Ca^{2+}$ myosin light chain kinase (MLCK) phosphorylates the myosin regulatory light chain (MLC) and thus mediates stress fiber contraction [101]. In addition, it was demonstrated that MLC may also be phosphorylated by Rho-kinase in a $Ca^{2+}$-independent manner [101]. The shortening of stress fibers during MLCK-induced stress fiber contraction occurs faster and to a larger extent than during Rho-kinase-mediated stress fiber contraction [101]. Due to the slower Rho-kinase-mediated phosphorylation of MLC,

Rho-dependent stress fiber shortening occurs over a longer time range than MLCK-mediated stress fiber contraction. These findings suggest that $Ca^{2+}$ induces rapid contraction, whereas Rho-kinase mediates sustained contraction [101]. As myofibroblasts generate continuous contraction [102], the Rho-kinase-dependent mechanism of stress fiber contraction appears to be of higher importance than the rapid $Ca^{2+}$-dependent response [102]. This hypothesis is supported by the findings which are presented hereafter. These findings also highlight the importance of a second system by which Rho-kinase regulates myofibroblast contraction. To be specific, Rho-kinase inhibits myosin phosphatase which dephosphorylates the MLC [103]. In granulation tissue, it was observed that inhibition of Rho-kinase-mediated inactivation of myosin phosphatase abrogated contraction of myofibroblasts [104]. Furthermore, pharmacological blockage of Rho-kinase and MLCK inhibited lysophosphatidic acid (LPA)-promoted myofibroblast contraction, respectively [105]. On the other hand, blockage of myosin phosphatase induced myofibroblast contraction even in the absence of LPA and also restored contraction after Rho-kinase inhibition [105]. In contrast, increase of intracellular calcium did not promote myofibroblast contraction [105]. Hence, the $Ca^{2+}$-independent Rho-kinase-mediated myofibroblast contraction may be necessary for myofibroblast contraction whereas the $Ca^{2+}$-dependent mechanism may be rather supporting but not sufficient to induce myofibroblast contraction [105].

### 1.6.4 Mechanical force-induced α-SMA gene expression

Mechanical forces that affect fibroblasts activate signaling pathways which mediate gene transcription. Hence, application of mechanical forces to fibroblasts results in phosphorylation of p38, which subsequently induces α-SMA gene expression in Rat-2 cells [106]. Interestingly, mechanical force-induced upregulation of α-SMA expression also requires binding of p38 to stress fiber-associated α-SMA in these cells [106]. Thus, α-SMA promotes its own expression in a feed forward loop. The mechanistic details however remain to be investigated. Intriguingly, in cardiac fibroblasts force-induced α-SMA expression requires intact actin filaments and activation of ERK [107]. The kinase p38, however, was demonstrated to mediate force-induced inhibition of α-SMA expression in this study [107]. Other authors propose that upon force-application FAK gets activated and regulates actin assembly *via* gelsolin and Type-I phosphatidylinositol 4-phosphate 5 kinase-gamma in NIH3T3 cells [108]. Subse-

quently, the actin-filament-regulated transcription co-activator MRTF-A promotes α-SMA expression in NIH3T3 cells [108].

# 2 Aim of the study

Several studies demonstrated that LRP1 is a modulator of the TGF-β1 signaling pathway. Transforming growth factor-β1 is a well established key inducer of fibroblast to myofibroblast transdifferentiation, a process which occurs during wound healing. The link between LRP1, TGFβ1 signaling and the acquisition of the myofibroblast phenotype becomes evident in kidney fibroblasts, in which CTGF-induced phosphorylation of LRP1 results in an increase of the TGF-β1-induced expression of the myofibroblast marker α-SMA. The mechanisms by which LRP1 regulates the differentiation of fibroblasts to myofibroblasts are cell-type specific and remain elusive in the lung.

In this context, the aim of the study was threefold:

1. to investigate whether LRP1 regulates the expression of α-SMA in lung fibroblasts
2. to elucidate the signaling pathway by which LRP1 regulates α-SMA expression
3. to decipher whether LRP1 influences myofibroblast functions, such as contraction, proliferation and migration

# 3 Material and methods

## 3.1 Materials

### 3.1.1 Equipment

| Name | Company |
|---|---|
| accuri C6 Flow Cytometer | BD Biosciences, Heidelberg, Germany |
| Cell culture incubator | Heraeus, Hanau, Germany |
| ChemiDoc™ Touch Imaging System | Bio-Rad Laboratories, Wiesbaden, Germany |
| Culture insert 2 well | ibidi, Planegg, Germany |
| Electrophoresis chambers | Bio-Rad, Wiesbaden, Germany |
| Falcon tubes | Greiner Bio-One, Frickenhausen, Germany |
| Filter tips: 10; 100; 1000 µl | Eppendorf, Wesseling, Germany |
| Gel blotting paper | GE Healthcare, München, Germany |
| LA-EA1 objective adapter | Sony, Berlin, Germany |
| Leica DM IL LED microscope | Leica, Wetzlar, Germany |
| Nex-3 camera | Sony, Berlin, Germany |
| Petri dishes | Greiner Bio-One, Frickenhausen, Germany |
| Pipetboy | Eppendorf, Wesseling, Germany |
| Pipets | Eppendorf, Wesseling, Germany |
| Power supply | Bio-Rad, Wiesbaden, Germany |
| StepOnePlus Real-Time PCR Machine | Applied Biosystems, Darmstadt, Germany |
| Spectra MAX190 microplate reader | Molecular Devices, Biberach an der Riß, Germany |
| TGradient Thermocycler | Biometra, Göttingen, Germany |
| Tissue culture dishes | Greiner Bio-One, Frickenhausen, Germany |
| TriStar$^2$ S LB 942 Multimode Reader | Berthold Technologies, Bad Wildbad, Germany |
| Water bath for cell culture | Medingen, Arnsdorf, Germany |

| | |
|---|---|
| Western blot chambers | Bio-Rad, Wiesbaden, Germany |
| Vortex machine | Scientific Industries, New York, USA |

### 3.1.2 Reagents

| **Product name** | **Company** |
|---|---|
| Adenosine triphosphate (ATP) | Roth, Karlsruhe, Germany |
| bovine serum albumin (BSA) | Roth, Karlsruhe, Germany |
| Coelenterazine | Cayman Chemical, Biomol, Hamburg, Germany |
| Coenzyme A trilithium salt | Sigma Aldrich, München, Germany |
| Corning® Collagen I, Rat Tail | Corning, Wiesbaden, Germany |
| cOmplete™, EDTA-free Protease Inhibitor Cocktail | Roche, Karlsruhe, Germany |
| Deoxynucleotide (dNTP) Mix | Thermo Scientific, Schwerte, Germany |
| Dithiothreitol | Sigma Aldrich, München, Germany |
| D-luciferin potassium salt | Cayman Chemical, Biomol, Hamburg, Germany |
| DNA ladder (100 bp, 1 kb) | Thermo Fisher Scientific, Darmstadt, Germany |
| Dulbecco's Modified Eagle Medium (DMEM) | Gibco, Darmstadt, Germany |
| DMEM: NutrientMixture F-12 | Gibco, Darmstadt, Germany |
| Ethanol | Roth, Karlsruhe, Germany |
| Ethidium bromide | Sigma Aldrich, München, Germany |
| Ethylenediaminetetraacetic acid (EDTA) | Roth, Karlsruhe, Germany |
| Ethylene glycol tetraacetic acid (EGTA) | Roth, Karlsruhe, Germany |
| Fetal calf serum (FCS) | Gibco, Darmstadt, Germany |
| Glycerol | Roth, Karlsruhe, Germany |
| Glycylglycine | Roth, Karlsruhe, Germany |
| 4-(2-Hydroxyethyl)-piperazine-1-ethanesulfonic acid (HEPES) | Roth, Karlsruhe, Germany |
| Lipofectamine™ 2000 transfection reagent | Invitrogen, Darmstadt, Germany |

| | |
|---|---|
| Lipofectamine™ 3000 transfection reagent | Invitrogen, Darmstadt, Germany |
| Magnesium sulfate | Roth, Karlsruhe, Germany |
| Methanol | Roth, Karlsruhe, Germany |
| Milk powder (fat reduced) | Roth, Karlsruhe, Germany |
| MultiScribe Reverse transcriptase | Applied Biosystems, Darmstadt, Germany |
| NP-40 | Roth, Karlsruhe, Germany |
| Opti-Minimal Essential Medium I (Opti-MEM™ I) reduced-serum medium | Gibco, Darmstadt, Germany |
| 5x passive lysis buffer | Promega, Mannheim, Germany |
| Penicillin/streptomycin | Gibco, Darmstadt, Germany |
| Phenylmethylsulfonyl fluoride (PMSF) | Roth, Karlsruhe, Germany |
| Platinum® SYBR® Green | Invitrogen, Darmstadt, Germany |
| Potassium chloride | Roth, Karlsruhe, Germany |
| Potassium dihydrogen phosphate | Roth, Karlsruhe, Germany |
| Propidium iodide | Roth, Karlsruhe, Germany |
| 10x reverse transcriptase (RT) buffer | Applied Biosystems, Darmstadt, Germany |
| RiboLock RNase Inhibitor | Thermo Scientific, Schwerte, Germany |
| RNase A | Thermo Scientific, Schwerte, Germany |
| 10x RT Random Primers | Applied Biosystems, Darmstadt, Germany |
| siLentFect™ Lipid transfection reagent | Bio-Rad Laboratories, Wiesbaden, Germany |
| Sodium azide | Roth, Karlsruhe, Germany |
| Sodium chloride | Roth, Karlsruhe, Germany |
| Sodium deoxycholate | Sigma Aldrich, München, Germany |
| Sodium dodecyl sulfate (SDS) | Roth, Karlsruhe, Germany |
| Sodium hydroxide (NaOH) | Roth, Karlsruhe, Germany |
| Sodium orthovanadate | Roth, Karlsruhe, Germany |
| Tris(hydroxymethyl)aminomethane (TRIS) | Roth, Karlsruhe, Germany |
| Triton-X-100 | Roth, Karlsruhe, Germany |

| | |
|---|---|
| Trypsin | Gibco, Darmstadt, Germany |
| Tween 20 | Roth, Karlsruhe, Germany |

## 3.2 Methods

### 3.2.1 Cell culture

Mouse embryonic fibroblasts (MEF) were cultured in Dulbecco's Modified Eagle Medium (DMEM) (Gibco, Darmstadt, Germany) supplemented with 10% heat-inactivated fetal calf serum (FCS) and 1% penicillin/streptomycin (both from Gibco). Human fibroblasts were derived from the lung parenchyma of patients with IPF or donors. They were maintained in DMEM: NutrientMixture F-12 (Gibco) supplemented with 10% heat-inactivated FCS and 1% penicillin/streptomycin and applied in experiments between the $2^{nd}$ – $6^{th}$ passage. Cell culture was performed at 37 °C in humidified air with 5% $CO_2$.

### 3.2.2 Cell treatment

Mouse embryonic fibroblasts ($2x10^5$ cells/well) were maintained in culture medium with 10% FCS on a 12-well plate for 24 h and then treated with 10 ng/ml TGF-β1 (R&D Systems, Wiesbaden, Germany) for 0, 0.5, 1, 4, 8, 10 or 14 h in serum-free medium or with 50 µM of the JNK1/2/3 inhibitor SP600125 or 20 µM of MAPK/ERK kinase 1/2 (MEK1/2) inhibitor PD98059 (both from Millipore, Darmstadt, Germany) in serum-free medium for 24 h.

Seventy-two hours after the transfection with siRNA directed against LRP1 or negative control siRNA, IPF lung fibroblasts were treated with 1 ng/ml TGF-β1 and/or 50 µM JNK 1/2/3 inhibitor SP600125 (Millipore, Darmstadt, Germany), 20 µM MEK1/2 inhibitor PD98059 (Merck, Darmstadt, Germany) and 10 µM p38 inhibitor SB203580 (InvivoGen, Toulouse, France) for 24 h. Aforementioned reagents were added directly to the culture medium containing the transfection solution. For time-dependent TGF-β1 stimulation (0, 8, 10, 12, 16 h), the culture medium with transfection solution was aspirated and 1 ng/ml TGF-β1 was administered in serum-free medium.

### 3.2.3 Protein isolation

Mouse embryonic fibroblasts and IPF lung fibroblasts were lysed in radioimmunoprecipitation assay buffer (RIPA). In this mixture of 50 mM Tris-HCl (pH 7.4), 150 mM NaCl, 1 mM ethylenediaminetetraacetic acid (EDTA), 1% Triton-X-100, 1% sodium deoxycholate, 0.1% sodium dodecyl sulfate (SDS), supplemented with 1 mM phenylmethylsulfonyl fluoride (PMSF), 1 mM sodium orthovanadate and an EDTA-free Protease Inhibitor Cocktail (Roche, Mannheim, Germany) the cells were incubated on ice for 30 min. The samples were vortexed every 5 min. Subsequently, the lysates were centrifuged at 9,300 g for 10 min at 4 °C. The supernatants were transferred to a fresh tube. The protein concentration was measured using the Pierce™ BCA Protein Assay Kit (Thermo Scientific™, Schwerte, Germany) according to the manufacturer's instruction. Briefly, 20 µl of the diluted protein lysate (dilution 1:5; diluent phosphate-buffered saline (PBS)) and of the bovine serum albumin (BSA) standard were plated in duplicates into a microtiter plate. Furthermore, BCA Reagent A and BCA Reagent B were mixed in a ratio 50:1 and 40 µl of this mixture was added to each test sample and to the BSA standard. The microtiter plate was incubated at 37 °C for 30 min. Ultimately, the absorbance was measured at 562 nm in a Spectra MAX190 microplate reader (Molecular Devices, Biberach an der Riß, Germany).

### 3.2.4 Western blotting

Ten or 20 µg cell lysates were subjected to SDS-polyacrylamide-gel electrophorese (PAGE) under reducing conditions, using β-mercaptoethanol as a reducing agent. Afterwards, the proteins were electrotransferred to a polyvinylidene fluoride (PVDF) membrane. Nitrocellulose membranes were used exclusively for the adhesion of phosphorylated proteins. Blocking of both types of membranes was performed with 5% non-fat milk (Roth, Karlsruhe, Germany) in Tris-buffered saline with Tween20 buffer (TBS-T; 5 mM Tris-Cl, 150 mM NaCl, 0.1% Tween 20 (pH 7.5)) for 1 h at room temperature. Membranes were incubated with the following primary antibodies: mouse anti-α-SMA (1:5,000; Chemicon international, Temecula, CA; catalog number: CBL171), rabbit anti-LRP1 (1:1,000; Abcam, Cambridge, UK; catalog number: ab92544), rabbit anti-SAPK/JNK (1:1,000; Cell Signaling Technology, Frankfurt am Main, Germany; catalog number: 9252), rabbit anti-phospho-JNK (T183/Y185) (1:500; R&D Systems; catalog number: AF1205), rabbit anti-c-Jun (1:1,000; Cell Sig-

naling Technology; catalog number: 9165), mouse anti-SMAD2/3 (1:1,000; BD Transduction Laboratories, Heidelberg, Germany; catalog number 610843), rabbit anti-phospho-SMAD2 (Ser465/467) (1:500; Cell Signaling Technology; catalog number: 3108), rabbit anti-phospho-SMAD2 (Ser245/250/255) (1:500; Cell Signaling Technology; catalog number: 3104), rabbit anti-phospho-SMAD3 (Ser423/425) (C25A9) (1:500; Cell Signaling Technology; catalog number: 9520), rabbit anti-p44/42 (ERK1/2) (1:1,000; Cell Signaling Technology; catalog number: 4695), mouse anti-phospho-p44/42 (1:1,000; Cell Signaling Technology; catalog number: 9106), rabbit anti-p38 (1:1,000; Cell Signaling Technology; catalog number: 9212), rabbit phospho-p38 (Thr180/Tyr182) (1:1,000; Cell Signaling Technology; catalog number: 4511). Thereafter, the membrane was probed with a peroxidase-labeled secondary antibody (1:5,000; all from Dako, Glostrup, Denmark; catalog number: P044701-2 (mouse) and P021702-02 (rabbit)). Amersham™ ECL Select™ Western Blotting Detection Reagent (GE Healthcare, München, Deutschland) was employed to induce the peroxidase reaction. The detection of proteins was performed with a ChemiDoc™ Touch Imaging System (Bio-Rad Laboratories, Wiesbaden, Germany). The membranes were stripped and reprobed with a mouse anti-β-actin antibody (1:10,000; Sigma Aldrich, München, Germany; catalog number: A1978) to determine the amount of proteins on the membrane.

### 3.2.5 RNA isolation and reverse transcriptase reaction

Isolation of RNA from MEF and IPF lung fibroblasts was executed with a peqGOLD Total RNA Kit (Peqlab, Erlangen, Germany) according to the manufacturer's instruction. One ng of RNA served as template in a cDNA synthesis reaction which also contained 2 µl 10x reverse transcriptase (RT) buffer (Applied Biosystems, Darmstadt, Germany), 0.8 µl deoxynucleotide (dNTP) Mix (25 mM; Thermo Scientific), 2 µl 10x RT Random Primers (25 µM; Applied Biosystems), 1 µl MultiScribe Reverse transcriptase (200 U/µl; Applied Biosystems), 1 µl of RiboLock RNase Inhibitor (40 U/µl; Thermo Scientific) and 3.2 µl nuclease-free water. The samples were initially incubated at 25 °C for 10 min, then at 37 °C for 2 h and finally heated at 85 °C for 5 min in a Tgradient Thermocycler (Biometra, Göttingen, Germany).

### 3.2.6 Real-time PCR

Real-time PCR (qPCR) was performed using a StepOnePlus Real-Time PCR Machine (Applied Biosystems) using the cycling conditions 95 °C for 6 min, followed by 45 cycles of 95 °C for 20 s, 55 °C for 30 s and 73 °C for 30 s. The qPCR reaction reagent contained 1 µl forward primer (400 nM), 1 µl reverse primer (400 nM), 12.5 µl Platinum® SYBR® Green (Invitrogen), 1 µl cDNA and 9.5 µl nuclease-free water. The primers which were employed in qPCR to amplify target gene transcripts are listed in table 1. Porphobilinogen deaminase (PBGD) served as a reference gene. Changes in the target gene expression are presented as $\Delta C_t$ calculated with the equation $\Delta C_t=(C_{tReference\ gene}- C_{tTarget\ gene})$. The efficiency of the qPCR reaction was assessed by dynamic range qPCR. To this end, qPCR was performed with four serial cDNA concentrations (undiluted, diluted 1:10, 1:100 and 1:1,000). Plotting of the $C_t$ values over the logarithmic values of the cDNA dilution factor was used to assess qPCR efficiency (slope of the graph of 2.0 = 100% efficiency). The exclusive amplification of the correct qPCR product was analyzed by agarose gel electrophoresis. In addition, a Reverse Transcription-qPCR control (RNA which had not been transcribed to cDNA was used as a template) was included in the qPCR to evaluate whether the amplification may occur from DNA contaminating the sample. Furthermore, a water control (sample does not contain cDNA) was included in the qPCR to assure that contamination of the reaction reagents did not contribute to the amplification signal.

**Table 1. List of primers used for qPCR**

| Gene | Spe-cies | Accession number | Nucleotide sequence (5' → 3') | Amplicon size (nt[1]) |
|---|---|---|---|---|
| *LRP1* | human | NM_002332.2 | F: TCT ACT TTG CCG ACA CCA CC<br>R: TGT CTT TTT GGG CCC ATC GT | 160 |
| *α-SMA* | human | NM_001613.3 | F: TCC CTG AAC ACC ACC CAG TG<br>R: AGC CCA GAG CCA TTG TCA C | 124 |
| *SMAD3* | human | NM_005902.3 | F: CCG ATG TCC CCA GCA CAT AA<br>R: CTG GTT CAG CTC GTA GTA | 96 |
| *PBGD* | human | NM_000190.3 | F: ACC CTA GAA ACC CTG CCA GAG AA<br>R: GCC GGG TGT TGA GGT TTC CCC | 124 |
| *α-SMA* | mouse | NM_007392.3 | F: GAT CAC CAT TGG AAA CGA ACG<br>R:<br>AGC ATA GAG ATC CTT CCT GAT GTC | 125 |
| *SMAD3* | mouse | NM_016769.4 | F: ACG CAG AAC GTG AAC ACC AA<br>R: GCG GCA GTA GAT AAC GTG AGG | 83 |
| *PBGD* | mouse | NM_013551.2 | F: TCC GGA GGC GGG TGT TGA GG<br>R: GCC AGA GAA AAG TGC CGT GGG | 116 |

[1]nt, nucleotide; [2]F, forward; [3]R, reverse

### 3.2.7 Subcellular fractionation

Mouse embryonic fibroblasts ($3x10^6$ cells/plate) were grown in 10 cm plates for 24 h and then washed twice with cold PBS and scraped into 2 ml PBS. Thereafter, a centrifugation at 3000 g for 3 min was performed and the pellet was resuspended in 500 µl cold hypotonic lysis buffer (20 mM 4-(2-Hydroxyethyl)-piperazine-1-ethanesulfonic acid (HEPES) (pH 7.9), 10 mM potassium chloride, 1 mM EDTA, 1 mM EGTA, 0,2% NP-40, 10% glycerol, 2 mM sodium orthovanadate and an EDTA-free Protease Inhibitor Cocktail). An incubation on ice for 10 min followed. The samples were centrifuged at 5,000 g for 5 min. The supernatant represented the cytosolic fraction and was frozen at -20 °C for further analysis. The pellet was resuspended in 100 µl hypertonic lysis buffer (20 mM HEPES (pH 7.9), 10 mM potassium chloride, 420 mM sodium chloride, 1 mM EDTA, 1 mM EGTA, 20% glycerol, 2 mM sodium orthovanadate and an EDTA-free Protease Inhibitor Cocktail) and incubated on ice for 45 min. Subsequently, the samples were centrifuged at 12,000 g for 10 min at 4 °C. The supernatant represented the nuclear fraction. It was stored at -20 °C for further investigation.

### 3.2.8 Inhibition of γ-secretase

Mouse embryonic fibroblasts (10,000 cells/well) were seeded into a 12-well plate. After 24 h, cells were treated with 0, 11.5, 23 and 46 µM of the γ-secretase inhibitor N-[N-(3,5-Difluorophenylacetyl)-L-alanyl]-S-phenylglycine t-butyl ester (DAPT; Sigma Aldrich) in culture medium containing 10% FCS for 72 h. The control cells received the vehicle control dimethyl sulfoxide (DMSO) in the same volume as corresponding to 46 µM DAPT. The analysis of LRP1 shedding was performed by western blotting. For analysis by qPCR, cells received 23 µM DAPT or the same volume of the vehicle control DMSO in culture medium with 10% FCS for 72 h.

### 3.2.9 Gene silencing by siRNA technology

Small interfering RNA (siRNA) directed against human LRP1 (sense sequence: 5‘-CCU GUA ACC UGC AGU GCU UTT-3‘) was designed with GeneAssist Custom siRNA Builder (Thermo Fisher Scientific, Darmstadt, Germany) and purchased from Microsynth (Balgach, Swiss). Commercially available siRNA directed against human

SMAD3 (Santa Cruz Biotechnology, Heidelberg, Germany, catalog number: Sc-38376) or human JNK1 (Invitrogen; catalog number: 10620318/10620319) and negative control siRNA (Invitrogen; catalog number: AM4637) were purchased. IPF lung fibroblasts ($2x10^5$ cells/well) were seeded onto a 12-well plate and cultivated for 24 h. Thereafter, cells were starved in serum-free DMEM: NutrientMixture F-12 for 24 h. Hundred nM siRNA directed against LRP1 or JNK1, 200 nM siRNA directed against SMAD3 or the same amount of negative control siRNA were diluted in 50 µl of Opti-Minimal Essential Medium I (Opti-MEM I) reduced-serum medium (Gibco). For the double knock-down experiments, two different siRNAs (100 nM siRNA directed against LRP1 + 100 nM siRNA directed against SMAD3 or 100 nM siRNA directed against LRP1 + 100 nM siRNA directed against JNK1) were combined in one sample in this step. Furthermore, 2.5 µl siLentFect™ Lipid transfection reagent (Bio-Rad Laboratories) were added to 47.5 µl of Opti-MEM™ I reduced serum medium and incubated for 5 min at room temperature. Afterwards, this sample was mixed with the siRNA-containing sample and subsequently incubated for 20 min at room temperature. Thereafter, 200 µl of Opti-MEM™ I reduced-serum medium were added. Cells were washed once with PBS and maintained in this transfection solution for 6 h. Afterwards, 1 ml of culture medium with 10% FCS was added. Eventually, the cells were further cultivated for 96 h. The efficiency of LRP1, SMAD3 and JNK1 gene silencing was assessed by western blotting and/or qPCR.

### 3.2.10 Membrane-based antibody array for the assessment of protein kinase phosphorylation

A Proteome Profiler Human Phospho-Kinase Array Kit (R&D Systems, catalog number: ARY003B) was used according to the manufacturer's instruction. Lysates of IPF lung fibroblasts which had been transfected with negative control siRNA or siRNA directed against LRP1 and had been either treated or untreated with TGF-β1 were employed.

### 3.2.11 Microarray

IPF or donor lung fibroblasts which had been derived from two different patients, respectively, were transfected with negative control siRNA or siRNA directed against LRP1. The efficacy of the silencing of LRP1 gene expression was assessed by

qPCR. Two hundred ng of the total RNA were purified, amplified and Cy3-labeled using a LIRAK kit (Agilent, Santa Clara, USA) according to the manufacturer's instruction. Thereafter, the Cy3-labeled aRNA was hybridized to 8x60K 60mer oligonucleotide spotted microarray slides (Human Whole Genome V3 agilent design ID 072363, Agilent) overnight and subsequently washed and dried according to the Agilent hybridization protocol. The dried slides were scanned at 2 µm/pixel resolution with a InnoScan is900 (Innopsys, Carbonne, France) and image analysis was undertaken using the Mapix 6.5.0 software (Innopsys). The calculated values for all spots were saved as GenePix results files. Analysis of the stored data was performed using the R software and the limma package (BioConductor). Mean spot signals were background corrected with an offset of 1 using the NormExp procedure on the negative control spots and the logarithms of the background-corrected values were quantile-normalized. These values were averaged for replicate spots per array. From different probes which were specific for the same NCBI gene ID, the probe with the maximum average signal intensity over the samples was chosen for subsequent analyses. Genes were ranked for differential expression with a moderated t-statistic. Pathway analyses were performed with gene set tests on the ranks of the t-values. All was performed by Dr. Jochen Wilhelm in the microarray core facility of the UGMLC in Giessen.

### 3.2.12 Dual-Luciferase Reporter Assay

Mouse embryonic fibroblasts (51,300 cells/well) were seeded onto a 48-well plate and starved in serum-free medium for 1 h on the next day. The transfection of pGL3-Basic-*pCAGA* firefly reporter and pRL-SV40 renilla reporter was performed using Lipofectamine™ 2000 transfection reagent (Life Technologies). To this end, 300 ng pGL3-Basic-*pCAGA* firefly reporter and 7 ng pRL-SV40 renilla reporter were diluted in 50 µl serum-free medium. Furthermore, 0.75 µl of Lipofectamine™ 2000 reagent were added to 49.25 µl serum-free medium. This mixture was incubated for 5 min at room temperature. Thereafter it was combined with the vector containing sample and incubated for 20 min at room temperature. Afterwards, the serum-free medium was removed from the cells and the aforementioned transfection solution was added. After 5 h of incubation, the transfection solution was replaced by culture medium with 10% FCS and the cells were incubated herein for 48 h.

IPF lung fibroblasts ($7x10^4$ cells/well) were seeded onto a 48-well plate. After attachment for 24 h, cells were starved in Opti-MEM™ I reduced-serum medium for 1 h and then transfected with pGL3-Basic-*pCAGA* firefly reporter and pRL-SV40 renilla reporter using Lipofectamine™ 3000 transfection reagent (Invitrogen). First, 140 ng of pGL3-Basic-*pCAGA* firefly reporter and 20 ng of pRL-SV40 renilla reporter were diluted in 12.80 µl of Opti-MEM™ I reduced-serum medium, second, 0.37 µl of p3000 reagent were added. In addition, 0.78 µl of Lipofectamine™ 3000 were incubated in 12.80 µl of Opti-MEM™ reduced-serum medium for 5 min at room temperature. Afterwards, 12.80 µl of this sample were mixed with the sample which contained the vectors and subsequently incubated for 10 min at room temperature. Thereafter, Opti-MEM™ I reduced-serum medium was removed from the cells and 24.40 µl of the transfection solution and 76.90 µl of Opti-MEM™ I reduced-serum medium were added to the cells. After 5 h of incubation, the transfection solution was removed and the cells were washed once with PBS. Thereafter, the cells were cultivated in culture medium with 10% FCS for 24 h, starved in serum-free medium for 5 h and then transfected with siRNA directed against LRP1 or with negative control siRNA. Cells were subsequently lysed by shaking in 100 µl/well 1x passive lysis buffer (Promega, Mannheim, Germany) for 10 min at room temperature. Thereafter, the activities of firefly and renilla luciferase in 10 µl of the cell lysate were measured in a white 96-well microplate (Berthold Technologies, Bad Wildbad, Germany) using a TriStar$^2$ S LB 942 Multimode Reader (Berthold Technologies). In the machine, 50 µl of firefly luciferase buffer (25 mM glycylglycine, 15 mM potassium dihydrogen phosphate (pH 8), 4 mM ethylene glycol tetraacetic acid (EGTA), 2 mM adenosine triphosphate (ATP), 1 mM dithiothreitol, 15 mM magnesium sulfate, 0.1 mM coenzyme A trilithium salt, 0.24 mM D-luciferin potassium salt) were added to the sample and the firefly luciferase activity was assessed by measurement of the generated luminescence for 7 s. After that, 50 µl of renilla luciferase buffer (1.1 mM sodium chloride, 2.2 mM EDTA, 0.22 mM potassium dihydrogen phosphate (pH 5.1), 0.44 mg/ml BSA, 1.3 mM sodium azide, 6.4 µM coelenterazine), which contains an inhibitor for firefly luciferase, were dispersed in the sample. Subsequently, renilla luciferase activity was measured by detecting the arising luminescence for 7 s. The transcriptional activity of SMAD3 was presented as the ratio of firefly luciferase-to-renilla luciferase luminescence values.

For Dual-Luciferase Reporter Assay with a vector containing AP1-binding consensus elements, IPF lung fibroblasts were seeded onto a 48-well plate. After attachment for 24 h, cells were transfected with siRNA directed against LRP1 or with negative control siRNA. After 24 h, cells were transfected with 140 ng of pGL4.44-AP1 firefly reporter and 20 ng of pRL-SV40 renilla reporter as described for the transfection of pGL3-Basic-*pCAGA* firefly reporter and pRL-SV40 renilla reporter in IPF lung fibroblasts. The collected transfection solution containing siRNA against LRP1 or control siRNA in culture medium with 10% FCS was added to the cells. An incubation for 48 h followed. Thereafter, the cells were prepared for measurement as described above.

### 3.2.13 Collagen gel contraction assay

The wells of a 24-well plate were precoated with 0.5 ml/well of 1% BSA in PBS (pH 7.4) for 2 - 3.5 h at 37 °C and rinsed twice with PBS. IPF lung fibroblasts were harvested 48 h after transfection with siRNA directed against LRP1 or negative control siRNA and 24 h after stimulation with 10 ng/ml TGF-β1. They were resuspended to reach a density of $2x10^5$ cells/ml in culture medium with 10% FCS. Rat tail collagen type I (0.78 mg/ml) in 0.02 M acetic acid (Corning, Wiesbaden, Germany) was added to the cells, followed by instant neutralization with 5.85 µl of 0.5 M sodium hydroxide (NaOH) per 0.5 ml sample. Subsequently, 243.9 µl/well of the solution were transferred to BSA-coated wells. Polymerization of collagen gels occurred during incubation at 37 °C for 1 h. Afterwards, collagen gels were detached from the well wall and bottom by gently canting the 24-well plate. Thereafter, 634 µl/well of the collected siRNA transfection solutions (siRNA directed against LRP1 or negative control siRNA) in culture medium (with 10% FCS) were added to the respective collagen gels. Further incubation therein for 48 h followed. Collagen gel contraction was documented after 3 and 24 h by taking photos with the Chemidoc™ Touch Imaging System (Bio-Rad) and collagen gel surface area was calculated using ImageJ.

### 3.2.14 Flow cytometry

Ninety-six hours after IPF lung fibroblasts had been transfected with control siRNA or siRNA directed against LRP1 in a 6-well plate, they were harvested and centrifuged at 160 g for 5 min. The pellet was resuspended in 5 ml PBS and centrifuged at 160 g

for 5 min. Three hundred µl PBS were added to the cell pellet and subsequently 1 ml 70% ethanol was given drop by drop to the cells under vortexing conditions. Thereafter, the cells were fixed for 1 h at 4 °C. Then, the samples were centrifuged at 160 g for 5 min and the cells were resuspended in 5 ml PBS. Centrifugation at 160 g for 5 min followed and cells were resuspended in 500 µl propidium iodide mix (20 µg/ml propidium iodide (Roth), 0.1% Triton X-100, 200 µg/ml RNase A (Thermo Scientific) in PBS). Subsequently, the samples were incubated at 37 °C for 15 min in the dark. The reaction was stopped by placing the samples on ice. An accuri C6 Flow Cytometer (BD Biosciences, Heidelberg, Germany) was used to measure the amount of DNA-bound propidium iodide. Data were analyzed with the accuri CFlow Plus (BD Biosciences) software.

### 3.2.15 Gap closure assay

IPF lung fibroblasts were transfected with siRNA directed against LRP1 or control siRNA. Forty-eight h after transfection and 24 h after stimulation with 10 ng/ml TGF-β1, cells were harvested and seeded (50,000 cells/pocket) in culture medium with 10% FCS into the two pockets of a culture insert (ibidi, Planegg, Germany) which had been placed into a 12-well plate. After 4 h, cells had attached to the well bottom and the culture insert was removed. Subsequently, 1.3 ml of the collected siRNA transfection solutions (containing siRNA directed against LRP1 or control siRNA) in culture medium (with 10% FCS) were added to respective cells. The migration of the cells into the gap between the two cell patches was documented after 0 h and 19 h using a Leica DM IL LED microscope (Leica, Wetzlar, Germany), a LA-EA1 objective adapter (Sony, Berlin, Germany) and a Nex-3 camera (Sony).

### 3.2.16 Statistics

Data are presented as mean values ± S.E.M. unless otherwise stated. Differences between two groups were calculated by using a Student's t-test, whereas differences between a larger number of groups were determined by analysis of variance (ANOVA) and Tukey's post hoc test. A value of $p<0.05$ was defined to be statistically significant. The aforementioned statistical analyses were executed in GraphPad Prism version 5.02 for Windows (GraphPad Software, La Jolla, CA).

# 4 Results

## 4.1 Microarray analysis of IPF and donor lung fibroblasts following LRP1-depletion

In order to identify genes regulated by LRP1 in IPF and donor lung fibroblasts, LRP1 was depleted in these cells and a microarray was performed. A pathway analysis of the microarray data was undertaken to identify Kegg pathways which are perturbed in IPF and donor lung fibroblasts following LRP1-knock-down. The Kegg pathways Lysosome, Protein processing in endoplasmic reticulum, Metabolic pathways, Glycosylphosphatidylinositol (GPI)-anchor biosynthesis, Valine, leucine and isoleucine degradation and N-Glycan biosynthesis were perturbed with high significance in both, IPF and donor lung fibroblasts after LRP1-depletion (Fig. 4 (not all labeled), Tab. 2, 3). However, only the perturbations of the Kegg pathways Lysosome and Protein processing in endoplasmic reticulum were with high significance different in IPF and donor lung fibroblasts after knock-down of LRP1 (Fig. 4). This can be seen in figure 4 because the larger the dot is, the higher is the significance for a different perturbation of the Kegg pathway in IPF and donor lung fibroblasts after LRP1-depletion.

Five Kegg pathways were perturbed with high significance in IPF lung fibroblasts but not in donor lung fibroblasts following LRP1-depletion (Fig. 4). Namely, they were Axon guidance, Regulation of actin cytoskeleton, Focal adhesion, Vascular smooth muscle contraction and Rap1 signaling pathway (Fig. 4). Interestingly, all of these Kegg pathways describe processes which are involved in the modulation of the cytoskeleton. The Kegg pathways which were perturbed with high significance in LRP1-deficient donor lung fibroblasts but not in LRP1-deficient IPF lung fibroblasts were Phagosome and Vibrio cholerae infection (Fig. 4). These Kegg pathways describe endocytic processes. Altogether, these results give a hint that the function of LRP1 may be switched from endocytic to signal transducing in IPF lung fibroblasts. By modulating signal transduction, LRP1 may regulate cytoskeleton remodeling in these cells. The 15 Kegg pathways which were most significantly perturbed following LRP1-depletion in IPF and donor lung fibroblasts are listed in table 2 and 3.

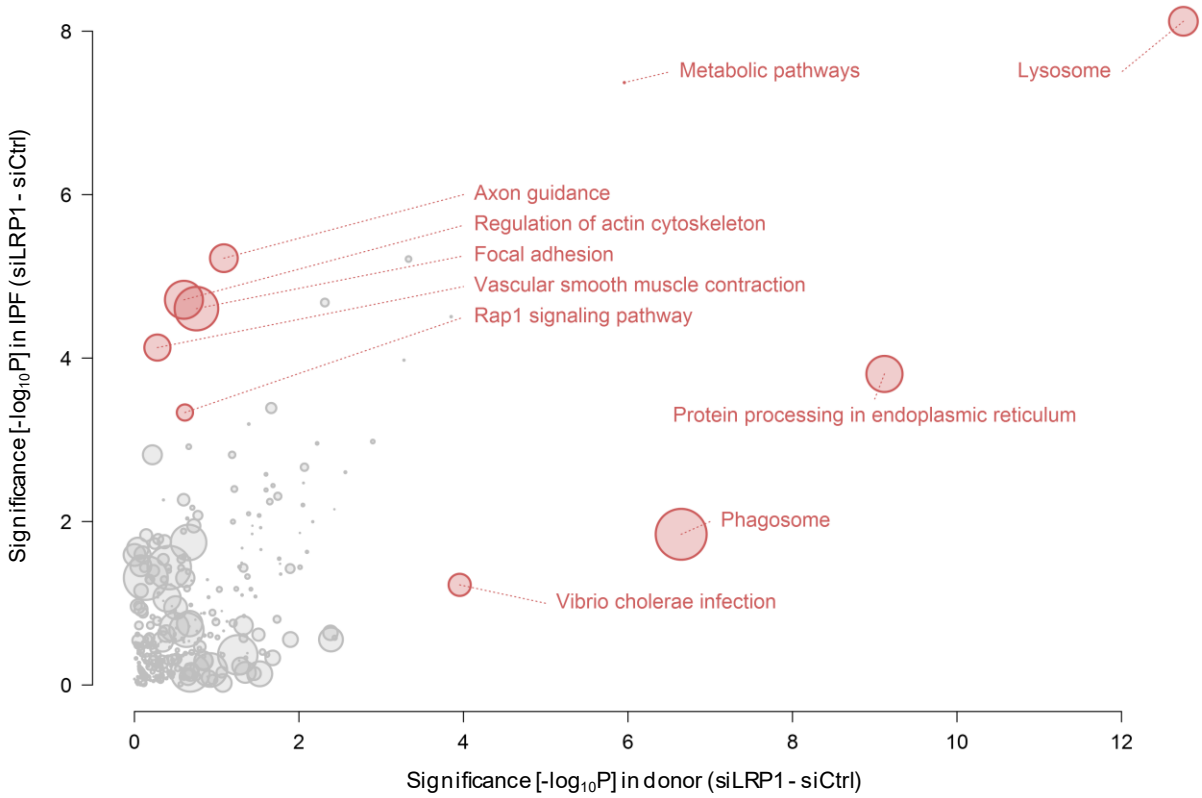


**Fig. 4: Microarray analysis of IPF and donor lung fibroblasts following LRP1-knock-down.** IPF and donor lung fibroblasts were transfected with siLRP1 or siCtrl and a microarray was performed. Scatter plot showing Kegg pathways which were perturbed in IPF and donor lung fibroblasts following LRP1-depletion (siLRP1 - siCtrl). The Kegg pathways are ranked according to the significance of perturbation [-$\log_{10}$ P]. Large dots indicate that the perturbation of the Kegg pathway is with high significance different in IPF and donor lung fibroblasts following LRP1-depletion. The experiment shows that depletion of LRP1 in IPF lung fibroblasts results in the significant perturbation of Kegg pathways which describe processes of cytoskeleton remodeling. In detail, the Kegg pathways Axon guidance, Regulation of actin cytoskeleton, Focal adhesion, Vascular smooth muscle contraction and Rap1 signaling pathway are significantly perturbed in IPF lung fibroblasts after LRP1-depletion. In contrast, knock-down of LRP1 in donor lung fibroblasts results in the significant perturbation of Kegg pathways which describe endocytic processes. The Kegg pathways Phagosome and Vibrio cholerae infection are significantly perturbed in LRP1-deficient donor lung fibroblasts. The Kegg pathways lysosome and protein processing in endoplasmic reticulum are significantly perturbed following LRP1-depletion in IPF and donor lung fibroblasts. In addition, the perturbation of these Kegg pathways is significantly different in these cell types after knock-down of LRP1.

**Table 2. Top 15 Kegg pathways perturbed with highest significance by LRP1-depletion in IPF lung fibroblasts.** The Kegg pathways Axon guidance, Regulation of actin cytoskeleton, Focal adhesion, Vascular smooth muscle contraction and Rap1 signaling pathway were perturbed with high significance in IPF lung fibroblasts but not in donor lung fibroblasts following LRP1-depletion. The aforementioned pathways are presented in bold font.

| **Kegg pathway** | **ID** | **Significance [-$\log_{10}$ P]** |
|---|---|---|
| Lysosome | 04142 | 8.12 |
| Metabolic pathways | 01100 | 7.37 |
| **Axon guidance** | 04360 | 5.22 |
| Valine, leucine and isoleucine degradation | 00280 | 5.21 |
| **Regulation of actin cytoskeleton** | 04810 | 4.71 |
| Proteasome | 03050 | 4.68 |
| **Focal adhesion** | 04510 | 4.61 |
| Glycosylphosphatidylinositol (GPI)-anchor biosynthesis | 00563 | 4.51 |
| **Vascular smooth muscle contraction** | 04270 | 4.13 |
| N-Glycan biosynthesis | 00510 | 3.97 |
| Protein processing in endoplasmic reticulum | 04141 | 3.81 |
| Oxidative phosphorylation | 00190 | 3.39 |
| **Rap1 signaling pathway** | 04015 | 3.33 |
| Steroid biosynthesis | 00100 | 3.19 |
| Type II diabetes mellitus | 04930 | 2.98 |

**Table 3. Top 15 Kegg pathways perturbed with highest significance by LRP1-depletion in donor lung fibroblasts.** The Kegg pathways Phagosome and Vibrio cholerae infection were perturbed with high significance in donor lung fibroblasts but not in IPF lung fibroblasts following LRP1-depletion. The aforementioned pathways are presented in bold font.

| **Kegg pathway** | **ID** | **Significance [-$\log_{10}$ P]** |
|---|---|---|
| Lysosome | 04142 | 12.75 |
| Protein processing in endoplasmic reticulum | 04141 | 9.12 |
| **Phagosome** | 04145 | 6.65 |
| Metabolic pathways | 01100 | 5.96 |
| **Vibrio cholerae infection** | 05110 | 3.95 |
| Glycosylphosphatidylinositol (GPI)-anchor biosynthesis | 00563 | 3.85 |
| Valine, leucine and isoleucine degradation | 00280 | 3.33 |
| N-Glycan biosynthesis | 00510 | 3.28 |
| Type II diabetes mellitus | 04930 | 2.90 |
| Collecting duct acid secretion | 04966 | 2.56 |
| Glycosaminoglycan biosynthesis - chondroitin sulfate / dermatan sulfate | 00532 | 2.43 |
| Nicotinate and nicotinamide metabolism | 00760 | 2.43 |
| Glycosaminoglycan degradation | 00531 | 2.39 |
| Cell adhesion molecules (CAMs) | 04514 | 2.38 |
| Proteasome | 03050 | 2.31 |

As described previously, LRP1 may regulate cytoskeleton remodeling in IPF lung fibroblasts. In the literature, remodeling of the cytoskeleton is described to be a main process during fibroblast to myofibroblast transdifferentiation [73–75]. An important example is the enhanced expression and incorporation of α-SMA into stress fibers [73–75]. Hence, it was next investigated in the present study whether LRP1 regulates α-SMA expression in IPF lung fibroblasts.

## 4.2 LRP1 suppresses α-SMA expression in IPF lung fibroblasts

The relationship between LRP1 and α-SMA expression was investigated. To this end, the gene expression of *LRP1* and *α-SMA* in the IPF lung fibroblasts from fifteen IPF patients was analyzed by qPCR (Fig. 5 A). The ∆Ct values of α-SMA were plotted against corresponding ∆Ct values of LRP1 and a linear regression was performed (Fig. 5 A). Thereby, it was shown that *LRP1* gene expression negatively correlates with the α-SMA mRNA level in IPF lung fibroblasts. Moreover, it was investigated whether LRP1 expression regulates *α-SMA* gene expression in MEF. To this end, the α-SMA mRNA levels were assessed by qPCR in LRP1-expressing and LRP1-knock-out MEF. This experiment revealed that the *α-SMA* gene expression is enhanced in LRP1-depleted MEF (Fig. 5 B).

Collectively, these data indicate that LRP1 suppresses α-SMA gene expression in IPF lung fibroblasts and MEF.

It was furthermore analyzed whether LRP1 also suppresses α-SMA on the protein level in IPF lung fibroblasts and MEF. For that purpose, LRP1 gene expression was silenced in IPF lung fibroblasts and western blotting was performed (Fig. 5 C). Depletion of LRP1 resulted in the increase of α-SMA protein levels in IPF lung fibroblasts. In MEF, the knock-out of LRP1 elevated α-SMA protein expression as well (Fig. 5 D). Hence, LRP1 suppresses α-SMA expression on the gene and protein level in IPF lung fibroblasts and MEF.

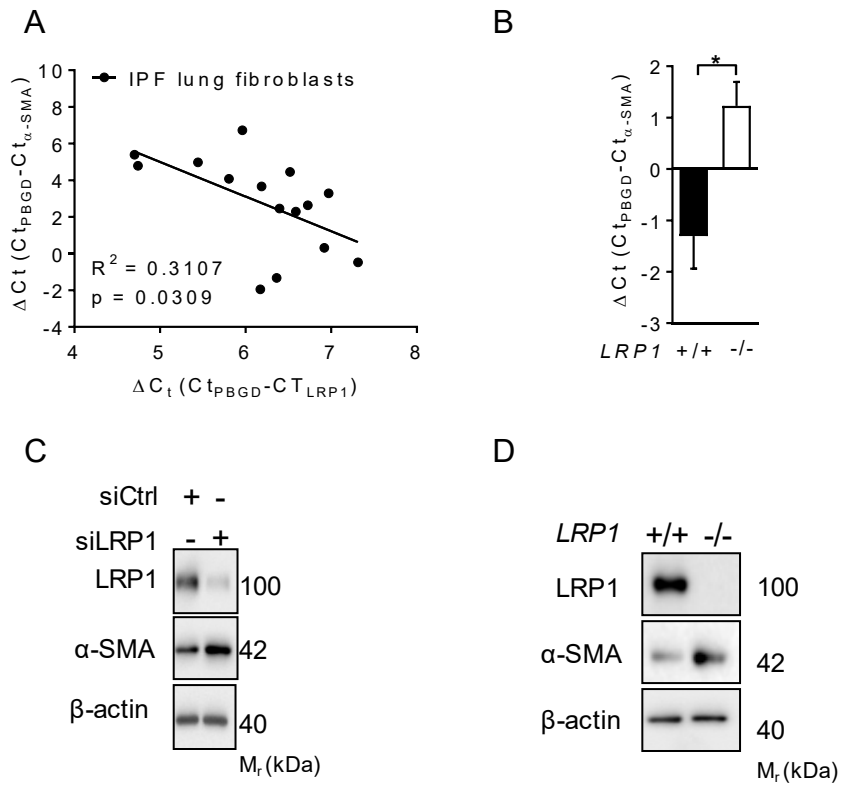


**Fig. 5: LRP1 suppresses α-SMA expression in IPF lung fibroblasts and mouse embryonic fibroblasts.** (A) The mRNA levels of LRP1 and α-SMA in the IPF lung fibroblasts from fifteen IPF patients were assessed by qPCR. PBGD was used as a reference gene. The ΔCt of α-SMA were plotted against the ΔCt values of LRP1. A linear regression was performed to describe the correlation of *LRP1* and *α-SMA* gene expression. (B) *α-SMA* gene expression was analyzed in LRP1-expressing and LRP1-knock-out MEF by qPCR. n=3. Data are expressed as ΔCt, using PBGD as a reference gene. LRP1 and α-SMA protein expression was investigated by western blotting in (C) LRP1-expressing and LRP1-deficient IPF lung fibroblasts (n=3) as well as in (D) LRP1-expressing and LRP1-knock-out MEF (n=3). β-actin served as a loading control. Representative western blots are shown. Panel (A) shows that LRP1 negatively correlates with the gene expression of α-SMA in IPF lung fibroblasts. Panel (C) shows that LRP1 suppresses α-SMA protein levels in these cells. Moreover, panels (B) and (D) show that LRP1 suppresses α-SMA gene and protein expression also in MEF.

## 4.3 LRP1 ICD does not serve as transcription factor to regulate α-SMA expression

The next step of the study was to decipher the mechanism by which LRP1 regulates the expression of α-SMA in IPF lung fibroblasts. It has been reported that LRP1 undergoes regulated proteolytic shedding [109,110]. During this process, metalloproteinases first mediate the shedding of the extracellular domain of LRP1 [109,110]. Thereby, a membrane-bound 25 kDa LRP1 fragment is generated [109,110]. When this fragment is further processed by γ-secretase, the carboxyterminal 12 kDa frag-

ment of LRP1 is liberated from the membrane [109,110]. This fragment is the intracellular domain (ICD) of LRP1 [110]. It was demonstrated that the ICD of LRP1 serves as a transcription factor and regulates *interferon γ* expression [109]. In the present study, LRP1-expressing MEF were used as a model system to investigate whether the ICD of LRP1 can regulate the gene expression of *α-SMA* and *SMAD3*. The latter is a major mediator of the canonical TGF-β1 pathway. SMAD3 was investigated as it had been demonstrated to regulate α-SMA expression [73]. LRP1-positive MEF were treated with the γ-secretase inhibitor DAPT. The efficiency of the inhibition of the γ-secretase-mediated processing of LRP1 was assessed by western blotting. Whereas the 25 kDa membrane-bound LRP1 fragment was absent in cells which were not treated with DAPT, this fragment was detectable after treatment of cells with 11.5, 23 or 46 µM DAPT for 72 h (Fig. 6 A). This indicated that the inhibition of γ-secretase by DAPT was efficient. Next, MEF were treated with 23 µM DAPT for 72 h and qPCR was performed. The α-SMA and SMAD3 mRNA levels were not altered by the inhibition of γ-secretase (Fig. 6 B, C). Hence, the ICD of LRP1 is not involved in the regulation of *α-SMA* and *SMAD3* in MEF.

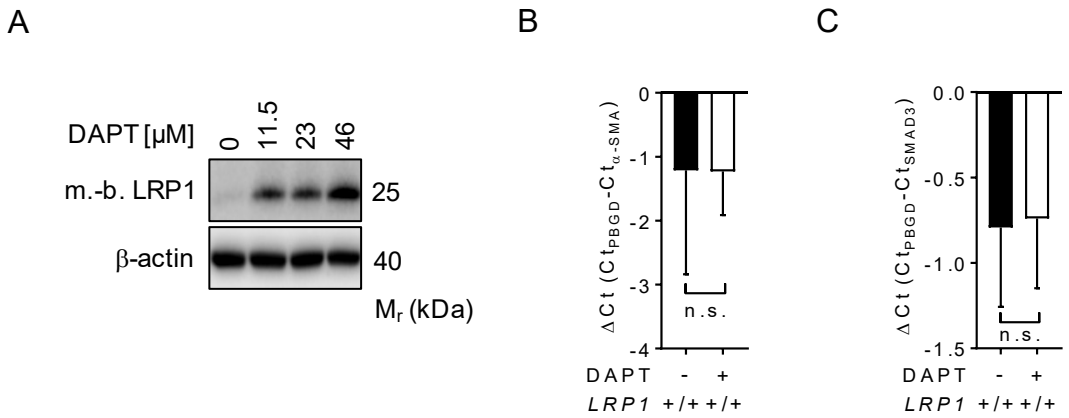


**Fig. 6: The intracellular domain of LRP1 does not regulate the expression of *α-SMA* and *SMAD3* as a transcription factor.** (A) LRP1-expressing MEF were treated with 0, 11.5, 23 and 46 µM of the γ-secretase inhibitor DAPT for 72 h. Thereafter, the protein expression of the membrane-bound LRP1 fragment (m.-b. LRP1) was determined by western blotting. β-actin was used as a loading control. n=3. Representative western blots are displayed. LRP1-expressing MEF were treated with 23 µM DAPT for 72 h and the mRNA levels of (B) α-SMA and (C) SMAD3 were assessed by qPCR. n=3. Data are presented as ΔCt, using PBGD as a reference gene. Collectively, these data reveal that liberation of LRP1 ICD by γ-secretase does not regulate *α-SMA* and *SMAD3* gene expression in MEF.

## 4.4 The regulation of α-SMA expression by LRP1 is independent of the canonical TGF-β1 pathway in IPF lung fibroblasts

Since LRP1 ICD is not a transcription factor in the regulation of α-SMA expression, it was next analyzed whether LRP1 regulates α-SMA expression by modulating signaling pathways in IPF lung fibroblasts. For instance, it has been reported that LRP1 can modulate the TGF-β1 signaling pathway [111,112]. As SMAD3, a major mediator of the canonical TGF-β1 signaling pathway, is known to promote α-SMA expression [73], it was investigated whether LRP1 modulates the expression or activation of SMAD3 in IPF lung fibroblasts. In addition, the effect of LRP1 on SMAD2, another major mediator of the canonical TGF-β1 signaling pathway, was analyzed.

LRP1-depletion did not affect the gene (Fig 7 A) and protein (Fig. 7 B) expression of SMAD3 in IPF lung fibroblasts as assessed by qPCR and western blotting. In contrast, the protein levels of SMAD2 were enhanced after silencing of LRP1 in these cells (Fig. 7 B). Furthermore, time-dependent treatment of LRP1-expressing and LRP1-depleted IPF lung fibroblasts with TGF-β1 revealed no changes in the activation of SMAD3 and SMAD2 as assessed by SMAD2/SMAD3 phosphorylation between these cells (Fig. 7 C).

Hence, these data reveal that LRP1 does not modulate the TGF-β1 signaling pathway by regulating SMAD3 and SMAD2 in IPF lung fibroblasts.

In MEF, however, knock-out of LRP1 resulted in enhanced SMAD3 mRNA (Fig. 7 D) and protein levels (Fig. 7 F). In order to determine the localization of SMAD3 in the cell, subcellular fractionation with LRP1-expressing and LRP1-deficient MEF was performed. Western blotting revealed higher amounts of SMAD3 in the nuclear fraction (NF) than in the cytosolic fraction (CF) when LRP1 is expressed in MEF (Fig. 7 E). After LRP1-depletion, the amounts of SMAD3 increased in both the cytosolic and the nuclear compartment in MEF (Fig. 7 E). These findings demonstrate that LRP1 may modulate the TGF-β1 signaling pathway by increasing SMAD3 protein expression and by promoting its translocation to the nucleus in MEF.

In order to investigate whether LRP1 modulates the activation of SMAD2 in MEF, LRP1-expressing and LRP1-deficient cells were time-dependently treated with TGF-β1. LRP1-knock-out shortened the duration of SMAD2 phosphorylation in the C-terminus (Ser465/467) and in the linker region (Ser245/250/255) in MEF (Fig. 7 F). Whereas phosphorylation in the C-terminus is required for the nuclear translocation

of SMAD2 [113–115], phosphorylation in the linker region can either promote or inhibit the translocation of SMAD2 to the nucleus [116,117]. Thus, the result demonstrates that LRP1 modulates the TGF-β1 signaling pathway by regulating the nuclear translocation of SMAD2 in MEF.

Interestingly, the findings made in MEF are contradictory to those made in IPF lung fibroblasts. Whereas LRP1 modulates SMAD2 and SMAD3 in MEF, LRP1 does not modulate the TGF-β1 signaling pathway in IPF lung fibroblasts.

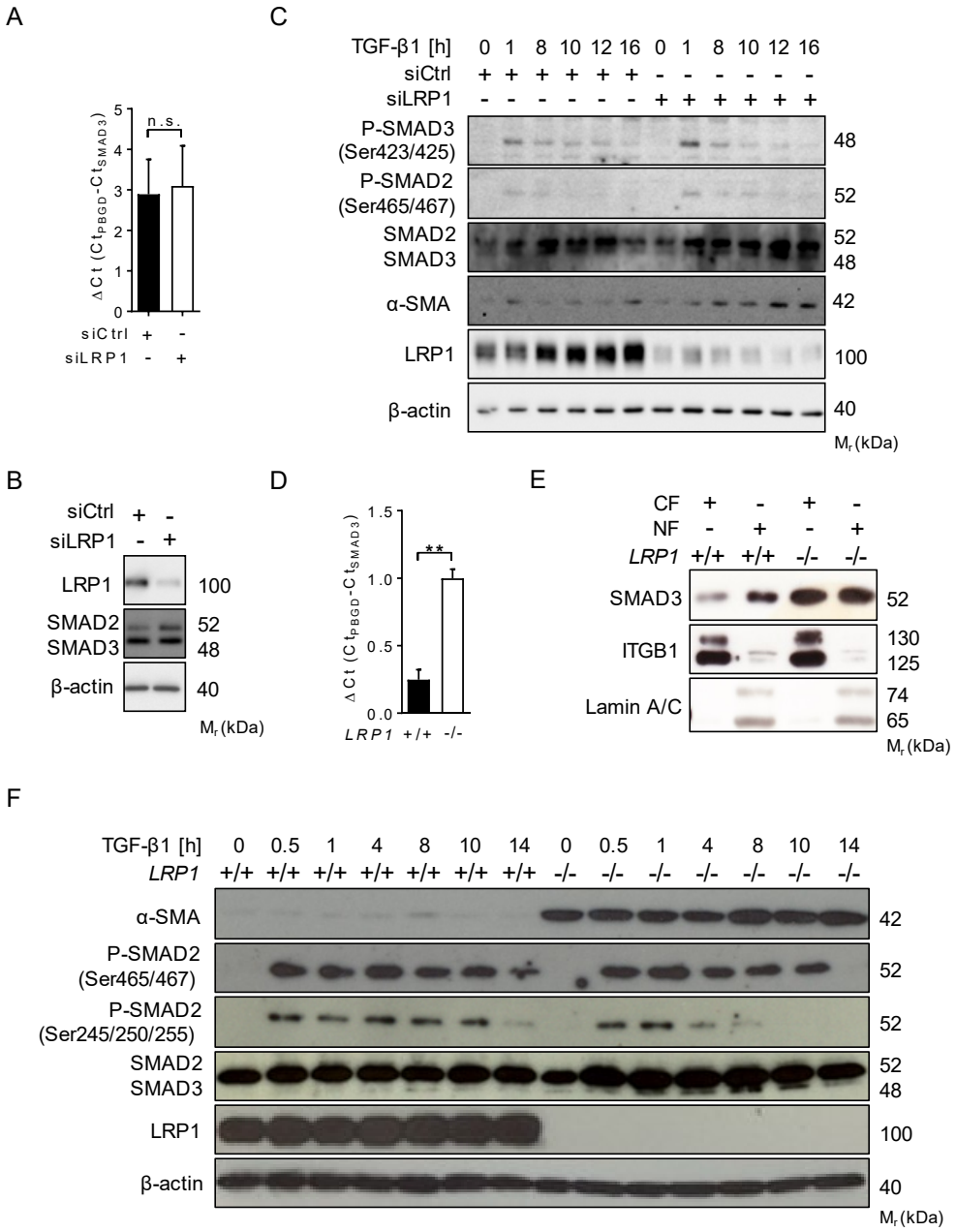


**Fig. 7: LRP1 does not regulate SMAD3 expression and activation in IPF lung fibroblasts.** LRP1 was depleted in IPF lung fibroblasts by siRNA. (A) SMAD3 mRNA levels were assessed by qPCR. Data are presented as ΔCt, using PBGD as a reference gene. n=3. *SMAD3* gene expression is not affected by LRP1-depletion in IPF lung fibroblasts. (B) The protein expression of SMAD2 and SMAD3

was determined by western blotting. β-actin served as a loading control. n=3. Representative western blots are shown. LRP1-deficiency results in increased SMAD2 protein expression in IPF lung fibroblasts. SMAD3 protein expression is not affected. (C) LRP1-expressing and LRP1-depleted IPF lung fibroblasts were treated with 1 ng/ml TGF-β1 for different time points. The protein expression of α-SMA, SMAD2, SMAD3 and LRP1 was analyzed. In addition, the activation of SMAD2 and SMAD3 was investigated by assessing the levels of P-SMAD2 (Ser465/467) and P-SMAD3 (Ser423/425). β-actin served as a loading control. n=1. Representative western blots are shown. LRP1 does not regulate SMAD3 and SMAD2 phosphorylation in IPF lung fibroblasts. (D) SMAD3 mRNA levels in LRP1-expressing and -knock-out MEF were assessed by qPCR. Data are presented as ΔCt, using PBGD as a reference gene. n=3. Knock-out of LRP1 enhances *SMAD3* gene expression in MEF. (E) Subcellular fractionation of LRP1-expressing and -deficient MEF was performed and the nuclear (NF) and cytosolic (CF) fractions were analyzed for the presence of SMAD3 by western blotting. Integrin β1 (ITGB1) served as a marker for the cytosolic fraction whereas lamin A/C was the marker for the nuclear compartment. n=3. Representative western blots are shown. LRP1-deficiency enhances the amounts of SMAD3 in both the cytosolic and nuclear fraction in MEF. (F) LRP1-expressing and LRP1-deficient MEF were treated with 10 ng/ml TGF-β1 for 0, 0.5, 1, 4, 8, 10 and 14 h. The protein levels of α-SMA, SMAD2, SMAD3 and LRP1 were analyzed by western blotting. In addition, the activation of SMAD2 was investigated by assessing the levels of P-SMAD2 (Ser465/467). Moreover, the phosphorylation of the linker region of SMAD2 was analyzed by assessing the levels of P-SMAD2 (Ser245/250/255). β-actin served as a loading control. n=3. Representative western blots are shown. Knock-out of LRP1 results in shortened phosphorylation in the C-terminus and linker region of SMAD2. Panels (A) - (C) indicate that LRP1 does not modulate the TGF-β1 signaling pathway by regulating SMAD2 and SMAD3 in IPF lung fibroblasts. However, panels (D) - (F) demonstrate that LRP1 regulates the TGF-β1 signaling pathway in MEF. In detail, LRP1 suppresses the expression of SMAD3 and its translocation to the nucleus in these cells. In addition, LRP1 may modulate the translocation of SMAD2 to the nucleus in MEF (panel (F)).

Although SMAD3 expression and activation were not affected by LRP1-depletion in IPF lung fibroblasts, further experiments were performed to analyze the effect of LRP1 knock-down on SMAD3. First, a Dual-Luciferase Reporter Assay with the SMAD3-binding consensus sequence CAGA [118] was executed with LRP1-expressing and LRP1-deficient IPF lung fibroblasts in order to measure the transcriptional activity of SMAD3. After LRP1-depletion, no change in the transcriptional activity of SMAD3 was observed under basal conditions in IPF lung fibroblasts (Fig. 8 A). In addition, knock-down of LRP1 did not affect SMAD3 transcriptional activity after treatment with TGF-β1 in these cells (Fig. 8 A). These data indicate that LRP1 does not regulate the transcriptional activity of SMAD3 in IPF lung fibroblasts. The aforementioned experiment was also performed with LRP1-expressing and LRP1-deficient MEF. The findings obtained in MEF are partially different than those obtained in IPF

lung fibroblasts. In detail, LRP1-depletion did not affect the transcriptional activity of SMAD3 under basal conditions. However, LRP1-depletion potentiated the transcriptional activity of SMAD3 in response to TGF-β1 in MEF (Fig. 8 B). These data indicate that LRP1 suppresses the TGF-β1-dependent transcriptional activity of SMAD3 in MEF.

Next, it was investigated whether SMAD3 is required for the suppression of α-SMA expression by LRP1 in IPF lung fibroblasts. To this end, SMAD3 and LRP1 were depleted either in combination or separately in these cells and α-SMA expression was assessed by qPCR and western blotting. On the mRNA level, LRP1-depletion increased α-SMA expression (Fig. 8 C). Additional knock-down of SMAD3 in LRP1-deficient IPF lung fibroblasts did not abolish the induction of *α-SMA* gene expression (Fig. 8 C). Thus, SMAD3 does not mediate LRP1-dependent suppression of *α-SMA* gene expression in IPF lung fibroblasts. After treatment of IPF lung fibroblasts with TGF-β1, the expected elevation of α-SMA mRNA levels after LRP1-depletion was not observed (Fig. 8 C). This may be explained by the reaching of a mRNA expression limit after TGF-β1-mediated increase of the *α-SMA* gene expression (Fig. 8 C). The efficiency of the knock-down of LRP1 and SMAD3 in this experiment was assessed by qPCR. Figure 8 D shows that silencing of *LRP1* gene expression efficiently decreased LRP1 mRNA levels. Knock-down of SMAD3 also efficiently diminished *SMAD3* gene expression (Fig. 8 E). The effect of LRP1- and SMAD3-depletion on the α-SMA protein levels in IPF lung fibroblasts is illustrated in figure 8 F and G. Knock-down of LRP1 increased the α-SMA protein expression in IPF lung fibroblasts under basal conditions and after treatment with TGF-β1 (Fig. 8 F, G). Under both conditions, the additional depletion of SMAD3 did not block the elevation of α-SMA protein expression after knock-down of LRP1 (Fig. 8 F, G). From this result it can be concluded that SMAD3 is not involved in the regulation of α-SMA protein expression by LRP1 in IPF lung fibroblasts. As visible in figure 8 F, silencing of *LRP1* efficiently reduced the LRP1 protein levels in IPF lung fibroblasts. Knock-down of SMAD3 also efficiently reduced the SMAD3 protein levels in these cells (Fig. 8 F). Hence, the depletion of LRP1 and SMAD3 was efficient in this experiment.

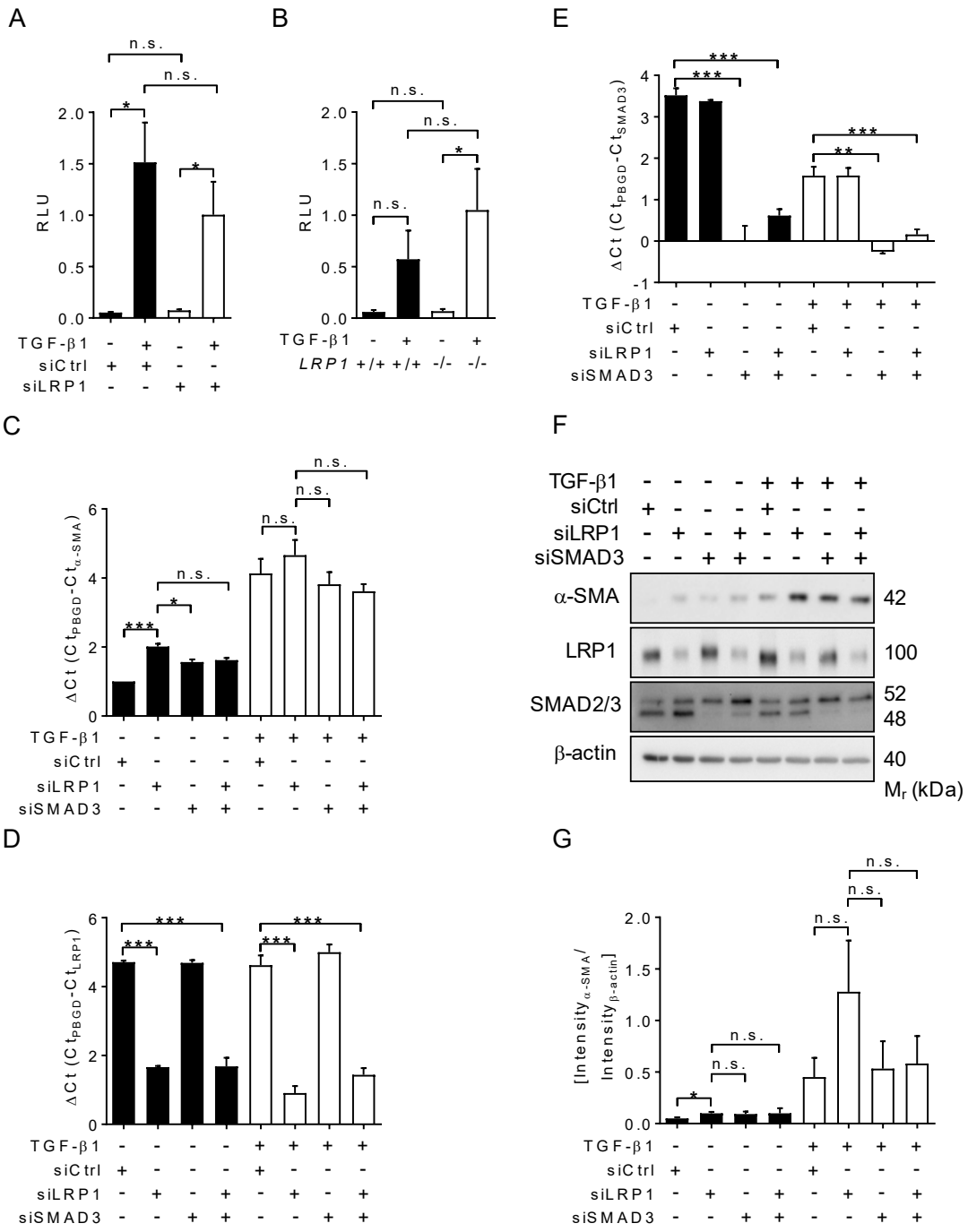


**Fig. 8: LRP1 does not regulate α-SMA expression *via* SMAD3 in IPF lung fibroblasts.** (A) IPF lung fibroblasts were transfected with siCtrl or siLRP1 as well as with pGL3-Basic-*pCAGA* firefly reporter and pRL-SV40 renilla reporter. Treatment with 1 ng/ml TGF-β1 was performed for 24 h. The transcriptional activity of SMAD3 was determined by Dual-Luciferase Reporter Assay. Data are expressed as mean values ± S.E.M. n=6. (B) LRP1-expressing and LRP1-deficient MEF were transfected with pGL3-Basic-*pCAGA* firefly reporter and pRL-SV40 renilla reporter and Dual-Luciferase Reporter Assay was executed after treatment with 10 ng/ml TGF-β1 for 24 h. Data are expressed as mean values ± S.E.M. n=3. IPF lung fibroblasts were transfected with siCtrl or siLRP1 and/or siSMAD3. The cells were either treated or untreated with 1 ng/ml TGF-β1 for 24 h. Measurement of (C) *α-SMA*, (D) *LRP1* and (E) *SMAD3* gene expression by qPCR. Data are expressed as ΔCt, using

PBGD as a reference gene. n=3. (F) Analysis of α-SMA, LRP1, SMAD2 and SMAD3 protein expression by western blotting, using β-actin as a loading control. n=4. Representative blots are shown. (G) Densitometric analysis of the α-SMA protein expression normalized to β-actin. n=4. Data are expressed as mean values ± S.E.M. Panel B shows that LRP1 suppresses the transcriptional activity of SMAD3 after TGF-β1-stimulation in MEF. However, panel A shows that LRP1 does not regulate the transcriptional activity of SMAD3 in IPF lung fibroblasts. Panels A, C and F indicate that SMAD3 does not mediate the increase of α-SMA gene and protein expression after LRP1-knock-down in IPF lung fibroblasts.

## 4.5 Analysis of kinase phosphorylation in IPF lung fibroblasts following LRP1-depletion

As demonstrated above, the control of α-SMA expression by LRP1 is not mediated by the canonical TGF-β1 pathway in IPF lung fibroblasts. In the literature, it was reported that LRP1-dependent gene expression can be mediated by numerous kinases, such as mitogen-activated protein kinases [119–121]. To identify kinases which activity is regulated by LRP1, a membrane-based antibody array which detects activating phosphorylations in kinases was performed. In this experimental system, antibodies which are specific for a distinct kinase are immobilized in duplicate on a nitrocellulose membrane. By incubation of protein lysates on the membrane, kinases are captured by these antibodies. In the present study, the protein lysates of LRP1-expressing and LRP1-deficient IPF lung fibroblasts either treated or untreated with TGF-β1 were analyzed (Fig. 9 A). The detection of phosphorylated kinases requires the incubation of the membrane with a mixture of biotinylated antibodies which are specific for the different phosphorylation sites of interest. In order to visualize phosphorylated kinases, chemiluminescent detection reagents are used. The intensity of the detected signal dots is proportional to the amount of the captured phosphorylated kinases (Fig. 9 A). Figure 9 A shows that the kinases JNK1/2/3 and ERK1/2 as well as c-Jun are phosphorylated in LRP1-expressing IPF lung fibroblasts under basal condition. Treatment of these cells with TGF-β1 increased the levels of these phosphorylated proteins (Fig. 9 A). In LRP1-depleted IPF lung fibroblasts, the basal amounts of phosphorylated JNK1/2/3, ERK1/2 and c-Jun were elevated in comparison to LRP1-expressing IPF lung fibroblasts (Fig. 9 A). In addition, higher levels of phosphorylated JNK1/2/3, ERK1/2 and c-Jun were detectable in LRP1-deficient than in LRP1-expressing IPF lung fibroblasts after treatment with TGF-β1. Collectively, these findings indicate that LRP1 may inhibit the phosphorylation of JNK1/2/3,

ERK1/2 and/or c-Jun in IPF lung fibroblasts under basal conditions and in response to TGF-β1. Thereby, LRP1 may suppress α-SMA expression in these cells.

The effect of LRP1 on the phosphorylation of all tested kinases was analyzed by densitometry. To this end, the pixel density of each signal dot which had been detected on the nitrocellulose membrane was assessed. Mean pixel densities were calculated from the duplicates. In order to highlight the effect of LRP1-depletion on the phosphorylation of the tested kinases, the densitometric data were not presented for all four conditions which are described in figure 9 A. Instead, the mean pixel densities obtained from LRP1-expressing IPF lung fibroblasts were subtracted from their counterparts obtained from LRP1-depleted IPF lung fibroblasts (siLRP1 - siCtrl). This difference describes the change of kinase phosphorylation after LRP1-depletion under basal conditions in IPF lung fibroblasts. In the same way, the difference of the mean pixel densities obtained from LRP1-expressing and LRP1-depleted IPF lung fibroblasts after treatment with TGF-β1 was calculated ((siLRP1 + TGF-β1) - (siCtrl + TGF-β1)). This difference describes the change of kinase phosphorylation after knock-down of LRP1 in IPF lung fibroblasts and treatment with TGF-β1. In figure 9 B, the change of kinase phosphorylation after LRP1-knock-down and TGF-β1-treatment ((siLRP1 + TGF-β1) - (siCtrl + TGF-β1)) was plotted against the change in kinase phosphorylation after LRP1-depletion under basal conditions (siLRP1 - siCtrl).

The first and fourth quadrant of the graph contain values which describe an increase of the kinase phosphorylation after LRP1-depletion. In contrast, the second and third quadrant contain values which describe a decrease of the phospho-kinase levels when LRP1 is depleted. The majority of values is concentrated around zero and thus is not affected by depletion of LRP1 in IPF lung fibroblasts. However, the values of P-ERK1/2, P-JNK1/2/3 and P-c-Jun are located in the first quadrant and hence their phosphorylation was increased following LRP1-depletion. In comparison to all investigated kinases, the phosphorylation of ERK1/2 was promoted to the most in LRP1-deficient IPF lung fibroblasts under basal conditions. Figure 9 B furthermore shows the effect of TGF-β1 on the phosphorylation of the investigated kinases after LRP1-depletion. In detail, the first and second quadrant contain values which describe a TGF-β1-mediated increase of the kinase phosphorylation after knock-down of LRP1. Values in the third and fourth quadrant indicate a TGF-β1-mediated decrease of the

kinase phosphorylation when LRP1 is absent. Since the values of ERK1/2, JNK1/2/3 and c-Jun are located in the first quadrant, TGF-β1 promoted their phosphorylation in LRP1-depleted IPF lung fibroblasts. This experiment highlights ERK1/2, JNK1/2/3 and c-Jun as potential mediators of LRP1-dependent signal transduction in IPF lung fibroblasts. It is imaginable that LRP1 may inhibit the phosphorylation of ERK1/2, JNK1/2/3 and/or c-Jun to suppress α-SMA expression in these cells. This may be observed under basal conditions and in response to TGF-β1.

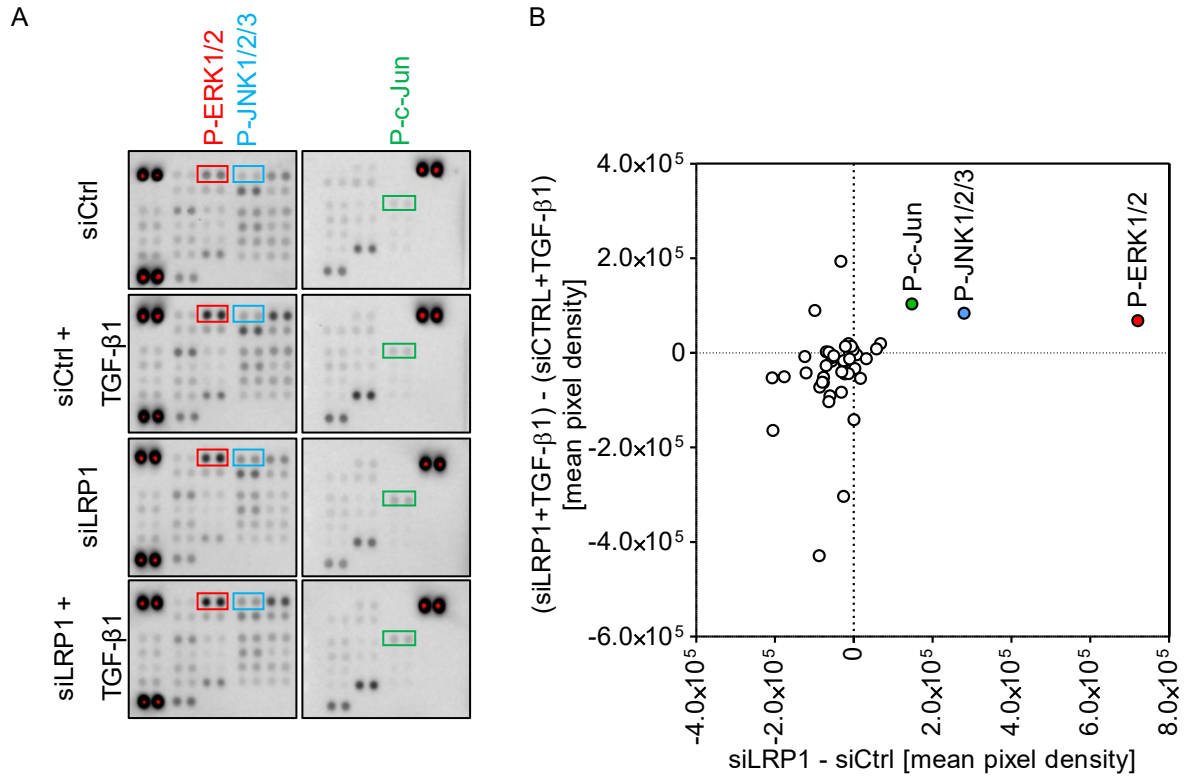


**Fig. 9: Analysis of kinase phosphorylation in LRP1-deficient IPF lung fibroblasts under basal conditions and after treatment with TGF-β1.** (A) A Proteome Profiler Human Phospho-Kinase Array was performed with protein lysates of LRP1-expressing and LRP1-depleted IPF lung fibroblasts either treated or untreated with 1 ng/ml TGF-β1 for 24 h. The signals of P-ERK1/2 (red), P-JNK1/2/3 (blue) and P-c-Jun (green) which occur in duplicate on the array membranes are highlighted. In the (B) densitometric analysis of the Proteome Profiler Human Phospho-Kinase Array, the difference ((siLRP1 + TGF-β1) - (siCtrl + TGF-β1)) of the mean pixel densities is plotted against the difference (siLRP1 - siCtrl) of the mean pixel densities. P-ERK1/2 (red), P-JNK1/2/3 (blue) and P-c-Jun (green) are highlighted. This experiment demonstrates that LRP1 may regulate the phosphorylation of ERK1/2, JNK1/2/3 and/or c-Jun in order to modulate signaling cascades in IPF lung fibroblasts. First quadrant: top right; second quadrant: top left; third quadrant: bottom left; fourth quadrant: bottom right.

## 4.6 LRP1 suppresses α-SMA expression by inhibiting the JNK signaling pathway in IPF lung fibroblasts

In chapter 4.5, it was described that LRP1 inhibits the phosphorylation of the kinases ERK1/2 and JNK1/2/3 as well as of the transcription factor c-Jun in IPF lung fibroblasts. In the present chapter, it is investigated whether these proteins mediate the LRP1-dependent regulation of α-SMA expression in IPF lung fibroblasts.

The most promising candidate among the aforementioned proteins is ERK1/2. In comparison to all investigated kinases, the phosphorylation of ERK1/2 was enhanced to the most following LRP1 silencing under basal conditions. In addition, TGF-β1 elevated ERK1/2 phosphorylation in LRP1-deficient IPF lung fibroblasts. In the literature, it was demonstrated that LRP1 activates ERK in order to potentiate TGF-β1-induced α-SMA expression in kidney fibroblasts [34].

The kinase MEK1/2 is the upstream activator of ERK1/2. Hence, blockage of MEK1/2 results in the inhibition of ERK1/2 activity. In order to determine whether ERK1/2 mediates LRP1-dependent α-SMA expression, MEK1/2 was blocked in LRP1-expressing and LRP1-deficient IPF lung fibroblasts by using the MEK1/2-specific inhibitor PD98059. The knock-down of LRP1 increased α-SMA expression in IPF lung fibroblasts as assessed by western blotting (Fig. 10 A, B). Treatment of cells with TGF-β1 elevated the α-SMA protein expression in both LRP1-expressing and LRP1-deficient IPF lung fibroblasts (Fig. 10 A, B). However, inhibition of MEK1/2 did not abrogate the induction of α-SMA expression following LRP1-depletion under basal conditions and after TGF-β1-stimulation (Fig. 10 A, B). Hence, LRP1 does not control ERK1/2 activation to suppress α-SMA expression in IPF lung fibroblasts.

It was furthermore investigated whether ERK1/2 mediates LRP1-dependent regulation of α-SMA expression in MEF. Knock-out of LRP1 led to the increase of α-SMA protein expression in these cells (Fig. 10 C). Pharmacological blockage of MEK1/2 in LRP1-expressing and -deficient MEF, however, had no effect on α-SMA expression (Fig. 10 C). This experiment demonstrates that ERK1/2 activation does not mediate the suppression of α-SMA by LRP1 in MEF.

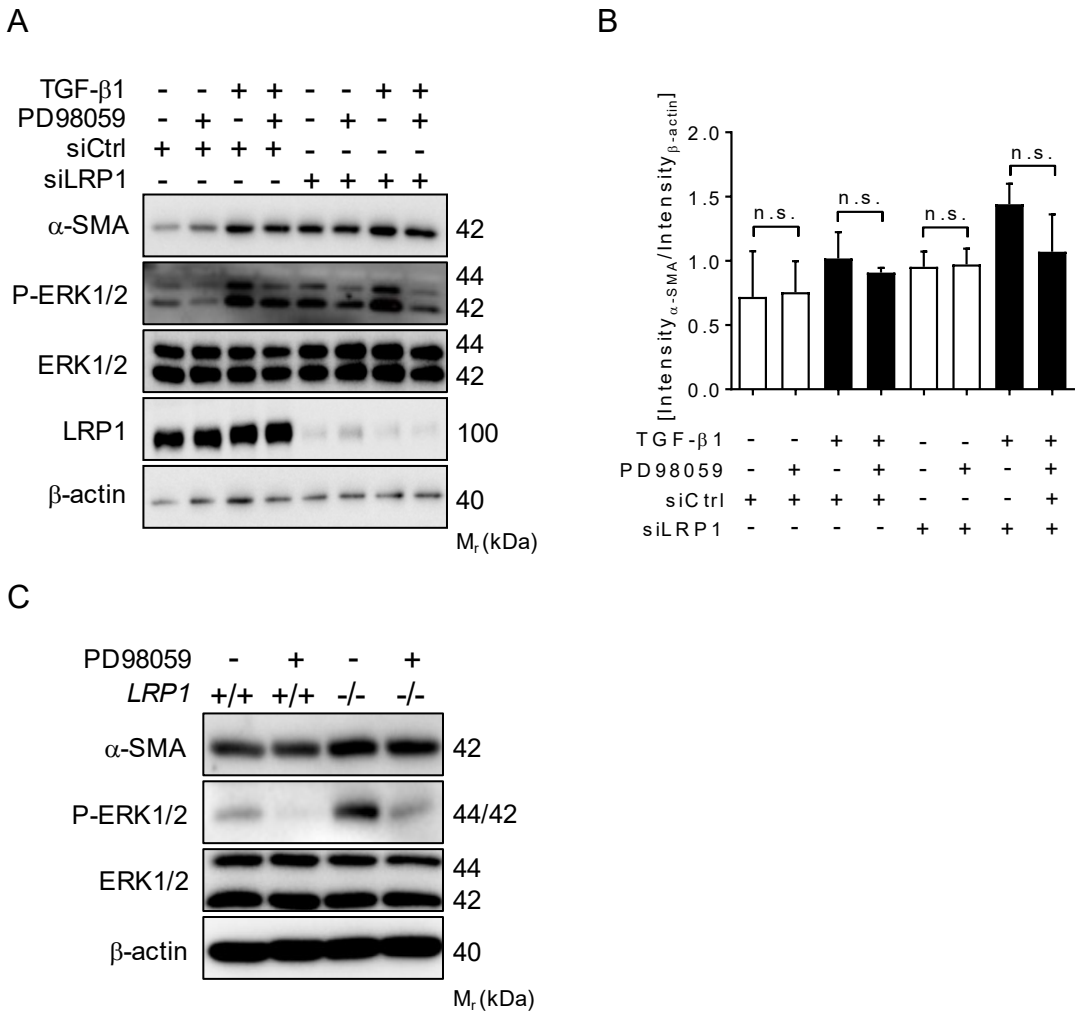


**Fig. 10: ERK1/2 has no effect on α-SMA expression following LRP1-depletion in IPF lung fibroblasts and MEF.** IPF lung fibroblasts were transfected with siLRP1 or siCtrl and treated with 1 ng/ml TGF-β1 and/or 20 µM MEK1/2 inhibitor PD98059 for 24 h. (A) The protein expression of α-SMA, ERK1/2 and LRP1 was assessed by western blotting. In addition, the activation of ERK1/2 was investigated by assessing the levels of P-ERK1/2. β-actin served as a loading control. n=3. Representative western blots are shown. (B) Densitometric analysis of α-SMA protein expression normalized to β-actin. n=3. (C) LRP1-expressing or -deficient MEF were treated with 20 µM MEK1/2 inhibitor PD98059 for 24 h. The protein expression of α-SMA and ERK1/2 was measured by western blotting. In addition, the activation of ERK1/2 was analyzed by assessing the levels of P-ERK1/2. β-actin served as a loading control. n=3. Representative western blots are displayed. Collectively, these data demonstrate that LRP1 does not suppress α-SMA by regulating ERK1/2 activation in IPF lung fibroblasts (panels (A) and (B)) and MEF (panel (C)).

As ERK1/2 did not mediate the suppression of α-SMA expression by LRP1 in IPF lung fibroblasts, JNK1/2/3 and its target c-Jun were investigated. The phosphorylation of both, JNK1/2/3 and c-Jun, was elevated following LRP1-depletion under basal conditions and after stimulation with TGF-β1 in IPF lung fibroblasts (Fig. 9 A, B). In

order to investigate whether JNK1/2/3 mediates LRP1-dependent suppression of α-SMA expression, JNK1/2/3 was inhibited with the JNK1/2/3 inhibitor SP600125 in LRP1-expressing and -deficient IPF lung fibroblasts. Knock-down of LRP1 enhanced α-SMA protein expression under basal conditions and after TGF-β1-stimulation in IPF lung fibroblasts (Fig. 11 A). Inhibition of JNK1/2/3 abrogated the increase of α-SMA following LRP1-depletion under both conditions (Fig. 11 A). In order to validate this result, the gene expression of LRP1 and JNK1 was silenced separately and in combination in IPF lung fibroblasts (Fig. 11 B). Thereafter, α-SMA protein expression was assessed by western blotting. LRP1-depletion increased α-SMA protein expression whereas JNK1-depletion did not affect α-SMA expression (Fig. 11 B). However, knock-down of JNK1 and LRP1 in combination abolished the induction of α-SMA expression which is observed following LRP1-depletion (Fig. 11 B). Collectively, these findings demonstrate that LRP1 inhibits JNK to suppress α-SMA expression in IPF lung fibroblasts. This was observed under basal conditions and following stimulation of IPF lung fibroblasts with TGF-β1.

In figure 11 B, also the relationship between LRP1, c-Jun and α-SMA is shown. To be specific, it is demonstrated that LRP1-depletion increases c-Jun protein levels in IPF lung fibroblasts (Fig. 11 B). Additional knock-down of JNK1 abrogated this increase of c-Jun protein expression (Fig. 11 B). Hence, JNK may mediate the LRP1-dependent suppression of α-SMA expression *via* c-Jun in IPF lung fibroblasts.

The role of JNK in the α-SMA regulation by LRP1 was also investigated in MEF. To this end, LRP1-expressing and -LRP1-defiecient MEF were treated with the JNK1/2/3 inhibitor SP600125 and the α-SMA expression was analyzed by western blotting. Whereas LRP1-depletion induced α-SMA protein expression, inhibition of JNK1/2/3 abolished this effect (Fig. 11 C). Thus, JNK1/2/3 mediates the LRP1-dependent suppression of α-SMA in MEF.

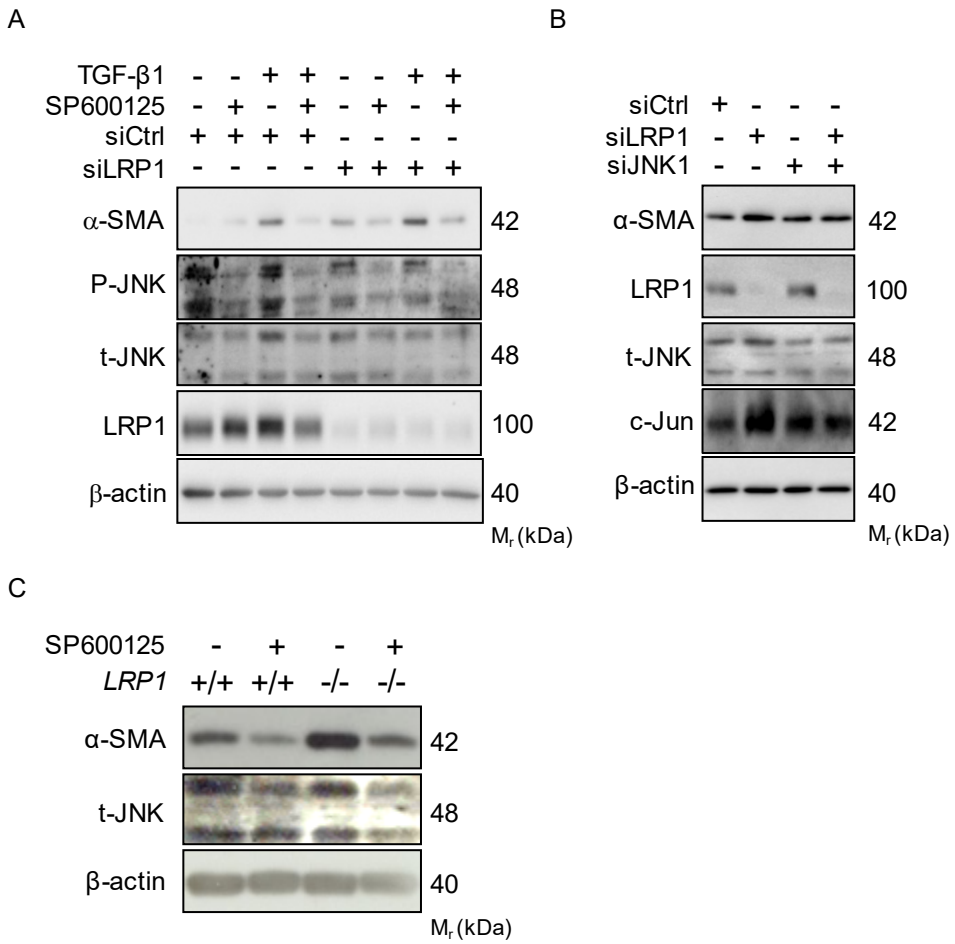


**Fig. 11: LRP1 suppresses α-SMA expression *via* JNK in IPF lung fibroblasts and MEF.** (A) IPF lung fibroblasts were transfected with siLRP1 or siCtrl and treated with 1 ng/ml TGF-β1 and/or 50 µM JNK1/2/3 inhibitor SP600125 for 24 h. The protein expression of α-SMA, t-JNK and LRP1 was analyzed by western blotting. Moreover, the activation of JNK was investigated by assessing the levels of P-JNK. β-actin served as a loading control. Representative western blots are shown. n=3. (B) Protein expression of α-SMA, LRP1, t-JNK and c-Jun in IPF lung fibroblasts after knock-down of LRP1 and/or JNK1 as assessed by western blotting. β-actin served as a loading control. n=3. Representative western blots are shown. (C) LRP1-expressing and LRP1-knock-out MEF were treated with 50 µM JNK1/2/3 inhibitor SP600125 for 24 h. Analysis of the protein expression of α-SMA and t-JNK was performed by western blotting. β-actin served as a loading control. n=2. Representative western blots are shown. Panels (A) and (B) indicate that LRP1-dependent suppression of α-SMA expression is mediated by JNK in IPF lung fibroblasts. JNK may mediate LRP1-dependent inhibition of α-SMA *via* c-Jun in these cells (panel B). Panel (C) shows that JNK mediates LRP1-dependent suppression of α-SMA in MEF.

In the present study, the role of the kinase p38 in the LRP1-dependent regulation of α-SMA expression was investigated in IPF lung fibroblasts. The interest in this kinase was based on its well descried role in the regulation of α-SMA expression during fibroblast to myofibroblast transdifferentiation. In detail, it has been demonstrated that

application of mechanical forces to fibroblasts results in the phosphorylation of p38 [106]. As a consequence, p38 promotes α-SMA expression in these cells [106].
However, it must be emphasized that the phosphorylation of p38 was only slightly affected by LRP1-depletion in IPF lung fibroblasts. Membrane-based antibody array revealed that knock-down of LRP1 slightly decreased the phosphorylation of p38 under basal conditions (siLRP1 - siCtrl: -60,703) and after TGF-β1-stimulation ((siLRP1 + TGF-β1) - (siCtrl + TGF-β1): -91,036). Hence, the results of the present study do not suggest p38 as a mediator of the LRP1-dependent suppression of α-SMA expression in IPF lung fibroblasts. Nonetheless, the effect of p38 on the LRP1-dependent regulation of α-SMA expression was investigated in these cells. To this end, LRP1-expressing and LRP1-depleted IPF lung fibroblasts were treated with the p38 inhibitor SB203580 and/or TGF-β1. Whereas TGF-β1 induced α-SMA protein expression in LRP1-expressing and LRP1-deficient IPF lung fibroblasts, inhibition of p38 had no effect on α-SMA protein expression in these both cell types (Fig. 12). Altogether, the data show that LRP1 does not regulate p38 to suppress α-SMA expression in IPF lung fibroblasts.

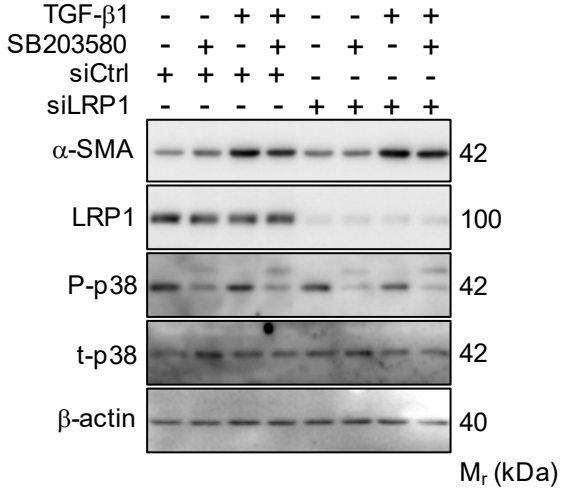


**Fig. 12: p38 is not involved in LRP1-dependent regulation of α-SMA expression in IPF lung fibroblasts.** LRP1-expressing and -deficient IPF lung fibroblasts were treated with 1 ng/ml TGF-β1 and/or 10 µM p38 inhibitor SB203580 for 24 h. The protein expression of α-SMA, LRP1 and t-p38 was measured by western blotting. In addition, the activation of p38 was investigated by assessing the levels of P-p38. β-actin served as a loading control. n=1. This experiment shows that p38 is not a mediator of LRP1-dependent suppression of α-SMA expression in IPF lung fibroblasts.

The transcription factor AP1, which exists as a number of dimeric complexes formed by members of the Jun (including c-Jun), Fos and ATF families, is a well described

downstream target of JNK1/2/3 [122]. As shown in figure 11 B, LRP1-depletion enhanced the protein level of c-Jun in a JNK1-dependent manner in IPF lung fibroblasts. In order to identify whether LRP1 regulates the transcriptional activity of AP1, LRP1-expressing and LRP1-deficient IPF lung fibroblasts were transfected with pGL4.44-AP1 firefly reporter and pRL-SV40 renilla reporter. The pGL4.44-AP1 firefly reporter contains six copies of an AP1-binding consensus element. Moreover, the cells were either treated or untreated with TGF-β1. Dual-Luciferase Reporter Assay demonstrated that LRP1-deficiency results in the increase of AP1 transcriptional activity (Fig. 13). In addition, TGF-β1 elevated the transcriptional activity of AP1 further and to a stronger extend in LRP1-depleted IPF lung fibroblasts than in control cells (Fig. 13). Altogether, these data indicate that LRP1 suppresses the transcriptional activity of AP1 under basal conditions in IPF lung fibroblasts. Furthermore, LRP1 limits the TGF-β1-induced increase of the AP1 transcriptional activity in these cells.

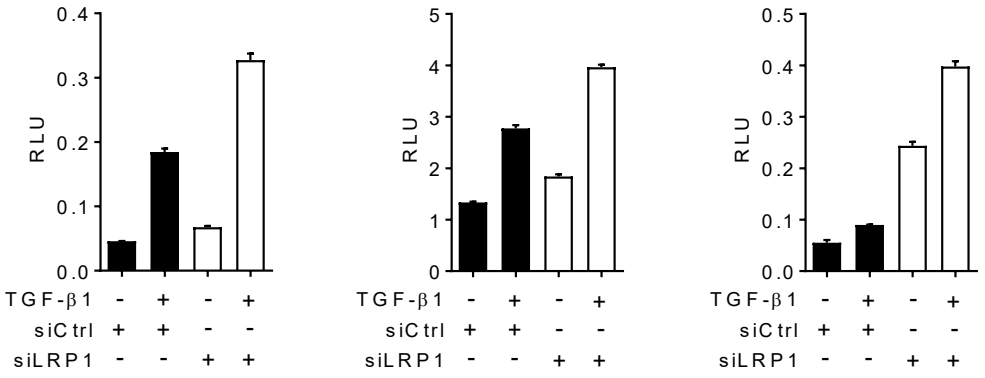


**Fig. 13: LRP1 suppresses the transcriptional activity of AP1 in IPF lung fibroblasts.** IPF lung fibroblasts were transfected with siLRP1 or siCtrl as well as with pGL4.44-AP1 firefly reporter and pRL-SV40 renilla reporter and treated with 1 ng/ml TGF-β1 for 24 h. Dual-Luciferase Reporter Assay was performed to determine the transcriptional activity of AP1. n=3. The results of all three experiments are presented separately. Per experiment, the measurement was performed in triplicate. Data are expressed as mean values ± S.E.M. This experiment reveals that LRP1 suppresses the transcriptional activity of AP1 under basal conditions in IPF lung fibroblasts. In addition, LRP1 limits the TGF-β1-mediated increase of AP1 transcriptional activity in these cells.

## 4.7 LRP1-deficiency enhances the contractile activity of IPF lung fibroblasts

As LRP1-depletion upregulated the myofibroblast marker α-SMA in IPF lung fibroblasts, it was further analyzed if loss of LRP1 also promotes the generation of the contractile myofibroblast phenotype. To this end, the contraction of floating collagen gels

by LRP1-expressing and LRP1-deficient IPF lung fibroblasts was assessed under basal conditions or in response to TGF-β1. The reduction of the collagen gel surface area during contraction negatively correlates with the contractile activity of the cells. Hence, the more the surface area of a collagen gel is reduced, the higher is the contractile activity of the cells in this collagen gel.

After 3 h, IPF lung fibroblasts had contracted the collagen gels (Fig. 14 A). However, the surface area of the collagen gels was similar under all conditions (Fig. 14 A, B). Thus, knock-down of LRP1 did not modulate the contractile activity of IPF lung fibroblasts at this time point (Fig. 14 A, B). In addition, TGF-β1 did not affect the contractile activity of IPF lung fibroblasts at the 3 h time point (Fig. 14 A, B). After 24 h, IPF lung fibroblasts further contracted the collagen gels (Fig. 14 A). LRP1-deficient IPF lung fibroblasts contracted the collagen gel more than LRP1-expressing IPF lung fibroblasts (Fig. 14 A). Accordingly, the surface area of the collagen gel containing LRP1-deficient IPF lung fibroblasts was smaller than the surface area of the collagen gel containing LRP1-expressing IPF lung fibroblasts (Fig. 14 C).

Moreover, stimulation with TGF-β1 potentiated the contraction of the collagen gels by LRP1-expressing and LRP1-depleted IPF lung fibroblasts (Fig. 14 A). Interestingly, this effect was stronger in LRP1-deficient than in LRP1-expressing IPF lung fibroblasts (Fig. 14 A). Accordingly, the surface area of the collagen gel containing LRP1-deficient, TGF-β1-stimulated IPF lung fibroblasts was the smallest in comparison to the surface area of the other collagen gels (Fig. 14 C). Altogether, these results demonstrate that LRP1 suppresses the contraction of IPF lung fibroblasts. Furthermore, LRP1 limits the TGF-β1-induced increase of the contractile activity of these cells.

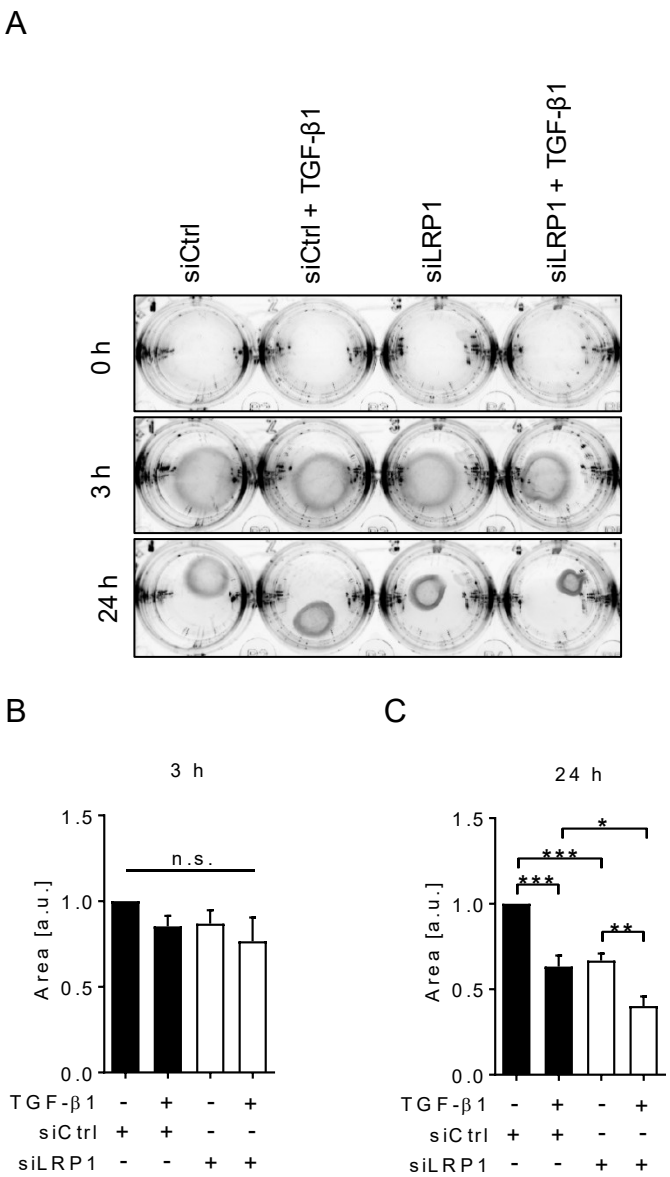


**Fig. 14: LRP1-deficiency increases the contractile activity of IPF lung fibroblasts.** (A) IPF lung fibroblasts were transfected with siLRP1 or siCtrl and embedded into floating collagen gels 48 h after siRNA transfection and 24 h after treatment with 10 ng/ml TGF-β1. The contraction of the collagen gels was documented after 0 h, 3 h and 24 h. n=5. Representative pictures are shown. The surface area of the collagen gels after (B) 3 h and (C) 24 h is presented in arbitrary units. n=5. Data are expressed as mean values ± S.E.M. Collectively, these data show that LRP1 inhibits the contractile activity of IPF lung fibroblasts. In addition, LRP1 limits the TGF-β1-mediated elevation of the contractile activity of these cells.

As there is evidence that myofibroblasts may show enhanced proliferation [123–125], it was analyzed whether LRP1 is involved in the proliferation of IPF lung fibroblasts. To this end, the DNA of LRP1-expressing and LRP1-deficient IPF lung fibroblasts was stained by propidium iodide. Subsequent analysis by flow cytometry revealed that the majority of IPF lung fibroblasts (around 80%) were in the G1 phase of the cell

cycle (Fig. 15 A). Ten percent of the cells were in the S phase and other ten percent of the cells were in the G2/M phase of the cell cycle (Fig 15 B, C). The knock-down of LRP1 had no effect on the proliferation of IPF lung fibroblasts as the amount of cells in the G2/M phase remained unaffected (Fig. 15 C). These data indicate that LRP1 does not regulate the proliferation of IPF lung fibroblasts.

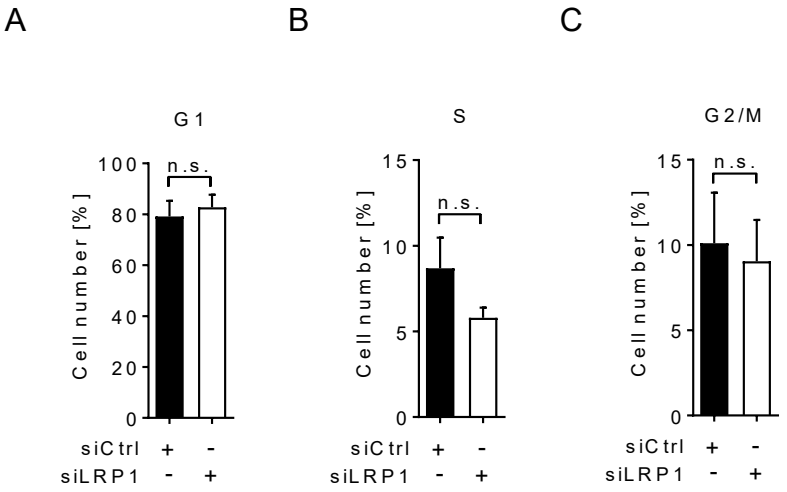


**Fig. 15: LRP1 does not regulate the proliferation of IPF lung fibroblasts.** IPF lung fibroblasts were transfected with siLRP1 or siCtrl for 96 h and cell proliferation was assessed by propidium iodide staining of the DNA. The detection of DNA-bound propidium iodide was performed by flow cytometry. Percentage of cells in the (A) G1, (B) S and (C) G2/M phase of the cell cycle. n=3. Data are expressed as mean values ± S.E.M. This experiment demonstrates that LRP1 does not regulate the proliferation of IPF lung fibroblasts.

Furthermore, the role of LRP1 in the migration of IPF lung fibroblasts was investigated. Therefore, LRP1-expressing and LRP1-deficient IPF lung fibroblasts were seeded into the two chambers of culture inserts and allowed to migrate into the gap between these two chambers after removal of the silicone insert. After 19 h, cells had migrated into the gap (Fig. 16 A) but LRP1-expressing and -deficient IPF lung fibroblasts showed no difference in the migratory potential (Fig. 16 A). In addition, TGF-β1 had no effect on the migration of IPF lung fibroblasts (Fig. 16 A). Hence, neither LRP1 nor TGF-β1 regulate the migratory potential of IPF lung fibroblasts. Figure 16 B shows the surface area of the cell layers which were formed after 19 h of migration under the four conditions. Here, it becomes also apparent that neither LRP1-depletion nor treatment with TGF-β1 affected the migratory potential of IPF lung fibroblasts.

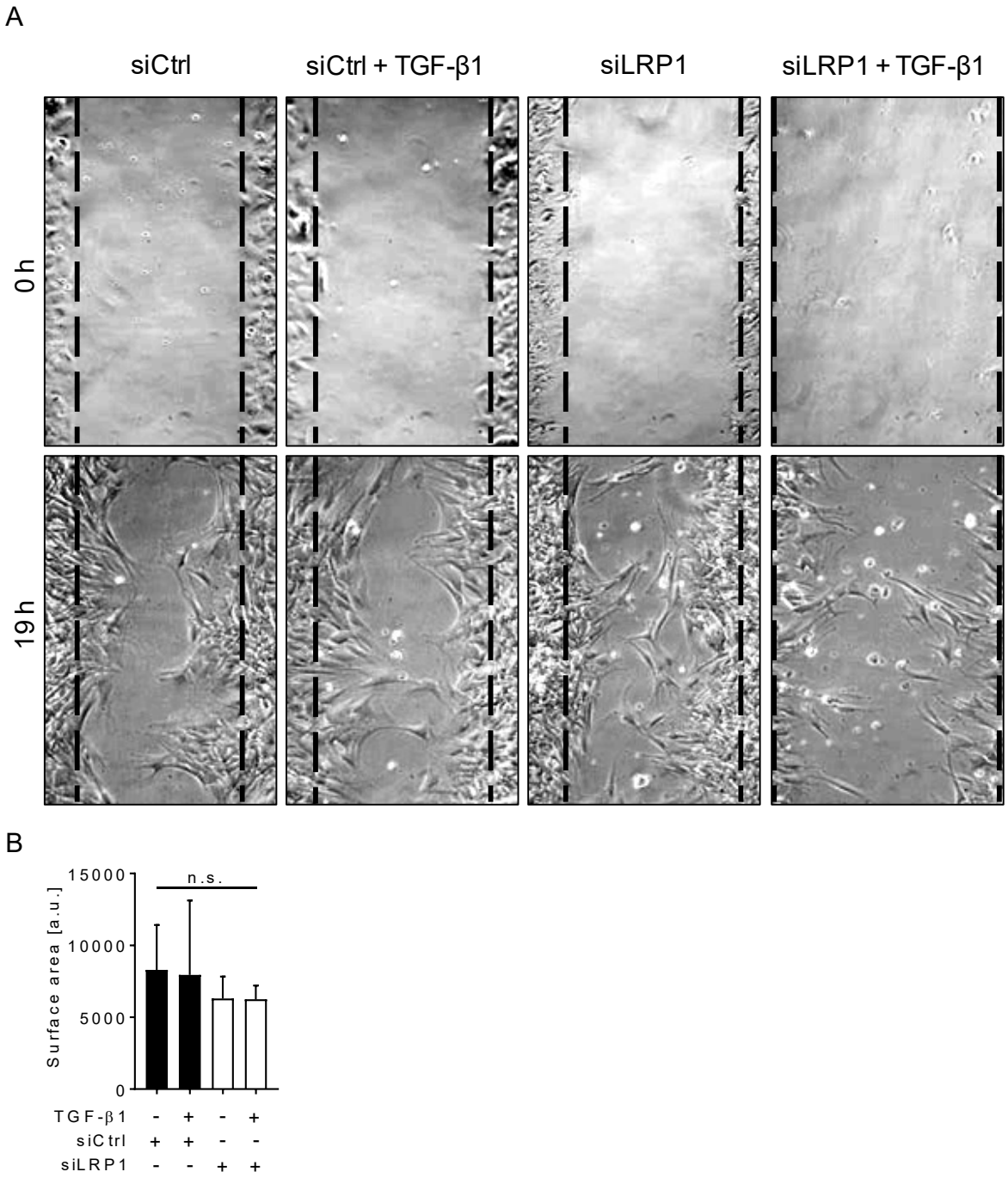


**Fig. 16: LRP1 does not regulate the migration of IPF lung fibroblasts.** After transfection of IPF lung fibroblasts with siLRP1 or siCtrl for 48 h and treatment with 10 ng/ml TGF-β1 for 24 h, cells were seeded into the chambers of a silicone insert. After removal of the silicone insert, cells migrated into the gap between the cell patches. (A) The cell migration was documented after 0 h and 19 h. n=4. Representative pictures are displayed. (B) The surface area of the cell layer in the gap after 19 h of migration is presented in arbitrary units for all four conditions. n=4. Data are expressed as mean values ± S.E.M. The experiment shows that neither LRP1 nor TGF-β1 regulate the migratory potential of IPF lung fibroblasts.

# 5 Discussion

## 5.1 LRP1 suppresses α-SMA expression in IPF lung fibroblasts

Wound healing is a process of tightly controlled tissue remodeling events. Dynamic changes in the ECM, cell migration, proliferation and differentiation belong to these events. Fibroblasts are of central importance during tissue remodeling. These cells first migrate into the lesion where they proliferate and form a large population [24]. Secondly, fibroblasts in this population differentiate to myofibroblasts, the key mediators of wound repair [24]. These α-SMA expressing, high contractile cells strongly secrete ECM components which rebuild an ECM matrix in the lesion [31,32]. Here, it becomes apparent that dysregulated acquisition and persistence of myofibroblasts lead to imbalanced tissue repair, such as scarring. Fibroblast to myofibroblast transdifferentiation is controlled in several manners, e.g. by cytokine expression and matrix rigidity. Interestingly, LRP1 was described to regulate fibroblast to myofibroblast transdifferentiation as well [34,126,127]. LRP1 is an endocytic receptor which is known to be involved in tissue remodeling, e.g. by regulating the catabolism of fibronectin and by modulating ECM-crosslinking or -degrading enzymes [7,16,36,42–44]. The functions of LRP1 in fibroblast to myofibroblast transdifferentiation are described hereafter. In kidney fibroblasts, CTGF mediates the phosphorylation of LRP1 which subsequently enhances the TGF-β1-induced α-SMA expression and thus the differentiation of fibroblasts to myofibroblasts [34]. In a similar manner, tissue plasminogen activator (tPA) promotes the TGF-β1-dependent induction of α-SMA and collagen I *via* LRP1 in kidney fibroblasts [126]. In detail, binding of tPA to LRP1 induces the phosphorylation of the latter [126]. As a consequence, LRP1 recruits β1 integrin and thus permits activation of integrin-linked kinase [126]. This kinase mediates a signaling which results in enhanced α-SMA and collagen I expression in kidney fibroblasts [126]. Hence, tPA promotes fibroblast to myofibroblast transdifferentiation in a LRP1-dependent manner in kidney fibroblasts [126]. Besides, tPA protects kidney fibroblasts from apoptosis *via* LRP1 [128]. In hepatic stellate cells, however, tPA-mediated phosphorylation of LRP1 results in the Akt activation and in the decreased α-SMA protein and *collagen I* gene expression [127]. Thus, LRP1 protects hepatic stellate cells from differentiation to myofibroblasts [127]. These findings indicate that the functions of LRP1 are cell type-specific. The role of LRP1 in the differentiation of

pulmonary fibroblasts to myofibroblast has not been described yet. In the present work, a microarray analysis was performed and demonstrated that the Kegg pathways which describe cytoskeleton remodeling processes are significantly perturbed in IPF lung fibroblasts but not in donor lung fibroblasts following LRP1-depletion. The finding that LRP1 affects pathways which are responsible for cytoskeleton rearrangements gives a hint that LRP1 may indeed be involved in the generation of the myofibroblast phenotype in IPF lung fibroblasts. Changes in the cytoskeleton adopt myofibroblasts to the enhanced mechanical stress which occurs during wound healing. In this process, the formation of stress fibers as well as the expression and incorporation of α-SMA into stress fibers are fundamental [73–75]. For instance, the incorporation of α-SMA into stress fibers permits the formation and maintenance of suFa [74,75]. suFa can transmit a fourfold higher external tension than mature Fa [75]. Moreover, α-SMA expression is a prerequisite for the expression of collagen by myofibroblasts [63]. Therewith, uncontrolled fibroblast to myofibroblast transdifferentiation leads to uncontrolled collagen deposition which results in scar formation. The fact that silencing of *LRP1* gene expression affects cytoskeleton-related Kegg pathways in IPF lung fibroblasts but not in donor lung fibroblasts indicates that this effect depends on the pathological condition. It is imaginable that the pathological constitution primes IPF lung fibroblasts. According to the Two-Hit Hypothesis, primed cells show an exaggerated reaction to a second hit. Hence, the myofibroblast phenotype may be easier induced in IPF lung fibroblasts than in donor lung fibroblasts. Indeed, it is observed that fibroblast-like cells which are located in fibroblastic foci of IPF lungs express α-SMA [123–125]. Thus, these cells are considered to represent the myofibroblast phenotype whereas donor lung fibroblasts rather represent the fibroblast phenotype without traits of myofibroblasts. The present study indicates that loss of LRP1 may be a second hit which triggers the uncontrolled differentiation of IPF lung fibroblasts to myofibroblasts. The consequence of this event may be scar formation. An explanation why LRP1 may be a second hit trigger in IPF lung fibroblasts is given hereafter.

The microarray revealed that knock-down of LRP1 significantly perturbed Kegg pathways which describe endocytic processes in donor lung fibroblasts but not in IPF lung fibroblasts. Therefore, priming of IPF lung fibroblasts may switch the function of LRP1 from endocytic to signal transducing in IPF lung fibroblasts. As a consequence, LRP1 becomes a regulator of fibroblast to myofibroblast transdifferentiation in these

cells. As mentioned above, α-SMA is expressed and incorporated into stress fibers during fibroblast to myofibroblast transdifferentiation [73–75]. Below, experiments which were performed to show whether LRP1 regulates α-SMA expression in IPF lung fibroblasts, are described. Analysis of LRP1 and α-SMA mRNA levels in IPF lung fibroblasts which were derived from different IPF patients revealed that lower levels of LRP1 correlate with higher α-SMA levels. Knock-out of LRP1 in MEF resulted in elevated *α-SMA* gene expression. In addition, LRP1-depletion enhanced α-SMA protein expression in IPF lung fibroblasts and MEF. Thus, LRP1 suppresses the generation of the myofibroblast phenotype in these cell types. Since fibroblast to myofibroblast transdifferentiation is crucial for wound healing, the expression of LRP1 may be transiently downregulated in order to induce α-SMA expression in fibroblasts after injury. Reexpression of LRP1 may occur in the resolution phase of wound healing and limit fibroblast to myofibroblast transdifferentiation. In contrast, permanently reduced LRP1 expression may promote the exaggerated acquisition of myofibroblasts in fibrosis. As the accumulation of α-SMA-positive myofibroblasts drives the progression of pulmonary fibrosis [63], loss of LRP1 in lung fibroblasts may accelerate the disease progression.

## 5.2 LRP1 ICD does not serve as transcription factor to regulate α-SMA expression

Besides its endocytic function, LRP1 can regulate the expression of genes by either modulating signaling cascades or *via* its ICD which can act as a transcription factor [110]. The liberation of the ICD requires the shedding of the extracellular domain of LRP1 by metalloproteinases and the subsequent processing of the membrane-bound fraction by γ-secretase [109,110]. LRP1 ICD as a transcription factor is known in the context of inflammation [109]. Therein, lipopolysaccharide (LPS) promotes LRP1 ectodomain shedding and thus the subsequent release of ICD [109]. LRP1 ICD limits the expression of interferon γ during the LPS-dependent inflammatory response [109]. The results of the present study, however, demonstrate that the ICD of LRP1 does not suppress *α-SMA* gene expression in MEF. This experiment was performed with MEF as a model system because it could not be conducted with IPF lung fibroblasts due to technical reasons.

## 5.3 The regulation of α-SMA expression by LRP1 is independent of the canonical TGF-β1 pathway in IPF lung fibroblasts

TGF-β1 is a key mediator of fibroblast to myofibroblast transdifferentiation [72]. This cytokine was found to induce α-SMA expression *via* the canonical mediator SMAD3 [73]. LRP1 was found to suppress the canonical TGF-β1 signaling in vascular smooth muscle cells [129]. Hence, it was investigated in the present study whether LRP1 modulates α-SMA expression in a SMAD3-dependent manner in IPF lung fibroblasts. The data of the present study indicate that neither the SMAD3 expression nor the SMAD3 activation are regulated by LRP1 in IPF lung fibroblasts. Furthermore, Dual-Luciferase Reporter Assay with the SMAD3-binding consensus sequence CAGA showed that LRP1 does not modulate the transcriptional activity of SMAD3 in these cells. Finally, it was also demonstrated that SMAD3 does not mediate LRP1-dependent suppression of α-SMA expression in IPF lung fibroblasts as knock-down of SMAD3 did not block the increase of α-SMA expression after LRP1-depletion. Intriguingly, an increase of the SMAD2 protein expression was observed in IPF lung fibroblasts following LRP1-depletion. However, this increase did not affect the activation of SMAD2 in LRP1-deficient IPF lung fibroblasts. The role of LRP1-dependent induction of SMAD2 in IPF lung fibroblasts remains to be investigated. Altogether, the data show that LRP1 does not modulate the canonical TGF-β1 signaling pathway in IPF lung fibroblasts.

It has to be emphasized that LRP1 has an opposite effect on SMAD3 expression in IPF lung fibroblasts and MEF. Whereas SMAD3 expression remained unaffected by LRP1-depletion in IPF lung fibroblasts, knock-out of LRP1 elevated the gene and protein expression of SMAD3 in MEF. In addition, subcellular fractionation revealed that SMAD3 levels in both, the cytoplasm and the nucleus are elevated when LRP1 is absent in MEF. Since knock-out of LRP1 in MEF elevated the SMAD3 levels in the nucleus, an increase of the transcriptional activity of SMAD3 was expected. However, the transcriptional activity of SMAD3 was not affected in LRP1-deficient MEF under basal conditions. Instead, LRP1-depletion enhanced the transcriptional activity of SMAD3 only in response to TGF-β1 in MEF. The finding that LRP1 suppresses the TGF-β1-dependent transcriptional activity of SMAD3 in MEF is opposed to the finding obtained in IPF. Whether the inhibition of SMAD3 transcriptional activity by LRP1 regulates TGF-β1-induced α-SMA expression in MEF remains to be investigated.

In the present study it was furthermore demonstrated that knock-out of LRP1 shortened the duration of phosphorylation in the C-terminus and the linker region of SMAD2 in MEF. Whereas phosphorylation of the SMAD2 C-terminus is required for the translocation of SMAD2 to the nucleus [113–115], phosphorylation in the linker region can either promote or block this process [116,117]. Further investigation is needed to assess whether LRP1 affects the transcriptional activity of SMAD2 and if so, whether LRP1 regulates α-SMA expression *via* SMAD2 in MEF.

The different effects of LRP1 on SMAD2 and SMAD3 in IPF lung fibroblasts and MEF may be explained by the properties of these cells. Whereas MEF are embryonic cells, IPF lung fibroblasts are terminally differentiated cells. The embryonic MEF have characteristics of fibroblasts but can also develop into tissues from all three germ layers [130]. This feature is called pluripotency and is a characteristic of embryonic stem cells. Terminally differentiated fibroblasts, such as IPF lung fibroblasts, are not pluripotent. Hence, IPF lung fibroblasts may differentiate to myofibroblasts by transdifferentiation. In this process, a differentiated cell type converts to another differentiated cell type without going through a pluripotent cell state. MEF, however, may rather undergo transdetermination in order to differentiate to myofibroblasts. In transdetermination, a progenitor cell switches lineage commitment in order to develop to a related cell type. Here, it becomes evident that several mechanisms may mediate the differentiation of fibroblasts to myofibroblasts, depending on the developmental state of the cell. Similarly, priming of IPF lung fibroblasts may modify the mechanisms by which IPF lung fibroblasts differentiate to myofibroblasts. These suggestions may explain the inconsistencies which were obtained concerning the effect of LRP1-depletion on SMAD2 and SMAD3 in IPF lung fibroblasts and MEF.

## 5.4 LRP1 suppresses α-SMA expression by inhibiting the JNK signaling pathway in IPF lung fibroblasts

LRP1 participates in signal transduction by regulating the activity of various kinases, such as mitogen-activated kinases, phosphatidylinositol 3-kinase/Akt and Rho-like GTPases [119–121,131,132]. As LRP1 does not have enzymatic functions, it serves as docking site for scaffolding and adaptor proteins which bring kinases and their substrates in close proximity [3,8–10]. In many cases, tyrosine phosphorylation of the cytoplasmic domain of LRP1 is required for the binding of scaffolding and adaptor proteins [8–10]. Also in fibroblast to myofibroblast transdifferentiation, LRP1 was de-

scribed to modulate signaling cascades. For instance, the previously mentioned tPA-mediated suppression of the myofibroblast phenotype in hepatic stellate cells requires the activation of Akt in a LRP1-dependent manner [127]. However, the promotion of the TGF-β1-induced differentiation of kidney fibroblasts to myofibroblasts by CTGF is mediated by LRP1-dependent activation of ERK1/2 [34]. The results of the present study demonstrate that the levels of activated ERK1/2 are increased after LRP1-depletion in IPF lung fibroblasts and MEF but that ERK1/2 is not involved in the LRP1-dependent regulation of α-SMA expression in these cell types. The kinase p38 was found to promote α-SMA expression following the application of mechanical forces to fibroblasts [106]. Since mechanical forces increase after injury, p38 may regulate fibroblast to myofibroblast transdifferentiation during wound healing. In the literature, p38 was demonstrated to be activated in a LRP1-associated manner during LRP1-dependent internalization of β-amyloid protein in neurons and astrocytes in the mouse brain [121]. However, a link between LRP1 and p38 in fibroblasts has not been described yet. In the present study, it was demonstrated that LRP1-depletion results only in the slight decrease of p38 activity under basal conditions and in response to TGF-β1 in IPF lung fibroblasts. Furthermore, pharmacological inhibition of p38 did also not affect α-SMA expression in LRP1-deficient IPF lung fibroblasts. From these findings it is concluded that LRP1 does not affect p38 activation to suppress α-SMA expression in IPF lung fibroblasts.

Since the present study demonstrated that P-JNK is increased after LRP1-depletion under basal conditions and following TGF-β1-stimulation in IPF lung fibroblasts it was investigated whether LRP1 regulates α-SMA *via* JNK. To this end, JNK was pharmacologically blocked in LRP1-deficient IPF lung fibroblasts and MEF and also a simultaneous knock-down of LRP1 and JNK1 was performed in IPF lung fibroblasts. Both, blocking of JNK and silencing of JNK1, abrogated α-SMA increase after LRP1-depletion. Thus, these experiments indicate that LRP1 suppresses α-SMA expression by inhibiting JNK in IPF lung fibroblasts. The present study describes for the first time that LRP1 regulates JNK activity in the context of fibroblast to myofibroblast transdifferentiation. In the literature, regulation of JNK by LRP1 has been described in other biological contexts. For instance, it was observed that LRP1 supports the invasion of follicular thyroid carcinoma cells by suppressing JNK and promoting ERK [120]. Another example is that LRP1 suppresses the JNK and NF-κB pathways in

microglia and thus limits the expression of pro-inflammatory cytokines in response to LPS [133].

The data of the present study furthermore revealed that the levels of active and total c-Jun, a downstream-target of JNK, are enhanced by LRP1 knock-down in IPF lung fibroblasts. In addition, the knock-down of JNK1 partially reversed the LRP1-mediated increase of total c-Jun. Depending on the biological context, c-Jun can serve as a component of the transcription factor AP1 [122]. In general, AP1 occurs as dimeric complexes which are formed by members of the Jun, Fos and ATF families [122]. In the present study, Dual-Luciferase Reporter Assay with a vector containing AP1-binding consensus elements revealed that the transcriptional activity of AP1 is enhanced after *LRP1* gene silencing under basal conditions in IPF lung fibroblasts. Depletion of LRP1 also enhances the TGF-β1-dependent transcriptional activity of AP1. Altogether, the data indicate that LRP1 suppresses α-SMA expression and therewith the generation of the myofibroblast phenotype by limiting the JNK/AP1 signaling pathway in IPF lung fibroblasts (Fig. 17). By inhibiting this signaling pathway, LRP1 can regulate α-SMA expression in two different manners in these cells (Fig. 17). First, LRP1 can suppress α-SMA expression independent of TGF-β1 (Fig. 17). Second, LRP1 can limit the TGF-β1-induced α-SMA expression in IPF lung fibroblasts (Fig. 17). In the literature, it had already been demonstrated that TGF-β1 can mediate α-SMA expression in human lung fibroblasts in a JNK-dependent manner [134]. TGF-β1 is a key inducer of fibroblast to myofibroblast transdifferentiation and its expression is tightly regulated during wound healing [72,135]. The capability of LRP1 to regulate α-SMA expression in the absence of TGF-β1 may implicate potential dangers. For instance, uncontrolled loss of LRP1 during wound healing may result in the ongoing differentiation of fibroblasts to myofibroblasts even when the TGF-β1 levels are declining in the later stage of wound healing. The potentiation of the TGF-β1-induced α-SMA expression following LRP1 loss may also prolong the phase of fibroblast to myofibroblast transdifferentiation during wound healing. The consequence of these scenarios would be the uncontrolled deposition of ECM components by myofibroblasts which leads to pathological tissue scarring.

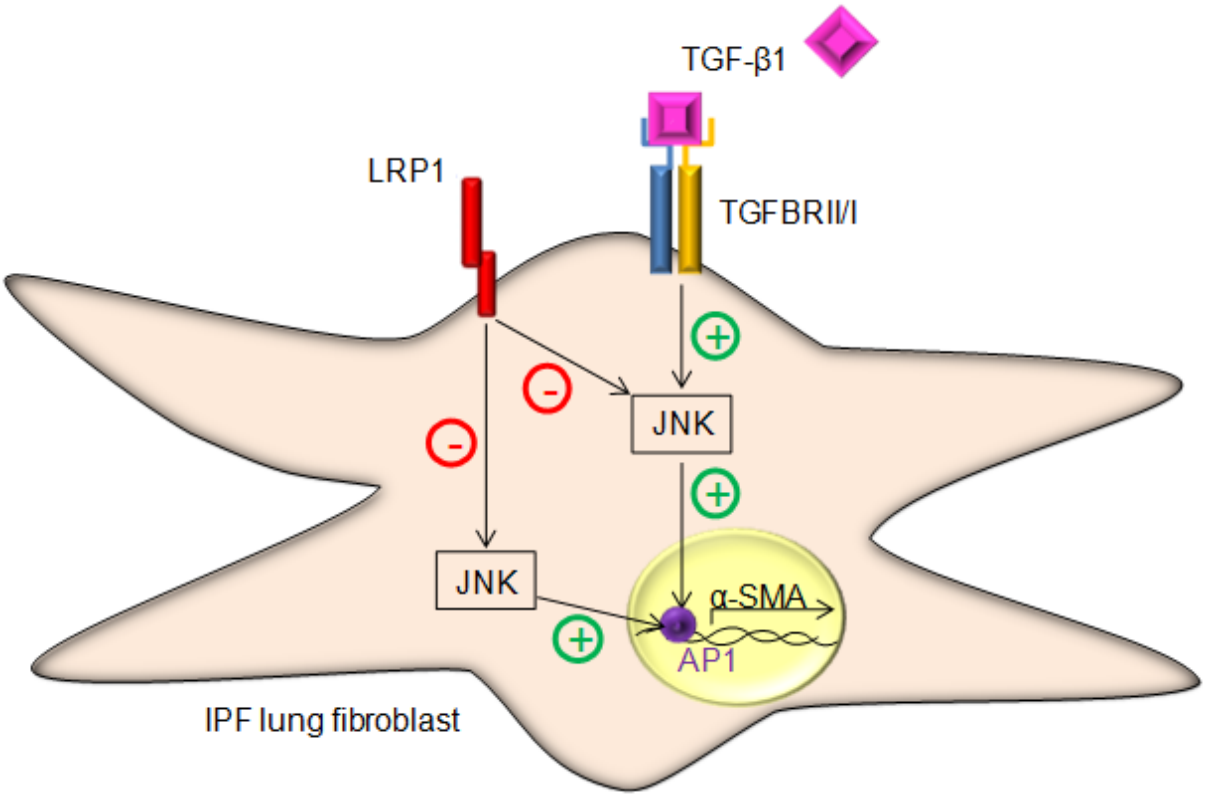


**Fig. 17: LRP1 suppresses α-SMA expression by inhibiting the TGF-β1-dependent and -independent JNK/AP1 signaling in IPF lung fibroblasts.** LRP1 suppresses α-SMA expression in IPF lung fibroblasts by inhibiting JNK which subsequently limits the transcriptional activity of AP1. By inhibiting the JNK/AP1 signaling pathway, LRP1 can suppress α-SMA expression independent of TGF-β1 in these cells. In addition, LRP1 can limit the TGF-β1-mediated induction of α-SMA by blocking the JNK/AP1 signaling in IPF lung fibroblasts. TGF-β1: transforming growth factor-β1; TGFBRII/I: transforming growth factor-β receptor type II/I; LRP1: low density lipoprotein receptor-related protein 1; JNK: c-Jun N-terminal kinase; α-SMA: α-smooth muscle actin.

Since LRP1 was demonstrated to suppress fibroblast to myofibroblast transdifferentiation by inhibiting the JNK/AP1 pathway, the latter is another potential therapeutic target to counteract uncontrolled acquisition of myofibroblasts after LRP1 loss in IPF lung fibroblasts. The orally active JNK inhibitor CC-930 blocks phosphorylation of c-Jun [136]. It was tested as anti-fibrotic drug in the house dust mite (HDM)-induced mouse model of airway fibrosis [137]. Therein, CC-930 reduced the levels of phosphorylated c-Jun in the lungs of HDM-treated mice. In addition, CC-930 inhibited the levels of MMP7, which is also an IPF marker, and collagen deposition after HSM-treatment [137]. CC-930 was tested in a phase II multicenter study of mild/moderate IPF [137]. In this study, a trend of decrease of MMP7 and SP-D in the plasma was described after treatment with CC-930 [137]. However, no conclusions about the effect of CC-930 on pulmonary function could be withdrawn [137]. In addition, the study was terminated early because of adverse events [137]. The most common adverse events were the increase of alanine aminotransferase (ALT), the increase of

aspartate aminotransferase (AST) and infection of the upper respiratory tract [137]. Since the increase of ALT and AST in the blood indicates liver damage, these adverse events showed that CC-930 exhibits liver toxicity. Hence, further development of JNK inhibiting drugs is needed.

### 5.5 LRP1-deficiency enhances the contractile activity of IPF lung fibroblasts

Myofibroblasts are characterized by high contractile activity [31]. This function requires the incorporation of α-SMA into stress fibers [73–75]. For instance, it was demonstrated that delivery of a fusion protein containing the N-terminal sequence AcEEED of α-SMA results in the selective removal of α-SMA from stress fibers [99]. As a consequence, the contractile activity of myofibroblasts decreased [100]. By contracting granulation tissue myofibroblasts support wound healing [33]. In addition, the contractile activity of myofibroblasts was described to promote their own maturation in a feed forward loop by activating latent TGF-β1 [89]. In this process integrins on the myofibroblast surface bind LAP in the latent TGF-β1 [89]. Thereafter, myofibroblast contraction induces conformational changes in the latent TGF-β1 and thus permits the liberation of active TGF-β1 [89]. The present study indicates that LRP1 suppresses α-SMA expression by inhibiting the JNK/AP1 pathway in IPF lung fibroblasts. It is furthermore demonstrated that LRP1-depletion results in increased contractile activity of these cells. Interestingly, this effect is even stronger in response to TGF-β1. Therewith, transient reduction of LRP1 expression in lung fibroblasts may contribute to the acquisition and persistence of the α-SMA-positive, high contractile myofibroblast phenotype during wound healing. In the literature, however, LRP1 was described to mediate the lactoferrin-induced increase in the contractile activity of WI-38 fibroblasts [138]. Lactoferrin is a ligand of LRP1 [139] and exerts multiple functions in wound healing, such as regulation of the inflammatory phase as well as fibroblast migration and proliferation [140]. In the lung, bronchial glands secrete lactoferrin into the airway lumen [141] where it protects the lung from antioxidants [142]. A change in the levels of lactoferrin has not yet been described in IPF. Hence, further research is required to investigate whether lactoferrin regulates the contraction of fibroblasts in IPF.

As a regulator of fibroblast to myofibroblast transdifferentiation, LRP1 may also be involved in the development of IPF. This chronic progressive disease is considered to result from repeated epithelial injury which is accompanied by expansion of the

fibroblast population [143]. A characteristic of IPF is the accumulation of myofibroblasts in the interstitial space and in the alveolar spaces where they excessively produce ECM and thus mediate scarring of the lung [143]. It is imaginable that LRP1 may be permanently lost in fibroblasts in IPF. The mechanisms by which LRP1 expression is regulated in IPF remain elusive. However, restoration of LRP1 expression in IPF lung fibroblasts may provide a therapeutic approach against IPF. In human retinal pigment epithelial cells, the LRP1 expression was elevated by TGF-β1 and TGF-β2 [144]. In the IPF lung, TGF-β1 levels are increased [145]. Hence, it would be interesting to investigate whether LRP1 expression may also be regulated by TGF-β1 in IPF lung fibroblasts. It is imaginable that this cytokine has a different effect in IPF lung fibroblasts than in human retinal pigment epithel cells. Thus, the enhanced levels of TGF-β1 in the IPF lung may suppress LRP1 expression in IPF lung fibroblasts. The expression of TGF-β2 is not changed in the IPF lung [145]. Therefore, TGF-β2 may not regulate LRP1 expression in IPF lung fibroblasts.

There is evidence that myofibroblasts may have enhanced proliferative properties in the fibrotic foci of IPF patients. For instance, inactivation of the transcription factor forkhead box O3a (FoxO3a) was identified to promote IPF lung fibroblast proliferation on polymerized type I collagen [123]. Polymerized type I collagen had been shown to suppress fibroblast proliferation [146]. Interestingly, immunostaining of lung tissue from IPF patients and controls identified inactive FoxO3a to localize mainly in the IPF fibroblastic foci [123]. As the majority of fibroblasts in fibroblastic foci are α-SMA-positive and hence represent the myofibroblast phenotype, inactivation of FoxO3a may indeed increase myofibroblast proliferation [123]. Another study identified low levels of the collagen receptor $\alpha_2\beta_1$ integrin in IPF lung fibroblasts and showed proliferation of these cells on polymerized type I collagen [124]. Moreover, cells in IPF fibroblastic foci were found to express low levels of $\alpha_2\beta_1$ integrin [124]. Hence, a decrease of $\alpha_2\beta_1$ integrin expression may promote myofibroblast proliferation in IPF. Other authors demonstrated that low levels of caveolin-1 enhance proliferation of primary mouse lung fibroblasts on polymerized type I collagen [125]. Furthermore, low expression of caveolin-1 was seen in IPF lung fibroblasts *in vitro* and in IPF fibroblastic foci *in vivo* [125]. These findings indicate that reduced caveolin-1 expression may promote myofibroblast proliferation in IPF. Intriguingly, LRP1 was described to modulate fibroblast proliferation. For example, LRP1-depletion switches the

TGF-β1 function from anti- to proproliferative [30]. In human hepatic stellate cells, LRP1 suppresses proliferation by inhibiting ERK1/2 activation and reducing extracellular levels of TGF-β [147]. However, in rat kidney interstitial fibroblasts, tPA promotes proliferation by LRP1 [148]. In detail, after phosphorylation in the C-terminus, LRP1 mediates phosphorylation of ERK1/2, p90RSK and GSK3β [148]. Ultimately, cyclin D1 is induced [148]. Cyclin D1 promotes proliferation by mediating G1-S-phase transition [149]. Despite the described role of LRP1 in fibroblast proliferation, the data of the present study indicate that LRP1 does not regulate the proliferative potential of IPF lung fibroblasts.

Besides the aforementioned enhanced proliferation of IPF lung fibroblasts *in vitro*, it was demonstrated that fibroblasts isolated from IPF patients show higher migratory activity than control cells [150]. In the literature, it was described that LRP1 regulates the migratory potential of fibroblasts. For instance, PAI-1 promotes migration of MEF by activating the β-catenin pathway and ERK1/2 in a LRP1-dependent manner [151]. Furthermore, LRP1 mediates activation, endocytosis and degradation of β1-integrin and thus facilitates migration of MEF on fibronectin [152]. LRP1 also suppresses migration of human hepatic stellate cells by regulating ERK1/2 activation and extracellular TGF-β levels [147]. The present study, however, reveals that LRP1 does not regulate the migratory potential of IPF lung fibroblasts.

Collectively, the present study demonstrates that LRP1 suppresses α-SMA expression and the generation of high contractile activity in IPF lung fibroblasts by inhibiting the JNK/AP1 pathway. By limiting the JNK/AP1 signaling, LRP1 regulates α-SMA expression in two manners in IPF lung fibroblasts. First, LRP1 suppresses α-SMA expression independent of TGF-β1. Second, LRP1 limits the TGF-β1-induced α-SMA expression. Hence, loss of LRP1 may prolong the phase of TGF-β1-induced differentiation of fibroblast to myofibroblast during wound healing. In addition, uncontrolled reduction of LRP1 levels may permit ongoing fibroblast to myofibroblast transdifferentiation even when TGF-β1 levels decline in the later stage of wound healing. As a consequence, exaggerated ECM deposition by myofibroblasts may occur and lead to pathological tissue scarring.

# 6 Conclusions

The differentiation of fibroblasts to myofibroblasts is a key event in wound healing. Myofibroblasts are characterized by α-SMA expression and high contractile activity. This cell type produces large amounts of ECM components which rebuild an ECM in the lesion. Hence, uncontrolled acquisition of myofibroblasts results in imbalanced wound repair, such as scarring. Fibroblast to myofibroblast transdifferentiation is regulated both by cytokines, such as TGF-β1, and by matrix rigidity. In addition, the endocytic receptor LRP1 was demonstrated to be involved in this process. Mostly, LRP1 was found to promote or suppress α-SMA expression by modulating the TGF-β1 responses. However, its role in the regulation of α-SMA expression in lung fibroblasts remained elusive.

In the present study, it was demonstrated that LRP1 suppresses α-SMA expression on the mRNA and protein level in IPF lung fibroblasts. Moreover, LRP1 suppressed the contractile activity of IPF lung fibroblasts. In order to regulate α-SMA expression, LRP1 inhibited the activity of JNK. As a consequence, the transcriptional activity of AP1 was reduced. Altogether, the present study proposes for the first time a mechanism by which LRP1 limits the differentiation of IPF lung fibroblasts to myofibroblasts. Therewith, it is assumed that LRP1 may protect the lung from scar formation after injury. However, further research effort is needed in order to prove this suggestion. Since scarring of the lung parenchyma occurs in IPF, future studies may investigate whether LRP1 expression is downregulated in the lung fibroblasts of IPF patients and whether LRP1 expression correlates with scarring and disease progression.

# 7 References

[1] J. Herz, D.K. Strickland, LRP: a multifunctional scavenger and signaling receptor, The Journal of clinical investigation 108 (2001) 779–784.

[2] Y. Li, J. Cam, G. Bu, Low-density lipoprotein receptor family, Molecular neurobiology 23 (2001) 53–67.

[3] J. Herz, U. Hamann, S. Rogne, O. Myklebost, H. Gausepohl, K.K. Stanley, Surface location and high affinity for calcium of a 500-kd liver membrane protein closely related to the LDL-receptor suggest a physiological role as lipoprotein receptor, The EMBO journal 7 (1988) 4119–4127.

[4] J.G. Neels, B.M. van den Berg, A. Lookene, G. Olivecrona, H. Pannekoek, A.J. van Zonneveld, The second and fourth cluster of class A cysteine-rich repeats of the low density lipoprotein receptor-related protein share ligand-binding properties, The Journal of biological chemistry 274 (1999) 31305–31311.

[5] T.-Y. Ling, C.-L. Chen, Y.-H. Huang, I.-H. Liu, S.S. Huang, J.S. Huang, Identification and characterization of the acidic pH binding sites for growth regulatory ligands of low density lipoprotein receptor-related protein-1, The Journal of biological chemistry 279 (2004) 38736–38748.

[6] I. Mikhailenko, F.D. Battey, M. Migliorini, J.F. Ruiz, K. Argraves, M. Moayeri, D.K. Strickland, Recognition of alpha 2-macroglobulin by the low density lipoprotein receptor-related protein requires the cooperation of two ligand binding cluster regions, The Journal of biological chemistry 276 (2001) 39484–39491.

[7] Y. Li, M.P. Marzolo, P. van Kerkhof, G.J. Strous, G. Bu, The YXXL motif, but not the two NPXY motifs, serves as the dominant endocytosis signal for low density lipoprotein receptor-related protein, The Journal of biological chemistry 275 (2000) 17187–17194.

[8] M. Trommsdorff, J.P. Borg, B. Margolis, J. Herz, Interaction of cytosolic adaptor proteins with neuronal apolipoprotein E receptors and the amyloid precursor protein, The Journal of biological chemistry 273 (1998) 33556–33560.

[9] W. Klug, A. Dietl, B. Simon, I. Sinning, K. Wild, Phosphorylation of LRP1 regulates the interaction with Fe65, FEBS letters 585 (2011) 3229–3235.

[10] H. Barnes, B. Larsen, M. Tyers, P. van der Geer, Tyrosine-phosphorylated low density lipoprotein receptor-related protein 1 (Lrp1) associates with the adaptor protein SHC in SRC-transformed cells, The Journal of biological chemistry 276 (2001) 19119–19125.

[11] H. Emonard, L. Théret, A.H. Bennasroune, S. Dedieu, Regulation of LRP-1 expression, Pathologie-biologie 62 (2014) 84–90.

[12] L. Wujak, J. Schnieder, L. Schaefer, M. Wygrecka, LRP1. A chameleon receptor of lung inflammation and repair, Matrix biology journal of the International Society for Matrix Biology (2017).

[13] T. Kanekiyo, J.R. Cirrito, C.-C. Liu, M. Shinohara, J. Li, D.R. Schuler, M. Shinohara, D.M. Holtzman, G. Bu, Neuronal clearance of amyloid-β by endocytic receptor LRP1, The Journal of neuroscience the official journal of the Society for Neuroscience 33 (2013) 19276–19283.

[14] G. Rastegarlari, J.N. Pegon, C. Casari, S. Odouard, A.-M. Navarrete, N. Saint-Lu, B.J. van Vlijmen, P. Legendre, O.D. Christophe, C.V. Denis, P.J. Lenting, Macrophage LRP1 contributes to the clearance of von Willebrand factor, Blood 119 (2012) 2126–2134.

[15] E.L. Saenko, A.V. Yakhyaev, I. Mikhailenko, D.K. Strickland, A.G. Sarafanov, Role of the low density lipoprotein-related protein receptor in mediation of factor VIII catabolism, The Journal of biological chemistry 274 (1999) 37685–37692.

[16] M. Wygrecka, J. Wilhelm, E. Jablonska, D. Zakrzewicz, K.T. Preissner, W. Seeger, A. Guenther, P. Markart, Shedding of low-density lipoprotein receptor–related protein-1 in acute respiratory distress syndrome, American journal of respiratory and critical care medicine 184 (2011) 438–448.

[17] P. Boucher, J. Herz, Signaling through LRP1: Protection from atherosclerosis and beyond, Biochemical pharmacology 81 (2011) 1–5.

[18] M. Shinohara, M. Tachibana, T. Kanekiyo, G. Bu, Role of LRP1 in the pathogenesis of Alzheimer's disease: evidence from clinical and preclinical studies, Journal of lipid research 58 (2017) 1267–1281.

[19] L. Lin, K. Hu, LRP-1: functions, signaling and implications in kidney and other diseases, International journal of molecular sciences 15 (2014) 22887–22901.

[20] A.P. Lillis, L.B. van Duyn, J.E. Murphy-Ullrich, D.K. Strickland, LDL receptor-related protein 1: unique tissue-specific functions revealed by selective gene knockout studies, Physiological reviews 88 (2008) 887–918.

[21] A. Rohlmann, M. Gotthardt, R.E. Hammer, J. Herz, Inducible inactivation of hepatic LRP gene by cre-mediated recombination confirms role of LRP in clearance of chylomicron remnants, The Journal of clinical investigation 101 (1998) 689–695.

[22] S.M. Hofmann, L. Zhou, D. Perez-Tilve, T. Greer, E. Grant, L. Wancata, A. Thomas, P.T. Pfluger, J.E. Basford, D. Gilham, J. Herz, M.H. Tschöp, D.Y. Hui, Adipocyte LDL receptor-related protein-1 expression modulates postprandial lipid transport and glucose homeostasis in mice, The Journal of clinical investigation 117 (2007) 3271–3282.

[23] M. Yepes, M. Sandkvist, E.G. Moore, T.H. Bugge, D.K. Strickland, D.A. Lawrence, Tissue-type plasminogen activator induces opening of the blood-brain barrier via the LDL receptor-related protein, The Journal of clinical investigation 112 (2003) 1533–1540.

[24] I.A. Darby, B. Laverdet, F. Bonté, A. Desmoulière, Fibroblasts and myofibroblasts in wound healing, Clinical, cosmetic and investigational dermatology 7 (2014) 301–311.

[25] R.A.S. Ariëns, T.-S. Lai, J.W. Weisel, C.S. Greenberg, P.J. Grant, Role of factor XIII in fibrin clot formation and effects of genetic polymorphisms, Blood 100 (2002) 743–754.

[26] N. Laurens, P. Koolwijk, M.P.M. de Maat, Fibrin structure and wound healing, Journal of thrombosis and haemostasis JTH 4 (2006) 932–939.

[27] T.A. Tucker, L. Williams, K. Koenig, H. Kothari, A.A. Komissarov, G. Florova, A.P. Mazar, T.C. Allen, K. Bdeir, L.V. Mohan Rao, S. Idell, Lipoprotein receptor-related protein 1 regulates collagen 1 expression, proteolysis, and migration in human pleural mesothelial cells, American journal of respiratory cell and molecular biology 46 (2012) 196–206.

[28] F. Blasi, N. Sidenius, The urokinase receptor: focused cell surface proteolysis, cell adhesion and signaling, FEBS letters 584 (2010) 1923–1930.

[29] J.C. Chapin, K.A. Hajjar, Fibrinolysis and the control of blood coagulation, Blood reviews 29 (2015) 17–24.

[30] S.S. Huang, T.-Y. Ling, W.-F. Tseng, Y.-H. Huang, F.-M. Tang, S.M. Leal, J.S. Huang, Cellular growth inhibition by IGFBP-3 and TGF-beta1 requires LRP-1, FASEB journal official publication of the Federation of American Societies for Experimental Biology 17 (2003) 2068–2081.

[31] B. Hinz, G. Celetta, J.J. Tomasek, G. Gabbiani, C. Chaponnier, Alpha-smooth muscle actin expression upregulates fibroblast contractile activity, Molecular biology of the cell 12 (2001) 2730–2741.

[32] F. Klingberg, B. Hinz, E.S. White, The myofibroblast matrix. Implications for tissue repair and fibrosis, The Journal of pathology 229 (2013) 298–309.

[33] B. Hinz, D. Mastrangelo, C.E. Iselin, C. Chaponnier, G. Gabbiani, Mechanical Tension Controls Granulation Tissue Contractile Activity and Myofibroblast Differentiation, The American journal of pathology 159 (2001) 1009–1020.

[34] M. Yang, H. Huang, J. Li, D. Li, H. Wang, Tyrosine phosphorylation of the LDL receptor-related protein (LRP) and activation of the ERK pathway are required for connective tissue growth factor to potentiate myofibroblast differentiation, FASEB journal official publication of the Federation of American Societies for Experimental Biology 18 (2004) 1920–1921.

[35] K.G.F. Gerritsen, N. Bovenschen, T.Q. Nguyen, D. Sprengers, M.P. Koeners, A.N. van Koppen, J.A. Joles, R. Goldschmeding, R.J. Kok, Rapid hepatic clearance of full length CCN-2/CTGF, Journal of cell communication and signaling 10 (2016) 295–303.

[36] A.M. Salicioni, K.S. Mizelle, E. Loukinova, I. Mikhailenko, D.K. Strickland, S.L. Gonias, The low density lipoprotein receptor-related protein mediates fibronectin catabolism and inhibits fibronectin accumulation on cell surfaces, The Journal of biological chemistry 277 (2002) 16160–16166.

[37] A. Gaultier, M. Hollister, I. Reynolds, E.-h. Hsieh, S.L. Gonias, LRP1 regulates remodeling of the extracellular matrix by fibroblasts, Matrix biology journal of the International Society for Matrix Biology 29 (2010) 22–30.

[38] J.M. Orban, L.B. Wilson, J.A. Kofroth, M.S. El-Kurdi, T.M. Maul, D.A. Vorp, Crosslinking of collagen gels by transglutaminase, Journal of biomedical materials research. Part A 68 (2004) 756–762.

[39] S.S. Akimov, A.M. Belkin, Cell-surface transglutaminase promotes fibronectin assembly via interaction with the gelatin-binding domain of fibronectin, Journal of cell science 114 (2001) 2989–3000.

[40] W. Bains, Transglutaminse 2 and EGGL, the protein cross-link formed by transglutaminse 2, as therapeutic targets for disabilities of old age, Rejuvenation research 16 (2013) 495–517.

[41] K.C. Olsen, R.E. Sapinoro, R.M. Kottmann, A.A. Kulkarni, S.E. Iismaa, G.V.W. Johnson, T.H. Thatcher, R.P. Phipps, P.J. Sime, Transglutaminase 2 and Its Role in Pulmonary Fibrosis, American journal of respiratory and critical care medicine 184 (2011) 699–707.

[42] E.A. Zemskov, I. Mikhailenko, D.K. Strickland, A.M. Belkin, Cell-surface transglutaminase undergoes internalization and lysosomal degradation, Journal of cell science 120 (2007) 3188–3199.

[43] H. Emonard, G. Bellon, L. Troeberg, A. Berton, A. Robinet, P. Henriet, E. Marbaix, K. Kirkegaard, L. Patthy, Y. Eeckhout, H. Nagase, W. Hornebeck, P.J. Courtoy, Low density lipoprotein receptor-related protein mediates endocytic clearance of pro-MMP-2.TIMP-2 complex through a thrombospondin-independent mechanism, The Journal of biological chemistry 279 (2004) 54944–54951.

[44] E. Hahn-Dantona, J.F. Ruiz, P. Bornstein, D.K. Strickland, The low density lipoprotein receptor-related protein modulates levels of matrix metalloproteinase 9 (MMP-9) by mediating its cellular catabolism, The Journal of biological chemistry 276 (2001) 15498–15503.

[45] A. Moustakas, S. Souchelnytskyi, C.H. Heldin, Smad regulation in TGF-beta signal transduction, Journal of cell science 114 (2001) 4359–4369.

[46] H.L. Moses, R.J. Coffey, E.B. Leof, R.M. Lyons, J. Keski-Oja, Transforming growth factor beta regulation of cell proliferation, Journal of cellular physiology. Supplement Suppl 5 (1987) 1–7.

[47] H.L. Moses, R. Serra, Regulation of differentiation by TGF-beta, Current opinion in genetics & development 6 (1996) 581–586.

[48] B.A. Hocevar, P.H. Howe, Analysis of TGF-beta-mediated synthesis of extracellular matrix components, Methods in molecular biology (Clifton, N.J.) 142 (2000) 55–65.

[49] N. Schuster, K. Krieglstein, Mechanisms of TGF-beta-mediated apoptosis, Cell and tissue research 307 (2002) 1–14.

[50] M.O. Li, Y.Y. Wan, S. Sanjabi, A.-K.L. Robertson, R.A. Flavell, Transforming growth factor-beta regulation of immune responses, Annual review of immunology 24 (2006) 99–146.

[51] J.W. Penn, A.O. Grobbelaar, K.J. Rolfe, The role of the TGF-β family in wound healing, burns and scarring, International journal of burns and trauma 2 (2012) 18–28.

[52] M. Whitman, Smads and early developmental signaling by the TGFbeta superfamily, Genes & development 12 (1998) 2445–2462.

[53] M. Shi, J. Zhu, R. Wang, X. Chen, L. Mi, T. Walz, T.A. Springer, Latent TGF-β structure and activation, Nature 474 (2011) 343–349.

[54] M. Wang, Di Zhao, G. Spinetti, J. Zhang, L.-Q. Jiang, G. Pintus, R. Monticone, E.G. Lakatta, Matrix metalloproteinase 2 activation of transforming growth factor-beta1 (TGF-beta1) and TGF-beta1-type II receptor signaling within the aged arterial wall, Arteriosclerosis, thrombosis, and vascular biology 26 (2006) 1503–1509.

[55] L. Zawel, J. Le Dai, P. Buckhaults, S. Zhou, K.W. Kinzler, B. Vogelstein, S.E. Kern, Human Smad3 and Smad4 Are Sequence-Specific Transcription Activators, Molecular Cell 1 (1998) 611–617.

[56] Y.E. Zhang, Non-Smad pathways in TGF-beta signaling, Cell research 19 (2009) 128–139.

[57] K.H. Wrighton, X. Lin, X.-H. Feng, Phospho-control of TGF-beta superfamily signaling, Cell research 19 (2009) 8–20.

[58] F. Furukawa, K. Matsuzaki, S. Mori, Y. Tahashi, K. Yoshida, Y. Sugano, H. Yamagata, M. Matsushita, T. Seki, Y. Inagaki, M. Nishizawa, J. Fujisawa, K. Inoue, p38 MAPK mediates fibrogenic signal through Smad3 phosphorylation in rat myofibroblasts, Hepatology (Baltimore, Md.) 38 (2003) 879–889.

[59] I. Yakymovych, P. ten Dijke, C.H. Heldin, S. Souchelnytskyi, Regulation of Smad signaling by protein kinase C, FASEB journal official publication of the Federation of American Societies for Experimental Biology 15 (2001) 553–555.

[60] M.E. Engel, M.A. McDonnell, B.K. Law, H.L. Moses, Interdependent SMAD and JNK signaling in transforming growth factor-beta-mediated transcription, The Journal of biological chemistry 274 (1999) 37413–37420.

[61] S. Mori, K. Matsuzaki, K. Yoshida, F. Furukawa, Y. Tahashi, H. Yamagata, G. Sekimoto, T. Seki, H. Matsui, M. Nishizawa, J.-i. Fujisawa, K. Okazaki, TGF-beta and HGF transmit the signals through JNK-dependent Smad2/3 phosphorylation at the linker regions, Oncogene 23 (2004) 7416–7429.

[62] A.K. Kamaraju, A.B. Roberts, Role of Rho/ROCK and p38 MAP kinase pathways in transforming growth factor-beta-mediated Smad-dependent growth inhibition of human breast carcinoma cells in vivo, The Journal of biological chemistry 280 (2005) 1024–1036.

[63] K. Zhang, M.D. Rekhter, D. Gordon, S.H. Phan, Myofibroblasts and their role in lung collagen gene expression during pulmonary fibrosis. A combined immuno-

histochemical and in situ hybridization study, The American journal of pathology 145 (1994) 114–125.

[64] K.K. Kim, M.C. Kugler, P.J. Wolters, L. Robillard, M.G. Galvez, A.N. Brumwell, D. Sheppard, H.A. Chapman, Alveolar epithelial cell mesenchymal transition develops in vivo during pulmonary fibrosis and is regulated by the extracellular matrix, Proceedings of the National Academy of Sciences of the United States of America 103 (2006) 13180–13185.

[65] B.C. Willis, J.M. Liebler, K. Luby-Phelps, A.G. Nicholson, E.D. Crandall, R.M. Du Bois, Z. Borok, Induction of epithelial-mesenchymal transition in alveolar epithelial cells by transforming growth factor-beta1, The American journal of pathology 166 (2005) 1321–1332.

[66] L.-J. Chen, H. Ye, Q. Zhang, F.-Z. Li, L.-J. Song, J. Yang, Q. Mu, S.-S. Rao, P.-C. Cai, F. Xiang, J.-C. Zhang, Y. Su, J.-B. Xin, W.-L. Ma, Bleomycin induced epithelial-mesenchymal transition (EMT) in pleural mesothelial cells, Toxicology and applied pharmacology 283 (2015) 75–82.

[67] K. Barth, J. Reh, A. Sturrock, M. Kasper, Epithelial vs myofibroblast differentiation in immortal rat lung cell lines--modulating effects of bleomycin, Histochemistry and cell biology 124 (2005) 453–464.

[68] R. Abe, S.C. Donnelly, T. Peng, R. Bucala, C.N. Metz, Peripheral blood fibrocytes: differentiation pathway and migration to wound sites, Journal of immunology (Baltimore, Md. 1950) 166 (2001) 7556–7562.

[69] R.J. Phillips, M.D. Burdick, K. Hong, M.A. Lutz, L.A. Murray, Y.Y. Xue, J.A. Belperio, M.P. Keane, R.M. Strieter, Circulating fibrocytes traffic to the lungs in response to CXCL12 and mediate fibrosis, The Journal of clinical investigation 114 (2004) 438–446.

[70] M. Schmidt, G. Sun, M.A. Stacey, L. Mori, S. Mattoli, Identification of circulating fibrocytes as precursors of bronchial myofibroblasts in asthma, Journal of immunology (Baltimore, Md. 1950) 171 (2003) 380–389.

[71] N. Hashimoto, H. Jin, T. Liu, S.W. Chensue, S.H. Phan, Bone marrow–derived progenitor cells in pulmonary fibrosis, The Journal of clinical investigation 113 (2004) 243–252.

[72] A. Desmoulière, A. Geinoz, F. Gabbiani, G. Gabbiani, Transforming growth factor-beta 1 induces alpha-smooth muscle actin expression in granulation tissue

myofibroblasts and in quiescent and growing cultured fibroblasts, The Journal of cell biology 122 (1993) 103–111.

[73] L. Gu, Y.-J. Zhu, X. Yang, Z.-J. Guo, W.-B. Xu, X.-L. Tian, Effect of TGF-beta/Smad signaling pathway on lung myofibroblast differentiation, Acta pharmacologica Sinica 28 (2007) 382–391.

[74] B. Hinz, V. Dugina, C. Ballestrem, B. Wehrle-Haller, C. Chaponnier, Alpha-smooth muscle actin is crucial for focal adhesion maturation in myofibroblasts, Molecular biology of the cell 14 (2003) 2508–2519.

[75] J.M. Goffin, P. Pittet, G. Csucs, J.W. Lussi, J.-J. Meister, B. Hinz, Focal adhesion size controls tension-dependent recruitment of alpha-smooth muscle actin to stress fibers, The Journal of cell biology 172 (2006) 259–268.

[76] V.J. Thannickal, D.Y. Lee, E.S. White, Z. Cui, J.M. Larios, R. Chacon, J.C. Horowitz, R.M. Day, P.E. Thomas, Myofibroblast differentiation by transforming growth factor-beta1 is dependent on cell adhesion and integrin signaling via focal adhesion kinase, The Journal of biological chemistry 278 (2003) 12384–12389.

[77] J.C. Horowitz, D.S. Rogers, V. Sharma, R. Vittal, E.S. White, Z. Cui, V.J. Thannickal, Combinatorial activation of FAK and AKT by transforming growth factor-beta1 confers an anoikis-resistant phenotype to myofibroblasts, Cellular signalling 19 (2007) 761–771.

[78] P. Chiarugi, E. Giannoni, Anoikis. A necessary death program for anchorage-dependent cells, Biochemical pharmacology 76 (2008) 1352–1364.

[79] H.Y. Zhang, S.H. Phan, Inhibition of myofibroblast apoptosis by transforming growth factor beta(1), American journal of respiratory cell and molecular biology 21 (1999) 658–665.

[80] H.Y. Zhang, M. Gharaee-Kermani, K. Zhang, S. Karmiol, S.H. Phan, Lung fibroblast alpha-smooth muscle actin expression and contractile phenotype in bleomycin-induced pulmonary fibrosis, The American journal of pathology 148 (1996) 527–537.

[81] B. Hinz, Masters and servants of the force: the role of matrix adhesions in myofibroblast force perception and transmission, European journal of cell biology 85 (2006) 175–181.

[82] C. Ffrench-Constant, L. van de Water, H.F. Dvorak, R.O. Hynes, Reappearance of an embryonic pattern of fibronectin splicing during wound healing in the adult rat, The Journal of cell biology 109 (1989) 903–914.

[83] H. Kosmehl, A. Berndt, D. Katenkamp, Molecular variants of fibronectin and laminin: structure, physiological occurrence and histopathological aspects, Virchows Archiv an international journal of pathology 429 (1996) 311–322.

[84] E. Balza, L. Borsi, G. Allemanni, L. Zardi, Transforming growth factor beta regulates the levels of different fibronectin isoforms in normal human cultured fibroblasts, FEBS letters 228 (1988) 42–44.

[85] L. Borsi, P. Castellani, A.M. Risso, A. Leprini, L. Zardi, Transforming growth factor-beta regulates the splicing pattern of fibronectin messenger RNA precursor, FEBS letters 261 (1990) 175–178.

[86] A.F. Muro, F.A. Moretti, B.B. Moore, M. Yan, R.G. Atrasz, C.A. Wilke, K.R. Flaherty, F.J. Martinez, J.L. Tsui, D. Sheppard, F.E. Baralle, G.B. Toews, E.S. White, An essential role for fibronectin extra type III domain A in pulmonary fibrosis, American journal of respiratory and critical care medicine 177 (2008) 638–645.

[87] M. Kurkinen, A. Vaheri, P.J. Roberts, S. Stenman, Sequential appearance of fibronectin and collagen in experimental granulation tissue, Laboratory investigation; a journal of technical methods and pathology 43 (1980) 47–51.

[88] C. Kuhn, J.A. McDonald, The roles of the myofibroblast in idiopathic pulmonary fibrosis. Ultrastructural and immunohistochemical features of sites of active extracellular matrix synthesis, The American journal of pathology 138 (1991) 1257–1265.

[89] P.-J. Wipff, D.B. Rifkin, J.-J. Meister, B. Hinz, Myofibroblast contraction activates latent TGF-beta1 from the extracellular matrix, The Journal of cell biology 179 (2007) 1311–1323.

[90] Z. Xing, G.M. Tremblay, P.J. Sime, J. Gauldie, Overexpression of granulocyte-macrophage colony-stimulating factor induces pulmonary granulation tissue formation and fibrosis by induction of transforming growth factor-beta 1 and myofibroblast accumulation, The American journal of pathology 150 (1997) 59–66.

[91] D. Andreutti, G. Gabbiani, P. Neuville, Early granulocyte-macrophage colony-stimulating factor expression by alveolar inflammatory cells during bleomycin-induced rat lung fibrosis, Laboratory investigation; a journal of technical methods and pathology 78 (1998) 1493–1502.

[92] C.J. Scotton, M.A. Krupiczojc, M. Königshoff, P.F. Mercer, Y.C.G. Lee, N. Kaminski, J. Morser, J.M. Post, T.M. Maher, A.G. Nicholson, J.D. Moffatt, G.J. Lau-

rent, C.K. Derian, O. Eickelberg, R.C. Chambers, Increased local expression of coagulation factor X contributes to the fibrotic response in human and murine lung injury, The Journal of clinical investigation 119 (2009) 2550–2563.

[93] X. Huang, Y. Gai, N. Yang, B. Lu, C.S. Samuel, V.J. Thannickal, Y. Zhou, Relaxin regulates myofibroblast contractility and protects against lung fibrosis, The American journal of pathology 179 (2011) 2751–2765.

[94] E. Fireman, I. Shahar, S. Shoval, G. Messer, S. Dvash, J. Grief, Morphological and biochemical properties of alveolar fibroblasts in interstitial lung diseases, Lung 179 (2001) 105–117.

[95] B. Hinz, G. Gabbiani, Mechanisms of force generation and transmission by myofibroblasts, Current opinion in biotechnology 14 (2003) 538–546.

[96] S. Tojkander, G. Gateva, G. Schevzov, P. Hotulainen, P. Naumanen, C. Martin, P.W. Gunning, P. Lappalainen, A molecular pathway for myosin II recruitment to stress fibers, Current biology CB 21 (2011) 539–550.

[97] J.J. Tomasek, G. Gabbiani, B. Hinz, C. Chaponnier, R.A. Brown, Myofibroblasts and mechano-regulation of connective tissue remodelling, Nature reviews. Molecular cell biology 3 (2002) 349–363.

[98] B. Hinz, P. Pittet, J. Smith-Clerc, C. Chaponnier, J.-J. Meister, Myofibroblast development is characterized by specific cell-cell adherens junctions, Molecular biology of the cell 15 (2004) 4310–4320.

[99] P. Pittet, K. Lee, A.J. Kulik, J.-J. Meister, B. Hinz, Fibrogenic fibroblasts increase intercellular adhesion strength by reinforcing individual OB-cadherin bonds, Journal of cell science 121 (2008) 877–886.

[100] B. Hinz, G. Gabbiani, C. Chaponnier, The NH2-terminal peptide of alpha-smooth muscle actin inhibits force generation by the myofibroblast in vitro and in vivo, The Journal of cell biology 157 (2002) 657–663.

[101] K. Katoh, Y. Kano, M. Amano, H. Onishi, K. Kaibuchi, K. Fujiwara, Rho-kinase--mediated contraction of isolated stress fibers, The Journal of cell biology 153 (2001) 569–584.

[102] A.K. Harris, P. Wild, D. Stopak, Silicone rubber substrata: a new wrinkle in the study of cell locomotion, Science (New York, N.Y.) 208 (1980) 177–179.

[103] K. Kimura, M. Ito, M. Amano, K. Chihara, Y. Fukata, M. Nakafuku, B. Yamamori, J. Feng, T. Nakano, K. Okawa, A. Iwamatsu, K. Kaibuchi, Regulation of

myosin phosphatase by Rho and Rho-associated kinase (Rho-kinase), Science (New York, N.Y.) 273 (1996) 245–248.

[104] J.J. Tomasek, M.B. Vaughan, B.P. Kropp, G. Gabbiani, M.D. Martin, C.J. Haaksma, B. Hinz, Contraction of myofibroblasts in granulation tissue is dependent on Rho/Rho kinase/myosin light chain phosphatase activity, Wound repair and regeneration official publication of the Wound Healing Society [and] the European Tissue Repair Society 14 (2006) 313–320.

[105] M. Parizi, E.W. Howard, J.J. Tomasek, Regulation of LPA-promoted myofibroblast contraction, Experimental cell research 254 (2000) 210–220.

[106] J. Wang, J. Fan, C. Laschinger, P.D. Arora, A. Kapus, A. Seth, C.A. McCulloch, Smooth muscle actin determines mechanical force-induced p38 activation, The Journal of biological chemistry 280 (2005) 7273–7284.

[107] J. Wang, H. Chen, A. Seth, C.A. McCulloch, Mechanical force regulation of myofibroblast differentiation in cardiac fibroblasts, American journal of physiology. Heart and circulatory physiology 285 (2003) H1871-81.

[108] M.W.C. Chan, P.D. Arora, P. Bozavikov, C.A. McCulloch, FAK, PIP5KIgamma and gelsolin cooperatively mediate force-induced expression of alpha-smooth muscle actin, Journal of cell science 122 (2009) 2769–2781.

[109] K. Zurhove, C. Nakajima, J. Herz, H.H. Bock, P. May, Gamma-secretase limits the inflammatory response through the processing of LRP1, Science signaling 1 (2008) ra15.

[110] P. May, Y.K. Reddy, J. Herz, Proteolytic processing of low density lipoprotein receptor-related protein mediates regulated release of its intracellular domain, The Journal of biological chemistry 277 (2002) 18736–18743.

[111] C. Cabello-Verrugio, E. Brandan, A novel modulatory mechanism of transforming growth factor-beta signaling through decorin and LRP-1, The Journal of biological chemistry 282 (2007) 18842–18850.

[112] W.-F. Tseng, S.S. Huang, J.S. Huang, LRP-1/TβR-V mediates TGF-β1-induced growth inhibition in CHO cells, FEBS letters 562 (2004) 71–78.

[113] S. Souchelnytskyi, K. Tamaki, U. Engström, C. Wernstedt, P. ten Dijke, C.-H. Heldin, Phosphorylation of Ser 465 and Ser 467 in the C Terminus of Smad2 Mediates Interaction with Smad4 and Is Required for Transforming Growth Factor-β Signaling, J. Biol. Chem. 272 (1997) 28107–28115.

[114] S. Abdollah, M. Macías-Silva, T. Tsukazaki, H. Hayashi, L. Attisano, J.L. Wrana, TβRI Phosphorylation of Smad2 on Ser 465 and Ser 467 Is Required for Smad2-Smad4 Complex Formation and Signaling, J. Biol. Chem. 272 (1997) 27678–27685.

[115] M. Macías-Silva, S. Abdollah, P.A. Hoodless, R. Pirone, L. Attisano, J.L. Wrana, MADR2 is a substrate of the TGFbeta receptor and its phosphorylation is required for nuclear accumulation and signaling, Cell 87 (1996) 1215–1224.

[116] M. Kretzschmar, J. Doody, I. Timokhina, J. Massagué, A mechanism of repression of TGFbeta/ Smad signaling by oncogenic Ras, Genes & development 13 (1999) 804–816.

[117] M.L. Burch, S.N.Y. Yang, M.L. Ballinger, R. Getachew, N. Osman, P.J. Little, TGF-beta stimulates biglycan synthesis via p38 and ERK phosphorylation of the linker region of Smad2, Cellular and molecular life sciences CMLS 67 (2010) 2077–2090.

[118] S. Dennler, S. Itoh, D. Vivien, P. ten Dijke, S. Huet, J.M. Gauthier, Direct binding of Smad3 and Smad4 to critical TGF beta-inducible elements in the promoter of human plasminogen activator inhibitor-type 1 gene, The EMBO journal 17 (1998) 3091–3100.

[119] S.C. Muratoglu, I. Mikhailenko, C. Newton, M. Migliorini, D.K. Strickland, Low density lipoprotein receptor-related protein 1 (LRP1) forms a signaling complex with platelet-derived growth factor receptor-beta in endosomes and regulates activation of the MAPK pathway, The Journal of biological chemistry 285 (2010) 14308–14317.

[120] B. Langlois, G. Perrot, C. Schneider, P. Henriet, H. Emonard, L. Martiny, S. Dedieu, LRP-1 promotes cancer cell invasion by supporting ERK and inhibiting JNK signaling pathways, PLoS ONE 5 (2010) e11584.

[121] K.-G. Ma, J. Lv, X.-D. Hu, L.-L. Shi, K.-W. Chang, X.-L. Chen, Y.-H. Qian, W.-N. Yang, Q.-M. Qu, The p38 mitogen-activated protein kinase signaling pathway is involved in regulating low-density lipoprotein receptor-related protein 1-mediated β-amyloid protein internalization in mouse brain, The international journal of biochemistry & cell biology 76 (2016) 75–86.

[122] M. Karin, Z.g. Liu, E. Zandi, AP-1 function and regulation, Current opinion in cell biology 9 (1997) 240–246.

[123] R.S. Nho, P. Hergert, J. Kahm, J. Jessurun, C. Henke, Pathological alteration of FoxO3a activity promotes idiopathic pulmonary fibrosis fibroblast proliferation on type i collagen matrix, The American journal of pathology 179 (2011) 2420–2430.

[124] H. Xia, J. Seeman, J. Hong, P. Hergert, V. Bodem, J. Jessurun, K. Smith, R. Nho, J. Kahm, P. Gaillard, C. Henke, Low α(2)β(1) integrin function enhances the proliferation of fibroblasts from patients with idiopathic pulmonary fibrosis by activation of the β-catenin pathway, The American journal of pathology 181 (2012) 222–233.

[125] H. Xia, W. Khalil, J. Kahm, J. Jessurun, J. Kleidon, C.A. Henke, Pathologic caveolin-1 regulation of PTEN in idiopathic pulmonary fibrosis, The American journal of pathology 176 (2010) 2626–2637.

[126] K. Hu, C. Wu, W.M. Mars, Y. Liu, Tissue-type plasminogen activator promotes murine myofibroblast activation through LDL receptor-related protein 1-mediated integrin signaling, The Journal of clinical investigation 117 (2007) 3821–3832.

[127] L.-I. Kang, K. Isse, K. Koral, W.C. Bowen, S. Muratoglu, D.K. Strickland, G.K. Michalopoulos, W.M. Mars, Tissue-type plasminogen activator suppresses activated stellate cells through low-density lipoprotein receptor-related protein 1, Laboratory investigation; a journal of technical methods and pathology 95 (2015) 1117–1129.

[128] K. Hu, L. Lin, X. Tan, J. Yang, G. Bu, W.M. Mars, Y. Liu, tPA protects renal interstitial fibroblasts and myofibroblasts from apoptosis, Journal of the American Society of Nephrology JASN 19 (2008) 503–514.

[129] P. Boucher, W.-P. Li, R.L. Matz, Y. Takayama, J. Auwerx, R.G.W. Anderson, J. Herz, LRP1 functions as an atheroprotective integrator of TGFbeta and PDFG signals in the vascular wall, PLoS ONE 2 (2007) e448.

[130] B. Yusuf, R. Gopurappilly, N. Dadheech, S. Gupta, R. Bhonde, R. Pal, Embryonic fibroblasts represent a connecting link between mesenchymal and embryonic stem cells, Development, growth & differentiation 55 (2013) 330–340.

[131] D. Safina, F. Schlitt, R. Romeo, T. Pflanzner, C.U. Pietrzik, V. Narayanaswami, F. Edenhofer, A. Faissner, Low-density lipoprotein receptor-related protein 1 is a novel modulator of radial glia stem cell proliferation, survival, and differentiation, Glia 64 (2016) 1363–1380.

[132] E. Mantuano, M. Jo, S.L. Gonias, W.M. Campana, Low density lipoprotein receptor-related protein (LRP1) regulates Rac1 and RhoA reciprocally to control Schwann cell adhesion and migration, The Journal of biological chemistry 285 (2010) 14259–14266.

[133] L. Yang, C.-C. Liu, H. Zheng, T. Kanekiyo, Y. Atagi, L. Jia, D. Wang, A. N'songo, D. Can, H. Xu, X.-F. Chen, G. Bu, LRP1 modulates the microglial immune response via regulation of JNK and NF-κB signaling pathways, Journal of neuroinflammation 13 (2016) 304.

[134] S. Hashimoto, Y. Gon, I. Takeshita, K. Matsumoto, S. Maruoka, T. Horie, Transforming growth Factor-beta1 induces phenotypic modulation of human lung fibroblasts to myofibroblast through a c-Jun-NH2-terminal kinase-dependent pathway, American journal of respiratory and critical care medicine 163 (2001) 152–157.

[135] M. Pakyari, A. Farrokhi, M.K. Maharlooei, A. Ghahary, Critical Role of Transforming Growth Factor Beta in Different Phases of Wound Healing, Advances in wound care 2 (2013) 215–224.

[136] V. Plantevin Krenitsky, L. Nadolny, M. Delgado, L. Ayala, S.S. Clareen, R. Hilgraf, R. Albers, S. Hegde, N. D'Sidocky, J. Sapienza, J. Wright, M. McCarrick, S. Bahmanyar, P. Chamberlain, S.L. Delker, J. Muir, D. Giegel, L. Xu, M. Celeridad, J. Lachowitzer, B. Bennett, M. Moghaddam, O. Khatsenko, J. Katz, R. Fan, A. Bai, Y. Tang, M.A. Shirley, B. Benish, T. Bodine, K. Blease, H. Raymon, B.E. Cathers, Y. Satoh, Discovery of CC-930, an orally active anti-fibrotic JNK inhibitor, Bioorganic & medicinal chemistry letters 22 (2012) 1433–1438.

[137] J.L.J. van der Velden, Y. Ye, J.D. Nolin, S.M. Hoffman, D.G. Chapman, K.G. Lahue, S. Abdalla, P. Chen, Y. Liu, B. Bennett, N. Khalil, D. Sutherland, W. Smith, G. Horan, M. Assaf, Z. Horowitz, R. Chopra, R.M. Stevens, M. Palmisano, Y.M.W. Janssen-Heininger, P.H. Schafer, JNK inhibition reduces lung remodeling and pulmonary fibrotic systemic markers, Clinical and translational medicine 5 (2016) 36.

[138] Y. Takayama, H. Takahashi, K. Mizumachi, T. Takezawa, Low density lipoprotein receptor-related protein (LRP) is required for lactoferrin-enhanced collagen gel contractile activity of human fibroblasts, The Journal of biological chemistry 278 (2003) 22112–22118.

[139] T.E. Willnow, J.L. Goldstein, K. Orth, M.S. Brown, J. Herz, Low density lipoprotein receptor-related protein and gp330 bind similar ligands, including plasminogen activator-inhibitor complexes and lactoferrin, an inhibitor of chylomicron remnant clearance, The Journal of biological chemistry 267 (1992) 26172–26180.

[140] Y. Takayama, R. Aoki, Roles of lactoferrin on skin wound healing, Biochemistry and cell biology = Biochimie et biologie cellulaire 90 (2012) 497–503.

[141] D. Bowes, A.E. Clark, B. Corrin, Ultrastructural localisation of lactoferrin and glycoprotein in human bronchial glands, Thorax 36 (1981) 108–115.

[142] V.L. Kinnula, C.L. Fattman, R.J. Tan, T.D. Oury, Oxidative stress in pulmonary fibrosis: a possible role for redox modulatory therapy, American journal of respiratory and critical care medicine 172 (2005) 417–422.

[143] T.E. King, A. Pardo, M. Selman, Idiopathic pulmonary fibrosis, The Lancet 378 (2011) 1949–1961.

[144] M. Hollborn, G. Birkenmeier, A. Saalbach, I. Iandiev, A. Reichenbach, P. Wiedemann, L. Kohen, Expression of LRP1 in Retinal Pigment Epithelial Cells and Its Regulation by Growth Factors, Invest. Ophthalmol. Vis. Sci. 45 (2004) 2033.

[145] N. Khalil, R.N. O'Connor, K.C. Flanders, H. Unruh, TGF-beta 1, but not TGF-beta 2 or TGF-beta 3, is differentially present in epithelial cells of advanced pulmonary fibrosis, American journal of respiratory cell and molecular biology 14 (1996) 131–138.

[146] S.L. Schor, Cell proliferation and migration on collagen substrata in vitro, Journal of cell science 41 (1980) 159–175.

[147] V. Llorente-Cortes, V. Barbarigo, L. Badimon, Low density lipoprotein receptor-related protein 1 modulates the proliferation and migration of human hepatic stellate cells, Journal of cellular physiology 227 (2012) 3528–3533.

[148] L. Lin, G. Bu, W.M. Mars, W.B. Reeves, S. Tanaka, K. Hu, tPA activates LDL receptor-related protein 1-mediated mitogenic signaling involving the p90RSK and GSK3beta pathway, The American journal of pathology 177 (2010) 1687–1696.

[149] M. Fu, C. Wang, Z. Li, T. Sakamaki, R.G. Pestell, Minireview. Cyclin D1: normal and abnormal functions, Endocrinology 145 (2004) 5439–5447.

[150] H. Suganuma, A. Sato, R. Tamura, K. Chida, Enhanced migration of fibroblasts derived from lungs with fibrotic lesions, Thorax 50 (1995) 984–989.

[151] N. Kozlova, J.K. Jensen, T.F. Chi, A. Samoylenko, T. Kietzmann, PAI-1 modulates cell migration in a LRP1-dependent manner via β-catenin and ERK1/2, Thrombosis and haemostasis 113 (2015) 988–998.

[152] L. Wujak, R.T. Böttcher, O. Pak, H. Frey, E. El Agha, Y. Chen, S. Schmitt, S. Bellusci, L. Schaefer, N. Weissmann, R. Fässler, M. Wygrecka, Low density lipoprotein receptor-related protein 1 couples β1 integrin activation to degradation, Cellular and molecular life sciences CMLS (2017).

# 8 Declaration

I declare that I have completed this dissertation single-handedly without the unauthorized help of a second party and only with the assistance acknowledged therein. I have appropriately acknowledged and cited all text passages that are derived verbatim from or are based on the content of published work of others, and all information relating to verbal communications. I consent to the use of an anti-plagiarism software to check my thesis. I have abided by the principles of good scientific conduct laid down in the charter of the Justus Liebig University Giessen „Satzung der Justus-Liebig-Universität Gießen zur Sicherung guter wissenschaftlicher Praxis“ in carrying out the investigations described in the dissertation.

Jennifer Schnieder

# 9 Acknowledgement

First of all, I would like to thank Prof. Dr. Malgorzata Wygrecka-Markart for giving me the opportunity to perform by doctoral studies in such an interesting field as wound healing and fibrosis. I appreciate the support you have given me throuout this time. My thanks also goes to Prof. Dr. Adriaan Dorresteijn for agreeing to be my first supervisor and for your constructive feedback on my thesis.

I want to express my thanks to all the people who accompanied me everyday in the laboratory. Special thanks to Dr. Lukasz Wujak who I could discuss all kinds of questions with. Moreover, I thank Dr. Miroslava Didiasova and Dr. Dariusz Zakrzewicz for your advice. My special thanks also goes to Yvonne Horn, Horst Thiele and Markus Schwinn, for sharing your broad methodical experience with me. Thanks for the good time we had together.
My thanks goes to Prof. Dr. Klaus T. Preissner and his group for all the feedback on my work and the good working atmosphere.

I would like to express my thanks to Dr. Jochen Wilhelm who performed the microarray for me and who patiently answered all my statistical questions.

Last but definitely not least, I would like to thank my family for always standing behind me. Thank you for believing in me and supporting me on my way.